

# **Increasing the Capacity of Wireless Networks Using Beamforming**

Yousef Ali Yousef

A Thesis  
in  
The Department  
of  
Electrical and Computer Engineering

Presented in Partial Fulfillment of the Requirements  
For the Degree of  
Doctor of Philosophy ( Electrical and Computer Engineering ) at  
Concordia University  
Montreal, Quebec, Canada

September 2018

© Yousef Ali Yousef, 2018

**CONCORDIA UNIVERSITY**  
**SCHOOL OF GRADUATE STUDIES**

This is to certify that the thesis prepared

By:                   Yousef Yousef

Entitled:           Increased Spectral Efficiency Using User Identification,  
Beamforming, and Tracking

and submitted in partial fulfillment of the requirements for the degree of

Doctor Of Philosophy (Electrical and Computer Engineering)

complies with the regulations of the University and meets the accepted standards with respect to originality and quality.

Signed by the final examining committee:

\_\_\_\_\_ Chair  
Dr. Luis Amador

\_\_\_\_\_ External Examiner  
Dr. René Landry

\_\_\_\_\_ External to Program  
Dr. Adel Hanna

\_\_\_\_\_ Examiner  
Dr. Anjali Agarwal

\_\_\_\_\_ Examiner  
Dr. Dongyu Qiu

\_\_\_\_\_ Thesis Co-Supervisor  
Dr. Reza Soleymani

\_\_\_\_\_ Thesis Co-Supervisor  
Dr. Yousef R. Shayan

Approved by \_\_\_\_\_  
Dr. Mustafa Mehmet Ali, Graduate Program Director

December 12, 2018

\_\_\_\_\_  
Dr. Amir Asif, Dean  
Gina Cody School of Engineering and Computer Science

# **Abstract**

## **Increasing the Capacity of Wireless Networks Using Beamforming**

**Yousef Ali Yousef, Ph.D.**

**Concordia University, 2018**

Wireless mobile communications are growing in an exponential manner, especially in terms of the number of users. Also, the demand for high Quality of Service (QoS) has become essential. Nowadays, subscribers are using more applications such as the internet, video conferencing, and high quality TV. These applications require high data rates. The Space Division Multiple Access (SDMA) is the key element that can enable reusing of the same channels among different users in the same cell to meet this demand.

For the application of SDMA in an efficient way, it is required to identify the users' positions and directions in the cell. The Direction of Arrival (DOA) algorithms can estimate the incident angles of all the received signals impinging on the array antenna. These algorithms give the DOAs of all relevant signals of the user sources and interference sources. However, they are not capable of distinguishing and identifying which one is the direction of the desired user. In this thesis, we have proposed to use a Reference Signal (RFS) known by the transmitter and the receiver to identify which one of the estimated DOAs is the DOA of the desired user in the cell. Using a RFS and applying the correlation concept, we can distinguish the desired signal from the others. Moreover, we have considered the Affine Projection Algorithm (APA) to enhance the accuracy of the estimated direction and to form a beam towards the desired user and nulls towards the interferers. Our simulation results assure that, in the presence of the RFS, the DOA algorithms can identify the direction of the desired user with high accuracy and resolution. We have investigated this concept on different DOA

algorithms such as Multiple Signal Classification (MUSIC), ROOT MUSIC, and Estimate the direction of arrival of Signals Parameters via Rotational Invariance Technique (ESPRIT) algorithms.

Moreover, we have introduced an approach for using the smart antennas (SA) to exploit the space diversity for the next generations of mobile communication systems. We have applied a combination of the MUSIC and the Least Mean Squares (LMS) algorithms. We have proposed the MUSIC algorithm for finding the directions of the users in the cell. In addition, we have considered the LMS algorithm for enhancing the accuracy of the DOA, performing the beam generation process, and keeping track of the users in the cell. Furthermore, we have proposed a scheduling algorithm that performs the scheduling in terms of the generated beams.

The space diversity, together with the time and frequency diversities of LTE (Long Term Evolution) results in a large capacity increase in the next generations of wireless mobile communication systems. Simulation results show that the proposed algorithm called Multiple Signal Classification and Least Mean Squares (MLMS), has the capability to converge and completely follow the desired user signal with a very high resolution. The convergence and the accurate tracking of the desired signal user take place after 13 iterations while in the traditional LMS, the convergence needs 85 iterations to take place. This means an 84.7% improvement over the traditional LMS algorithm for the same number of calculations in each iteration. In contrast to the traditional LMS algorithm, the proposed algorithm can work in the presence of high level of interference. Furthermore, the proposed scheduling scheme based on beamforming shows a gain of 15% in the total aggregated throughput for each  $10^\circ$  decrease in the beam size. The proposed model provides an optimum, complete, and practical design for the next generations of the mobile communication systems. In this model, we have proposed a mechanism to find the direction of each user in the cell, enhance the accuracy of the obtained DOAs, and perform scheduling based on the generated beams.

In addition, we have presented an approach for Frequency Reuse (FR) based on beamforming for 5G. We have implemented a synthesizer in order to smartly form the desired beam shape and make the nulls deeper. We have taken the advantage of the SAs, beamforming capabilities, and the radiation pattern (RP) synthesizing techniques to build up a FR scheme for 5G. Also, we have developed a formula for calculating the Signal to Interference and Noise Ratio (SINR) in terms of the desired and the interferers directions. The objective is to maintain the SINR at the minimum acceptable levels required by the LTE while reducing the beam sizes, and hence increase the FR factor. The simulation results show that with a Uniform Linear Antenna (ULA) of 11 elements, we can achieve the desirable SINR levels using beams of  $10^0$  width, which improves the FR factor from 1 to 18, and subsequently increases the number of mobile users.

# *Acknowledgements*

All praise go to Allah Almighty, Who provided me this opportunity to contribute a drop in the sea of knowledge which He blessed to the human being. I only desire betterment to the best of my power; and my success can only come from Allah. In Him I Trust, and unto Him I look.

It is with great pleasure to acknowledge the efforts of many people who helped and facilitated my PhD program. First of all, my deepest gratitude goes to my supervisor, Prof. Yousef Shayan, for his passionate guidance, support throughout my studies at Concordia University. Secondly, I gratefully thank my Co-supervisor, Prof. Reza Solymani, for his supervision, advice, encouragement, help and support throughout all the struggling period of my research. He was always there to listen to my ideas and discuss them.

Thirdly, I would like to record the role of my mother and my father in achieving this destination. Their prayers, encouragement, love and affection were a brilliant help to keep me focused during this study. Also, I heartily acknowledge the prayers of my sister and all other friends as they played a vital role in the completion of this dissertation.

Fourthly, I also extend my sincere gratitude to my wife and daughters, who were so patient, and allowed me to spend extra time on this research.

Fifthly, I would like to gratefully thank the beamforming expert, my friend Dr. Jala Srar for his great help and support during my research work. He was always helping me whenever I needed him especially for the beamforming side of my research.

Sixthly, I would like to gratefully thank my friend Ahmad Amin who was involved in part of my work for his great help.

Finally, I am also very grateful to all the members in my Wireless Research Group for their friendship and support to help me finish my study. I am also thankful to all of my friends in Canada and Libya for their moral support during this study to boost my determination to achieve this goal.

*Dedicated to my parents, wife, and daughters*

# Contents

<b>List of Figures</b>	<b>xii</b>
<b>List of Tables</b>	<b>xv</b>
<b>List of Abbreviations</b>	<b>xvi</b>
<b>List of Symbols</b>	<b>xx</b>
<b>1 Chapter 1: Introduction</b>	<b>1</b>
1.1 Mobile Generations . . . . .	1
1.2 Literature Review . . . . .	6
1.2.1 Direction of Arrival . . . . .	6
1.2.2 Adaptive Beamforming Algorithms . . . . .	8
1.2.3 Scheduling . . . . .	10
1.2.4 Frequency Reuse . . . . .	11
1.2.5 Fifth Generation of Mobile Communications . . . . .	14
1.3 Objectives and Contributions . . . . .	16
1.4 Organization . . . . .	17
<b>2 Chapter 2: Background</b>	<b>18</b>
2.1 Antennas . . . . .	18
2.1.1 Principle of Array Antennas . . . . .	19
2.1.2 Two Elements Antenna Array . . . . .	20

2.1.3	N Element Linear Array Antennas (Uniform Amplitude and Spacing)	21
2.1.4	Smart Antennas . . . . .	22
2.2	Digital Beamforming . . . . .	23
2.2.1	Switched Digital Beamforming . . . . .	24
2.2.2	Adaptive Digital Beamforming . . . . .	25
2.3	Multiple Access in Frequency Domain . . . . .	26
2.3.1	OFDM . . . . .	26
2.3.2	OFDMA . . . . .	29
2.3.3	SC-FDMA . . . . .	31
<b>3</b>	<b>Chapter 3: Direction of Arrival Algorithms for User Identification for 5G</b>	<b>33</b>
3.1	Direction of Arrival Algorithms . . . . .	33
3.1.1	MUSIC Algorithm . . . . .	35
3.1.2	Root MUSIC Algorithm . . . . .	36
3.1.3	ESPRIT Algorithm . . . . .	37
3.2	System Model . . . . .	39
3.3	Accuracy Enhancement . . . . .	41
3.4	Simulation Results . . . . .	43
3.5	Conclusion . . . . .	49
<b>4</b>	<b>Chapter 4: Adaptive Beamforming for 5G</b>	<b>50</b>
4.1	Adaptive Beamforming Algorithms . . . . .	50
4.2	Wiener Solution . . . . .	51
4.3	Steepest Descent Method . . . . .	53
4.4	Least Mean Square . . . . .	54
4.5	Proposed Tracking Model . . . . .	55
4.6	Simulation Results . . . . .	59

4.7	Conclusion . . . . .	61
<b>5</b>	<b>Chapter 5: Scheduling Based on Beamforming</b>	<b>62</b>
5.1	Scheduling in LTE . . . . .	62
5.2	Modelling DS and NDS calls . . . . .	64
5.3	Resource Allocation Formula in OFDM System . . . . .	66
5.4	Modeling the utility function of the requested services . . . . .	68
5.5	Scheduling Procedure . . . . .	73
5.6	Simulation Results . . . . .	74
5.7	Conclusion . . . . .	76
<b>6</b>	<b>Chapter 6: Frequency Reuse Based on Beamforming for 5G</b>	<b>77</b>
6.1	The Concept of Transmit Beamforming . . . . .	78
6.2	Radiation Pattern Shaping . . . . .	79
6.3	Proposed Frequency Reuse Mechanism . . . . .	80
6.3.1	SINR Calculation . . . . .	81
6.3.2	Frequency Reuse Plan . . . . .	84
6.4	Worst Case Scenario Calculations . . . . .	87
6.4.1	Detailed Procedure . . . . .	89
6.5	Simulation Results . . . . .	93
6.6	Conclusion . . . . .	97
<b>7</b>	<b>Chapter 7: Conclusion and Future Work</b>	<b>98</b>
7.1	Conclusion . . . . .	98
7.2	Future Work . . . . .	99
7.2.1	Compare between the LMS, RLS, and APA adaptive beamforming algorithms in the presence of the correlator . . . . .	100

7.2.2	Calculating the system capacity based on the proposed frequency reuse and beamforming . . . . .	100
7.2.3	Analyze the performance of the proposed scheduling and frequency reuse schemes in the presence of more than two QoS classes . . . . .	100
7.2.4	Designing the best antenna for the proposed frequency reuse based on beamforming . . . . .	101

<b>Bibliography</b>		<b>102</b>
---------------------	--	------------

# List of Figures

1.1	(a) Frequency reuse-3 model in GSM, (b) Frequency reuse-7 model in GSM	12
1.2	(a) Strict FFR technique, (b) Soft FFR technique	13
2.1	Antenna Radiation Mechanism	19
2.2	Two element antenna array	20
2.3	N elements antenna array	22
2.4	(a) Dipole Pattern, (b) Array Factor, (c) Multiplication Result	23
2.5	Digital Beamformer	24
2.6	Switched Beamforming	25
2.7	Adaptive Beamforming	26
2.8	OFDM and FDMA Spectrum	27
2.9	OFDM Block Diagram	28
2.10	Cyclic Prefix Diagram	29
2.11	Users Diversity	30
2.12	OFDM Resource Blocks	30
2.13	OFDMA Resource Blocks	31
3.1	N Element Uniform Linear Antenna	34
3.2	Antenna Receiver Model	34
3.3	Two Identical Overlapped Sub-arrays	37
3.4	Affine Adaptive Beamforming System	42

3.5	DOA Estimation using MUSIC Algorithm for 10 Elements ULA at (a) $SNR = 10dB$ and (b) $SNR = 0dB$ . . . . .	44
3.6	Generate a Beam towards the Desired User and Nulls towards the Interferes in (a) Cartesian coordinates (b) Polar coordinates . . . . .	46
3.7	the Angles Associated with the Root Music Algorithm (a) at $SNR = 10dB$ and (b) $SNR = 0dB$ . . . . .	47
4.1	The Classes of Beamforming Algorithms . . . . .	51
4.2	Adaptive Beamformer . . . . .	52
4.3	MLMS Algorithm . . . . .	55
4.4	Convergence of MLMS and LMS Algorithms . . . . .	60
4.5	Tracking Capability of MLMS and LMS Algorithms . . . . .	60
5.1	Two Dimensional Markov Chain . . . . .	65
5.2	Utility Function of (a) DS and (b) NDS Applications . . . . .	68
5.3	Scheduler Flowchart . . . . .	73
5.4	Total aggregated Data Rate at different beam sizes . . . . .	75
5.5	Total Occupied Subchannels at Different Beam Sizes . . . . .	75
6.1	A General Beamforming System . . . . .	78
6.2	Four Beamformers Located at the Cell Center . . . . .	81
6.3	Four beamformers at the center and mobile placed at $P(r, \theta_1)$ . . . . .	82
6.4	A mini-cluster composed of two cells . . . . .	84
6.5	Cluster of six cells . . . . .	85
6.6	A combination of mini-clusters and clusters in one FR plan . . . . .	86
6.7	(a) Cluster of 6, (b) 12, (c) 18, and 36 cells . . . . .	87
6.8	Worst Case Scenario . . . . .	88
6.9	The proposed Configuration . . . . .	90

6.10	Cluster of 24 beams and mobile placed at a beam boundary. . . . .	94
6.11	Beam shape in the Cartesian coordinates with $HPBW = 15^\circ$ centered at $90^\circ$ . . . . .	94
6.12	Beam shape in the Polar coordinates with $HPBW = 15^\circ$ centered at $90^\circ$ and $SLL = 28.7\text{ dB}$ . . . . .	95
6.13	Beam shape in the Cartesian coordinates with $HPBW = 10^\circ$ centered at $90^\circ$ . . . . .	95
6.14	Beam shape in the Polar coordinates with $HPBW = 10^\circ$ centered at $90^\circ$ and $SLL = 28.8\text{ dB}$ . . . . .	96
6.15	Beam size with number of antenna elements. . . . .	97

# List of Tables

3.1	MUSIC Algorithm Results . . . . .	45
3.2	The obtained DOAs using Root MUSIC algorithm . . . . .	48
3.3	The obtained DOAs using ESPRIT algorithm . . . . .	48
5.1	Parameters of CQI . . . . .	64
5.2	Total aggregated throughput Gain . . . . .	76

# List of Abbreviations

**G & Generation**

**ABF & Adaptive Beamforming**

**AC & Alternate Current**

**AF & Array Factor**

**AMC & Adaptive Modulation and Coding**

**APA & Affine Projection Algorithm**

**AWGNC & Additive White Gaussian Noise**

**BLMS & Bessel Least Mean Square**

**BPSK & Binary Phase Shift Keying**

**BSC & Base Station Controller**

**BTS & Base Transceiver Station**

**CAC & Call Admission Control**

**CDMA & Code Division Multiple Access**

**CEB & Channel Estimated Based**

**CGM & Conjugate Gradient Method**

**CoMP & Coordinate Multiple transmission and reception**

**CP & Cyclic Prefix**

**CQI & Channel Quality Indicator**

**CS/CB & Coordinate Scheduling / Beamforming**

**CSI & Channel Status Indicator**

**CSW & Circuit Switching**

**DFT & Discrete Fourier Transform**

**DFT-S-OFDM & Discrete Fourier Transform Spread Orthogonal Frequency Division Multiplexing**

**DOA & Direction Of Arrival**

**DR & Despread Respread**

**DS & Delay Sensitive**

**DSP & Digital Signal Processing**

**EDGE & Enhanced Data for GSM Evolution**

**EF & Elementary Factor**

**eMBMS & evolved Multimedia Broadcast Multicast Service**

**eNB & e Node**

**ESPERIT & Estimate of Signal parameters via Rotational Invariance Techniques**

**FDD & Frequency Division Duplexing**

**FDMA & Frequency Division Multiple Access**

**FFR & Fractional Frequency Reuse**

**FM & Frequency Modulation**

**FR & Frequency Reuse**

**FD-MIMO & Full Dimension Multiple Input Multiple Output**

**GMSK & Gaussian Minimum Shift Keying**

**GPRS & General Packet Radio Service**

**GSM & Global System for Mobile communications**

**H-ARQ & Hybrid Automatic Repeat Request**

**HSCSD & High Speed Circuit Switched Data**

**HSDPA & High Speed Downlink Packet Access**

**HSUPA & High Speed Uplink Packet Access**

**ICI & Inter Cell Interference**

**ICIC & Inter Cell Interference Coordination**

**IDFT & Inverse Discrete Fourier Transform**

**ITU & International Telecommunication Union**

**LAA & Licensed Assisted Access**

**LBS & Location Based Service**

**LCS & Location Service**

**LMS & Least Mean Square**

**LLMS & LLeast Mean Square**

**LTE & Long Term Evolution**

**MBMS & Multimedia Broadcast Multimedia Service**

**MIMO & Multiple Input Multiple Output**

**ML & Maximum Like**

**MLMS & MUSIC and Least Mean Square**

**MMS & MultimediaMessage Service**

**MSE & Main Square Error**

**MUSIC & MUtiple SIgnal Classification**

**NDS & Non Delay Sensitive**

**NLMS & Normalized Least Mean Square**

**OFDM & Orthogonal Frequency Division Multiplexing**

**OFDMA & Orthogonal Frequency Division Muliple Access**

**OQPSK & Orthogonal Quadreture Phase Shift Keying**

**PAPR & Power Average Peack Ratio**

**PR & Property Restoral**

**PSK & Phase Shift Keying**

**QAM & Quadrature Amplitude Modulation**

**QoS & Quality of Service**

**QPSK & Quadrature Phase Shift Keying**

**RP & Radiation Pattern**

**RFS & RFerence Signal**

**RLMS & Recurssive Least Mean Square**

**RLS & Recurssive Least Square**

**RNC & Radio Network Controller**

**RS & Reference Signal**

**SA & Smart Antenna**

**SC-FDMA & Single Carrier Frequency Division Multiple Access**

**SDMA & Space Division Multiple Access**

**SINR & Signal to Interference and Noise Ratio**

**SMI & Sample Matrix Inversion**

**SMS & Short Message Service**

**SNR & Signal Noise Ratio**

**TDD & Time Division Duplexing**

**TDMA & Time Division Multiple Access**

**UE & User Equipment**

**ULA & Uniform Linear Antenna**

**UMTS & Universal Mobile Telecommunication Service**

**UI & User Identifier**

**WiMAX & Worldwide Interoperability for Microwave Access**

# List of Symbols

$d$  & Element Spacing

$\theta$  & Angle

$\phi$  & Angle

$\lambda$  & Wave length

$(\cdot)$  & Complex conjugate

$(\cdot)^H$  & Hermitian transpose

$(\hat{\cdot})_{est}$  & Estimated value

$E \cdot$  & Expectation

$dB$  & decibel

& Gradient

$\Delta$  & The Difference between two Frequencies

$\beta$  & Electric phase deference between the two adjacent elements

$I_0$  & Complex phasor current

$\beta$  & Electric phase deference between the two adjacent elements

$k$  & Wave number

$L$  & Dipole length

$E$  & Electric field intensity vector

$\eta$  & Intrinsic impedance

$\mu$  & Step size

$\Gamma$  & Gamma function

$J_\nu$  & Bessel function

$c$  & Speed of light

$\Theta_i$  & Time delay of signal arriving to element  $i$

$AF$  & Array factor

$U(\theta)$  & Radiation density

$f$  & Frequency

$f_i$  & Frequency of Subcarrier Number  $i$

$f_j$  & Frequency of Subcarrier Number  $j$

$T_s$  & Sampling Period

$max$  & Maximization

$\bar{R}_{xx}$  & Correlation matrix of the desired signal  $x_{des}$

$\bar{R}_{x_{des} x_{des}}$  & Correlation matrix of the signal  $x$

$\bar{R}_{nn}$  & Correlation matrix of the noise signal

$\bar{R}_{ss}$  & Correlation matrix of the source signal

$\bar{r}_{xd}$  & Cross-correlation vector

$e(.)$  & Error signal

$\bar{n}$  & Noise signal

$\bar{s}$  & Source signal

$\bar{w}$  & Weighting vector

$\bar{w}_{opt}$  & Optimum weighting vector

$corr$  & Correlation function

$arg$  & arg function

$\bar{\gamma}$  & Transformation matrix

$SNR$  & Signal to the noise ratio

$\Psi$  & Smoothing factor

$control$  & Control signal

$s_{ref}$  & Source reference signal

$A_i$  & Total traffic rate of service class  $i$

$\lambda_i$  & Arriving rate of service class  $i$

$\mu_i$  & Leaving rate of service class  $i$

$R_i$  & Total bit rate

$\alpha$  & Index

$B$  & Bandwidth

$f_{ds}$  & Frequency assigned to the delay sensitive services

$f_{nds}$  & Frequency assigned to the non delay sensitive services

$f_{max}$  & maximum frequency

$sgn$  & Sign function

$V$  & Utility scale

$u_i(\cdot)$  & Utility function of the service  $i$

$p_w$  & Power

$C_i$  & Constraint number  $i$

$\mathcal{L}$  & Lagrange

$S_{des}$  & Power of the desired user signal

$S_{interferer}$  & Power of the interferers

$A$  & Frequency set A

$B$  & Frequency set B

$BS_i$  & Base station number  $i$

$SINR_{BS_i}$  & Signal to the noise and interference ration at base station number  $i$

$SINR_{at\ mobile}$  & Signal to the noise and interference ration at the mobile

$y_{UI}$  & Signal strength at the user identifier

$ref(t)$  & Reference signal as function of time

$clk$  & Clock function

# Chapter 1: Introduction

## 1.1 Mobile Generations

Mobile communication has gone through different generations. Each generation has introduced some new features. The earliest generation of mobile communications was completely analog. They used Frequency Division Multiple Access/Frequency Division Duplexing (FDMA/FDD) and analog Frequency Modulation (FM). They started by using a powerful transmitter on a tall building [1]. Afterwards, the powerful transmitter was replaced by lower power base stations using the cellular concept.

The second generation (2G) was introduced in order to provide high speech quality and meet the higher demand for mobile communication [2]. In addition to high quality voice calls, 2G also offered the Short Message Service (SMS), facsimile and security features. It is known also as Global System for Mobile communication (GSM). The start of data services with 2G was through Circuit Switched technique (CSW) [3].

High Speed Circuit Switched Data (HSCSD) represents the first improvement to the GSM. It enabled certain users to occupy more than one time slot to get higher data rates. It is considered as only a software upgrade of GSM. Furthermore, HSCSD implements channel estimation to decide whether there is a need to send redundant information to correct the expected errors or not. If the signal is strong enough, there is no need for such information.

This increases the data rates from 9.6 *kbps* to 14.4 *kbps* per time slot [4]. In case of strong signal and the traffic is low, a user can occupy up to four time slots which gives 57.6 *kbps*.

The second stage of 2G improvements was through introducing the General Packet Radio Service (GPRS). GPRS represents both hardware and software upgrades of 2G. It allowed data to be sent through a packet switching technique where there is no reservation for channel while the user is not using it. In GPRS, the information is partitioned into small packets to be sent to the transmitter, then it reassembles this information again at the receiver. GPRS offers data rates up to 171.2 *kbps*. This can be achieved using the weakest coding scheme which means the signal strength is maximum. It also uses four coding schemes depending on the channel estimation status [5]. Enhanced data rates for GSM Evolution (EDGE) represents the third stage of 2G improvements. It applies nine different coding schemes. These schemes are applied based on the channel estimation status. Also, EDGE applies either Gaussian Minimum Shift Keying (GMSK) or 8-ary Phase Shift Keying (PSK) modulation. Furthermore, each symbol is represented by three bits. This enables sending larger data per one time slot [6]. The data rates go up to 60 *kb* per time slot and up to 480 *kb* per eight time slots.

3G was designed to give mobile users high speed data rates. Moreover, 3G design offers multimedia services such as Multimedia Message Services (MMS) and video conferencing. 3G represents hardware and software upgrades of 2G and replaced certain components as well. For example, Base Transceiver Station (BTS) was replaced by eNodeB. Another example is Base Station Controller (BSC) which was replaced by Radio Network Controller (RNC). 3G promised to provide speeds of 144 *kbps* in the rural areas with high speed mobility. For the indoor areas with slow mobility, 3G promised to provide speeds of 384 *kbps*. Moreover, it promised to offer speeds of 2 *Mbps* for fixed applications such as home or office use [7].

There are two separate standards for 3G approved by the International Telecommunication Union (ITU). The first standard is Code Division Multiple Access 2000 (cdma2000).

This standard was established to be suitable for North America. The second standard is Universal Mobile Telecommunication Service (UMTS) which was established to work in countries that already have GSM networks such as European countries and Japan [8].

Later on, the 3.5G came into the picture. 3.5G is known also as High Speed Downlink Packet Access (HSPDA). HSPDA was suggested in Release 5 of the UMTS [9]. It represents software upgrade of UMTS. HSPDA had promised high data rates of 10 *Mbps* which is five times the UMTS promised data rates. In order to achieve these data rates, HSPDA has introduced several new technologies such as Adaptive Modulation and Coding scheme (AMC), fast cell selection, Hybrid Automatic Request (H-ARQ) and fast packet scheduling .

Fast packet scheduling is one of the main features that add extras to HSPDA. It manages the channels allocation. In addition, it determines which user is going to transmit during the current time interval. Furthermore, HSPDA considers the channel conditions and applies scheduling based on these conditions. In case of very good channel conditions, HSPDA gives the opportunity to use high level modulation schemes which offers high data rates as a result. Thereafter, High Speed Uplink Packet Access (HSUPA) was suggested in Release 6 for UMTS. It is called some times as 3.75G. It had introduced the HSPDA technologies for the uplink connection. HSUPA is able to support data rates up to 5.8 *Mbps* [10].

LTE stands for Long Term Evolution. It was developed by the Third Generation Partner Project (3GPP). In some references, the term LTE refers to the 4G of mobile communications [11]. In December 2010, the name 4G was given by the ITU to all releases of LTE. The name was given also to Worldwide Interoperability for Microwave Access (WiMAX) and any technology with "substantially better" achievement than that is achieved by 3G . LTE was designed to achieve several targets. One of these targets is to provide high data rates at the speed of 100 *Mbps* for downlink transmission and 50 *Mbps* for uplink transmission. Another target is to make LTE mainly packet switched domain. Furthermore, LTE developers aimed to reduce the cost and the power consumption. In addition to all, LTE was designed

to offer flexible and efficient spectrum utilization [3]. In order to achieve these goals, LTE included some key technologies that enabled LTE to reach these targets. These key technologies include Orthogonal Frequency Division Multiple Access (OFDMA) as multiple access for downlink, Single Carrier Frequency Division Multiple Access (SC-FDMA) for uplink communication, dynamic scheduling and Multiple Input Multiple Output antennas (MIMO). LTE has started with Release 8 and is now in Release 12. Each release has some new feature updates that are added to the previous one.

Release 8 has been actively introduced in December 2008. It includes group of key features and technologies that differentiate it from the earlier versions of mobile communication. The first key feature is the improvement of the spectrum efficiency. This is achieved by adopting the OFDMA for down-link and SC-FDMA for uplink connection. The second key feature is the provided high data rates which go up to 300 *Mbps* for downlink and up to 75 *Mbps* for uplink [12]. The third key feature is the packet based network. This feature avoids the cost and the complexity that come along with the circuit switched networks. Release 8 has implemented some key technologies in order to offer these features. The first key technology is the implementation of OFDMA for down-link and SC-FDMA for up-link. The second one is the support of spatial multiplexing via MIMO technique. The third one is that, Release 8 has faster physical layer control mechanisms.

Release 9 is actually a completion of Release 8. Some specifications were targeted in Release 8 but were not finalized. One of these specifications is evolved Multimedia Broadcast/Multicast Services (eMBMS). Another specification is the Location Services (LCS) which is also known as Location Based Service (LBS) [13]. This service enables an application to detect the geographical position of the mobile. Furthermore, Release 9 has added enhancement for beamforming techniques.

Release 10 LTE-Advanced supports peak data rates of 1 *Gbps* for downlink and 500 *Mbps* for uplink. Moreover, it supports mobility up to 350 *km/h* and for some bands up to 500 *km/h*.

In this Release, the Multimedia Broadcast/Multicast Services (MBMS) is improved compared to Release 9. The key features of Release 10 is the support of so called carrier aggregation. Carrier aggregation can be defined as the aggregating number of carriers of the same or different bandwidths to increase the total bandwidth for one user. Each carrier is called carrier component. LTE-Advanced permits User Equipment (UE) to aggregate up to five carrier components with maximum bandwidth of 20 MHz for each [14]. This gives each UE ability to collect 100 MHz as maximum aggregated bandwidth. There are other key features for up-link such as clustered SC-FDMA. The clustered SC-FDMA means the adoption of Discrete Fourier Transform Spread OFDMA (DFT-S-OFDMA). DFT-S-OFDMA differs from SC-FDMA in the sense that it enables the allocation of non-contiguous groups of sub-carriers for single UE.

The main key advantages of Release 11 are Coordinated Multipoint transmission and reception (CoMP), enhanced physical downlink control channel, elimination of the interference among different radio access techniques, mobile data communication enhancement and machine type enhancement [15]. The working principle is, as the mobile get closer to the cell edge, the serving cell signal becomes weaker while the interfering signals coming from the neighboring cell becomes stronger. Using CoMP, neighboring antennas contribute to increase the received power at the cell edge, decreasing the interference and raising the collected data rates. There are many techniques to implement CoMP. One of these techniques is known as Coordinated Scheduling/Beamforming (CS/CB). In CS/CB, only one point can transmit which is selected via regular handover scheme and is periodically changed. Scheduling decisions of the neighboring points are coordinated to minimize the interference that they are transmitting to the destination mobile. This can be done by sending different resource blocks. The beamforming decisions can also coordinate among the neighboring points. There are other techniques to implement CoMP such as Joint Processing.

Release 12 presents some new features in order to enhance its performance. These features include dynamic adaptation of the TDD, enhancement of machine-type communications, enhancement of mobile data applications, and device-to-device communications [16].

Release 13 has three main technology classes [17]. The first class is the Full Dimension MIMO (FD-MIMO) which is placed to enhance the spectral efficiency. The second class includes the utilization of new frequency resources such as Licensed Assisted Access (LAA) for using unlicensed spectrum. The third technology class includes supporting of new services such as MTC.

Release 14 features [18] include introducing the usage of the latency reduction techniques, enhancing the work on the unlicensed spectrum, the enhancement of the MTC, using of massive multi antenna systems which includes high resolution feedback, introducing dynamic measurements of the reference signals (CSI-RS) allocation and better usage of the reference signal resources. Release 14 features include also the enhancement of the eMBMS services, and enhanced positioning.

In this research, we have proposed novel concepts and techniques that can be implemented in the coming generations of the wireless mobile communications. These concepts and techniques will significantly improve the already provided data rates.

## **1.2 Literature Review**

### **1.2.1 Direction of Arrival**

The present DOA algorithms are capable of figuring out the directions of the incoming signals. However, they cannot distinguish the desired user signal direction from the interferers. The DOA techniques can be classified into four categories [19]. The first category is the conventional techniques where the beamforming and null steering are used to estimate the DOAs. The DOAs of the incoming signals are estimated by doing a search on the output

power spectrum to find the power peaks. These peaks are used to determine the DOAs of the incoming signals. Capon's minimum variance is an example of the conventional techniques. The second category is subspace based techniques. These techniques build the DOA estimation based on the received data. There are two main algorithms of this category [20]. The first algorithm is the MUSIC algorithm which is based on the decomposition of the eigenvalues of the estimated correlation matrix of the received signal into signal subspace and noise subspace, then the noise subspace is used to estimate the DOAs [21]. The second algorithm is the ESPRIT algorithm which use the signal subspace to estimate the DOAs [22]. The third category is the Maximum Likelihood (ML) techniques. These techniques have high computational complexity which make them less popular. ML techniques have advantages over other techniques when the Signal to Noise Ratio (SNR) levels are low, and the signals are highly correlated. The last category is the integrated techniques which mix the subspace-based techniques with the property of rest-oral.

The accuracy of the DOA algorithms have been studied in many research articles. In [23], a comprehensive study had been performed on several DOA algorithms. The comparison is carried out between the assumed transmitted directions and the estimated directions using different DOA algorithms. In [24], the authors have studied the relationship between the system resolution and the mean square error. In [25], the authors have studied the DOA accuracy in the presence of unknown mutual coupling coefficients. Furthermore, they have developed an algorithm to estimate the mutual coupling coefficients. In [26], the authors have used the MUSIC algorithm to find the DOAs of the coming signal replicas received by the mobile station in order to place nulls in the direction of interferers. This scheme is proposed to work in an indoor environment. In [27], the multi-path components are used for position estimation purpose through considering the time difference of the arrival between these components. In [28], an evaluation of the MUSIC and ESPRIT algorithms is performed. This evaluation is carried out using different parameters such as the number of mobile users and the number of

time samples acquired.

The transmission of the reference signals between the base station and the user is very vital in mobile communications. It has been adopted by the Long Term Evolution (LTE). The reference signals can be described as a predefined signal (sequence of bits) known by the transmitter and the receiver. In addition, the reference signals utilize a predetermined resource elements. There are two main types of the reference in LTE [29]. The first type is the down link reference signals. These signals provide the mobile with the amplitude and phase reference to estimate the Channel Status Indicator (CSI) and calculate the Channel Quality Indicator (CQI) consequently. The second type of the reference signals is the up-link reference signals. This type of reference signals are used in channel estimation procedure done by the base station. The APA algorithm is attractive mainly for its fast convergence rate, fast tracking, and low steady state. It uses the Mean Square Error (MSE) method to reduce the error of intercepting the transmitted signal caused by the noise and the channel fading [30]. The corrupted signal passes through a filter that tends to suppress the noise while leaving the signal unchanged. The comparison with the classical adaptive filter algorithms such as LMS and Recursive Least Square (RLS) shows that the APA provides a good performance in the presence of noise and fading effect [31]. The APA is better attenuative than Normalized Least Mean Square (NLMS) in applications where the input signals are highly correlated . The APA updates the weights based on the current and previous input vectors while NLMS updates the weights based only on the current input vector.

### **1.2.2 Adaptive Beamforming Algorithms**

Adaptive beamforming is the key feature of the smart antennas. The basis of the adaptive beamforming is to find out the optimum weights of the antenna elements by implementing one of the adaptive beamforming algorithms. These weights are calculated such that they adjust the main lobe of the antenna towards the desired direction and suppressing the interfering

signals. In [32] [35], a new adaptive array beamforming algorithm is proposed, studied and evaluated. This algorithm is called Recursive Least mean Square Algorithm (RLMS). It is composed of Recursive Least Square (RLS) stage followed by LMS stage. The implemented combination shows better results than if LMS or RLS are implemented separately. Nevertheless, the complexity still exists. Furthermore, the execution time is longer.

In [36] [38], the authors implemented two algorithms. Each one of these algorithms is composed of two LMS stages with some differences between the two algorithms. The first algorithm is called LLMS and the second one called LMS-LMS. The results show rapid convergence within a small number of iterations. However, in this algorithm, the complexity is about the double of LMS algorithm of one stage. In [39], the authors have analyzed the performance of four different adaptive algorithms. These algorithms are LMS, Recursive Least Square (RLS), Conjugate Gradient Method (CGM), and Kalaman based normalized LMS algorithms. They have found that, the LMS algorithm offers the best results in terms of the beamforming pattern. Nevertheless, it has slow convergence which strongly depends on the step size. Furthermore, they have shown that, the RLS algorithm has a faster convergence among all of the algorithms under test. However, in RLS, the side lobes are not completely removed. In addition, the CGM algorithm gives a better beamforming pattern. The authors have suggested the Kalaman based normalized LMS algorithm as the most suitable one for wireless communications. In this thesis, we introduce the use of the scheduling based on beamforming in the whole cell area rather than at the cell edges. The optimized algorithm starts with finding the direction of the users, then, we feed the results to the LMS algorithm to generate beams in the directions of the desired users, nulls in the directions of interfezers, and keep tracking of the users in the cell.

### 1.2.3 Scheduling

The scheduling is about managing the allocation of the available resources in an efficient manner. The scheduling is performed to enhance the spectral efficiency and the aggregated data rate of each user. As a result of multiuser diversity, the channel quality may differ from user to user due to the multipath transmission. Also, for a single user, the channel quality may differ from time to time due to the users' movement. Therefore, the scheduling rules should be performed according to the channels quality status. In general, a scheduler tends to maximize the system efficiency by distributing all available resources to the well-suited users while keeping a proportional fairness among them. In addition, any scheduler is trying to satisfy the QoS requirements of dissimilar traffic flows along with maximizing the system capacity and aggregate data rates. The scheduling based on beamforming is applied partially in LTE in Releases 11,12, and 13 [29]. This is done through the cooperation between the different antennas in the adjacent cells. This property is called Coordinated Multipoint transmission and reception (CoMP). CoMP means that the neighboring antennas take their scheduling decisions in a way that increases the power towards the desired user and decreases the interference. In [40], an algorithm that implements the joint orthogonal beamforming and scheduling in Multiple Input Multiple Output (MIMO) antennas is proposed. The scheduling is done through finding the sets of the orthogonal weighting vectors via performing an exhaustive search. In [41], an opportunistic beamforming is introduced in order to rise up the overall throughput. In [42], the authors have studied the advantages of implementing coordinating transmission schemes. In [43] [45], the authors have considered that every node is provided with a SA, digital beamforming, and space division multiplexing capabilities. The proposed cross layer frame work is designed to operate for the last mile internet connection in wireless mesh networks. They also have used the integer linear programming to get to the optimum solution. The authors mainly have divided the nodes into logical groups such that these nodes can work together without causing any interference.

The utility function is a measure of the satisfaction. The satisfaction might be analyzed in terms of the users satisfactions or in terms of the QoS requirements. In [46], the scheduling is done based on the satisfaction characteristics of five classes of services. In this paper, we consider only two classes of services which are the Delay Sensitive (DS) and Non Delay Sensitive (NDS) classes .

#### **1.2.4 Frequency Reuse**

The number of mobile subscribers is increasing exponentially. Furthermore, the need for high QoS applications has become fundamental. These days, mobile subscribers are asking for more applications with high quality such as the video conferencing, and high quality TV [47]. These applications require a high bandwidth while the available bandwidth is very limited. The key element to fulfill this exponentially increasing demand is by implementing an efficient frequency reuse plan that can meet this increasing demand. In the mobile cellular networks, there is always a difficulty in choosing a proper frequency reuse plan that can satisfy the required QoS of the mobile users. The Inter Cell Interference (ICI) represents the main challenge of any implemented frequency reuse scheme. Large ICI values lead to small SINR values at the cell edges [48].

The earliest mobile networks were built based on using a single high transmitting antenna with maximum power that might cover the intended coverage area. In contrast, the 2G of the mobile communication networks is built based on splitting the entire coverage area into small subareas called cells. Each cell has a low power transmitter that might cover it. The cells are grouped into sets called clusters. The whole available bandwidth is divided between the cells of each cluster. Then, it is reused per cluster [49]. The simplest frequency reuse plan is achieved by reusing the available frequency band by factor of  $1/m$ , where  $m$  represents the number of the cells in the cluster. Figures 1.1(a), and 1.1(b) illustrate the frequency reuse plans of frequency reuse factor equal to  $1/3$  and  $1/7$  respectively. The third generation (3G)

of the mobile communication networks uses the Code Division Multiple Access (CDMA) as multiple access technique. This keeps the ICI is minimum [29].

Although, these frequency reuse plans offer a very acceptable ICI values, they repre-

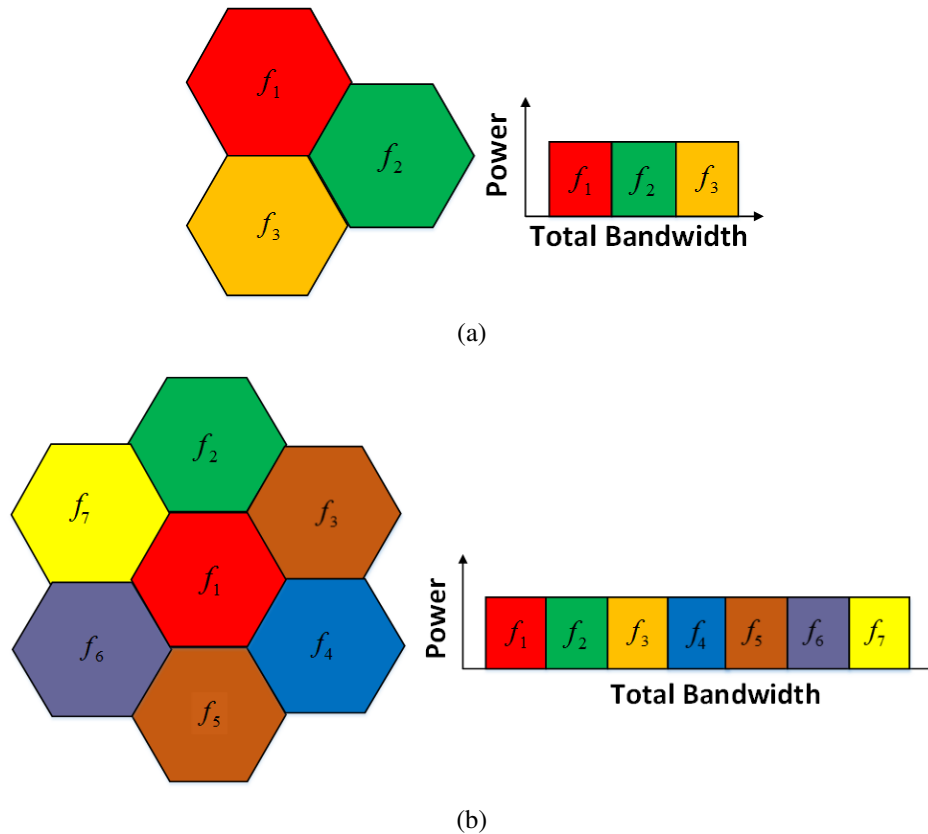


FIGURE 1.1: (a) Frequency reuse-3 model in GSM, (b) Frequency reuse-7 model in GSM

sent a large capacity loss and poor spectrum efficiency usage. This loss is by factor of  $1/m$ . LTE has adopted the OFDMA as a radio access technique along with the advanced antenna technologies [50]. Since the conventional cellular mobile networks struggle from the poor spectrum efficiency, LTE aims to implement a frequency reuse plan of frequency reuse factor equal to one to achieve higher capacities. Inter-Cell Interference Coordination (ICIC) is a technique where each cell allocates its resources in a way that improves the whole network performance. Fractional Frequency Reuse (FFR) is an ICIC technique introduced for OFDMA based wireless networks [51]. The concept of the FFR is based on dividing each

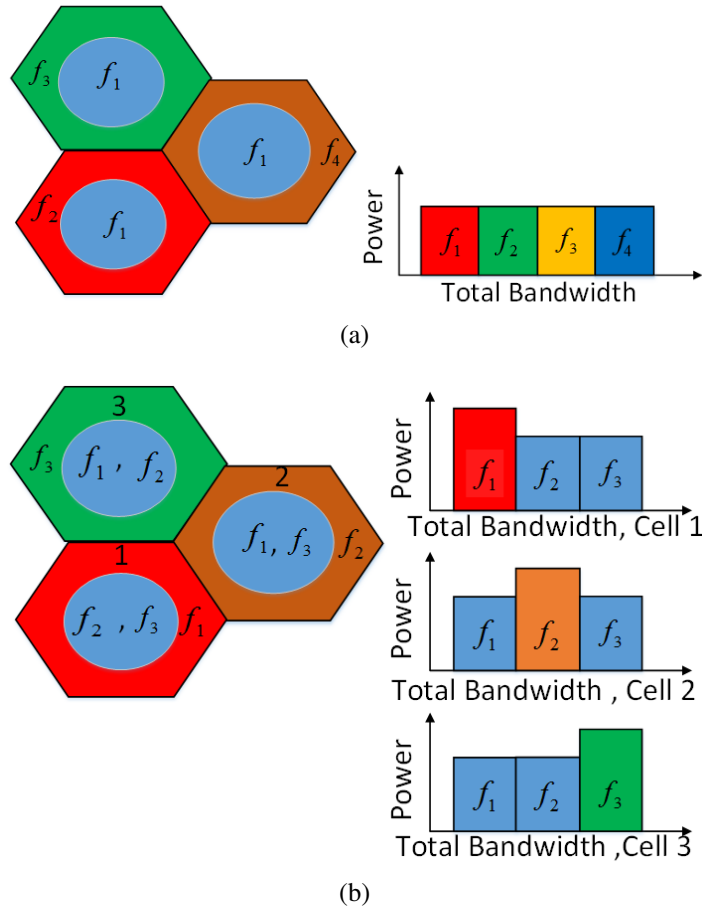


FIGURE 1.2: (a) Strict FFR technique, (b) Soft FFR technique

cell into two parts, inner part and outer part. The available bandwidth is allocated in a way that the cell-edge users do not interfere with each other. The FFR has two modes, Strict FFR mode and Soft FFR mode [52]. In the Strict FFR mode, the available bandwidth is partitioned into two sub-bands. The first sub-band is allocated to the inner part of each cell in the cluster with frequency reuse factor equal to one. The second sub-band is allocated to the outer parts of the cells in the cluster with a frequency reuse factor equal to  $1/m$ . Figure (1.2)(a) shows the Strict FFR of reuse factor equal to one for the inner parts and frequency reuse factor equal to  $1/3$  for the outer parts.

In the Soft FFR, the available bandwidth is divided into sub-band groups [53]. These groups are allocated between the inner and the outer parts of the cluster cells in a way that

keeps the ICI is minimum and the frequency reuse factor equal to one. This is illustrated in Figure (1.2) (b).

### **1.2.5 Fifth Generation of Mobile Communications**

5G represents the next generation of mobile communications. It is supposed to provide high data rates to the mobile users. These rates are expected to be in the range of tens of gigabits per second (Gb/s) [54]. There are five main research directions in the way towards the 5G. These directions include millimeter waves, massive MIMO, full duplex, small cells, and beamforming [55]. The millimeter waves (mm Wave) are in the range of 30 Ghz [56]. In this range, there are greater bandwidths available to be utilized. In the massive MIMO direction, the base stations are equipped with an extensive number of antennas [57]. These antennas are used to simultaneously serve large number of co channel users. The full duplex direction refers to using transceivers that can transmit and receive at the same time [58].

The smaller cells direction is used to increase the overall system capacity. The small cells are referred to as pico and femto cells with ranges of 10-200 m [59]. The authors in [60] have combined the femto cell with the relay mobile in one concept called Mobile Femto (MFemto) cell. Since the wireless users spend 80% of their calling times in the indoor areas while they spend 20% of their calling times in the outdoor areas, the authors in [61] have proposed to separate the indoor and outdoor users in two different scenarios in one potential cellular structure. This increases the overall system complexity. The beamforming research direction refers to using beamforming techniques in order to identify the best data delivery route for a specific user, in addition to decrease the interference coming from nearby users [62]. Applying the beamforming techniques might significantly enhance the system capacity, decreases the interference, and reduces the power consumption which satisfies the 5G needs [63]. In [64], the authors have designed a three dimensional beamforming by appending the vertical beamforming along with the horizontal beamforming. However, this technique can

not adapt with the users movements. In [54], the authors have studied the three dimensional beamforming as a promising technique for 5G. They have shown that the three dimensional beamforming may increase the data rate of each user and reduces the inter-sector interference. The authors in [65] have proposed a real time three dimensional hybrid beamforming technique for 5G. This proposed technique includes implementing of large scale antenna arrays at small cell.

Increasing the system capacity and efficiently utilizing the available resources represent one of the most challenging issues for 5G. An efficient FR plan is required to significantly increase the system capacity in a bid to fulfill the 5G high data rate requirements. Designing an appropriate FR plan for 5G is a hard task to do. This is because any suggested FR plan should meet the exponentially increasing demand on data and the limited available bandwidth. In [66], the author has mentioned the soft FR as one of the most powerful tools for increasing the system capacity in 5G. He proposed a multi-level soft FR and resource allocation scheme in order to increase the spectral efficiency at the cell edge. In [67], the authors have addressed the spectral efficiency demands for 5G. They have suggested a method for clustering, FR, and resource allocation for 5G. They have proposed to deal with each apartment in a building as a femto cell, then they apply the FR based on this assumption. In [68], a new resource allocation for heterogeneous networks is introduced. Instead of dividing the standard cells into inner part and outer parts as its applied in the recent releases of the LTE, the authors have divided each standard cell into a number of parts. Although the authors in [66 - 68] have considered the ICIC, they did not put a mechanism on how to handle the handover. In 5G proposals the emphasis is on cell-free operation and full FR. In order to implement full FR or even dense FR, other enabling technologies have to be used. One of these techniques is the digital beamforming which represents one of the fundamental technologies for 5G networks.

### 1.3 Objectives and Contributions

The number of subscribers in mobile communications is growing exponentially. There is an increase in both, the number of users and the quality of services that users are asking for. This exponential growth has put a lot of pressure on the operators to meet this highly increasing demand. This is happening while the available resources are limited.

The main objective of this thesis is to efficiently use the available bandwidth and increase the number of the mobile users. The SDMA is a fundamental scheme that can enable reusing of the same channels among different users in the cell. To implement the SDMA efficiently, it is required to identify the users positions in the cell. The existing DOA algorithms are able to estimate the directions of the incoming signals. However, they can not declare which signal belongs to which user and identify the desired users directions consequently.

The first contribution of this research is the introduction of the DOA algorithms to the cellular system [69]. The DOA algorithms themselves can give only estimations to the directions of the coming signals. However, they can not distinguish which one is the desired user signal and consequently they can not recognize the desired user direction. Using a RFS known by the transmitter and the receiver and applying the correlation concept, the proposed scheme enables the DOA algorithms to recognize the desired user signal and the desired user direction.

The second contribution of this research is to practically implement the adaptive beamforming algorithms [70]. By using the first contribution and providing the initial information to the adaptive beamforming algorithms, we enable the adaptive beamforming algorithms to converge much faster and work at high levels of interference and very low levels of SINR .

After knowing the direction of the desired user and proving the capability of tracking, we have proposed to feed this information to the proposed optimal scheduler. This represents the third contribution of this research.

The fourth contribution of this thesis is introducing the implementation of the synthesizing techniques along with the adaptive beamforming algorithms. This has allowed us to make an efficient control on the shape of the radiation pattern and send deep nulls towards the interferers.

The fifth contribution is the introduction of an efficient FR plan based on the knowledge of the desired users and the interferers directions. We have built up the proposed FR plan according to the SINR worst case scenarios.

## **1.4 Organization**

This thesis is organized as follows. In Chapter 2, we give a background about the antennas, digital beamforming, and the multiple access in frequency domain. In Chapter 3, we introduce the direction of arrival algorithms for the user identification in the cellular networks. The proposed beamforming tracking algorithm MLMS is presented in Chapter 4. Chapter 5 includes the proposed scheduling scheme. In Chapter 6, we introduce an efficient frequency reuse plan based on beamforming. Finally, Chapter 7 includes the conclusion and the possible future work.

# Chapter 2: Background

In this chapter, we present a background about the subjects that are used in this thesis and related to our research work. The first section includes an overview of the antennas, then we illustrate the beamforming concept and types. Finally, we briefly describe the LTE multiple access techniques in frequency domain.

## 2.1 Antennas

The antenna is an electronic device that converts the waves from the electric form to the electromagnetic form at the transmitter. The opposite process is applied at the receiver. The antenna radiation mechanism is explained in Figure (2.1). This figure shows that, in the first stage of the Alternating Current (AC), there are electric field lines formed by the electric charges. When the polarity is converted due to the change of the AC signal, there will be new electric field lines formed and the previous ones will be propagated. The same result can be achieved through the bending of the electric wires to change the acceleration of the electric charges movements.

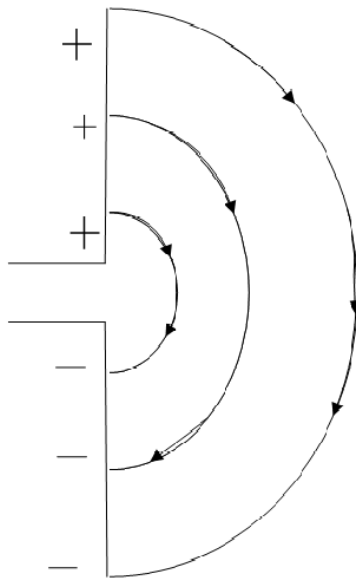


FIGURE 2.1: Antenna Radiation Mechanism

The propagation of electromagnetic waves takes the form of so called antenna radiation pattern. The antenna radiation pattern can be defined as the geographical representation of its radiated power.

In very brief, the antennas can be classified according to their radiation pattern into three categories, the first category is the omnidirectional antennas which radiate the same amount of power in one plane, the second category is the directive antennas which focus their radiation in a certain direction, while the third category is so called isotropic antennas. The isotropic antennas radiate the same amount of power in all planes. This class represents an ideal case which does not exist in the reality. It is used as a mathematical reference for comparison.

### 2.1.1 Principle of Array Antennas

The array antennas are designed to have directive radiation patterns (high gain) to satisfy the higher requirement of wireless communication. The array antenna is composed of a set

of identical radiating elements. These elements are arranged in an electrical and geometrical form. The array antenna elements are all active in some configurations. In other configurations, there are some elements which are passive. They work mainly as directors.

The array elements can be arranged in linear, planar, and circular geometric configurations. The superior geometric configuration for wireless applications is the planar configuration because it enables the array antenna to scan in three dimensions.

### 2.1.2 Two Elements Antenna Array

The two elements array antenna is the basic antenna array. This antenna is composed of two dipoles. These dipoles are placed vertically to y axes as shown in Figure (2.2).

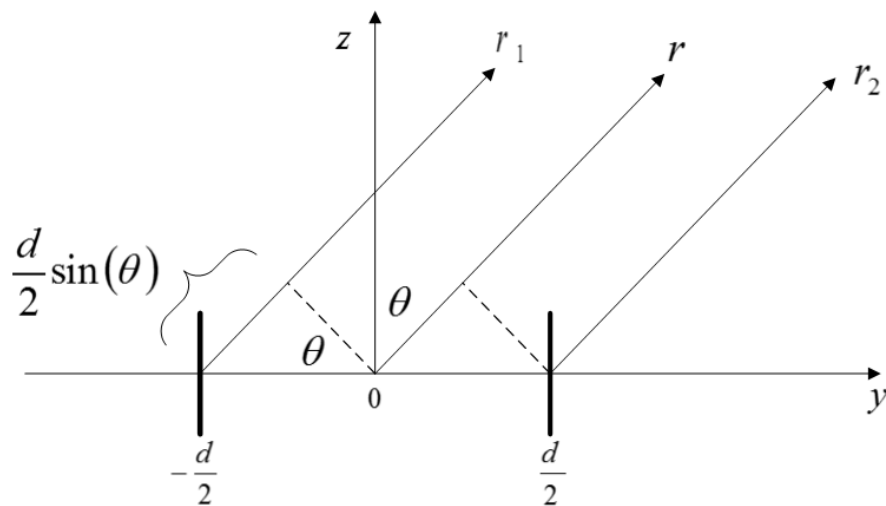


FIGURE 2.2: Two element antenna array

They are separated by distance  $d$ . The electric field is calculated at the distance  $r$  from the origin, where  $r$  is  $\gg d$ .

The vectors  $r_1, r_2$  and  $r_3$  are assumed to be parallel to each other.

$r_1$  and  $r_2$  can be defined approximately as:

$$r_1 = r + \frac{d}{2} \sin(\theta) \tag{2.1}$$

$$r_2 = r + \frac{d}{2} \sin(\theta) \quad (2.2)$$

assuming that,  $I_0 e^{-j\frac{\beta}{2}}$  and  $I_0 e^{+j\frac{\beta}{2}}$  are the phasor elements of element one and two respectively [19].

Further, it is possible to assume:

$$r = r_1 = r_2 \quad (2.3)$$

$$E_\theta = \frac{jk\eta I_0 e^{-j\frac{\beta}{2}} L \sin(\theta)}{4\pi r_1} e^{-jkr_1} + \frac{jk\eta I_0 e^{+j\frac{\beta}{2}} L \sin(\theta)}{4\pi r_2} e^{+jkr_2} \quad (2.4)$$

$$E_\theta = \underbrace{\frac{jk\eta I_0 L e^{-jkr}}{4\pi r}}_{\text{Element Factor}} \sin \theta \underbrace{\left( 2 \cos\left(\frac{kd \sin \theta + \beta}{2}\right) \right)}_{\text{Array Factor}} \quad (2.5)$$

The radiation pattern of the array antenna can be obtained by multiplying the Array Factor (AF) with the Element array Factor (EF).

The Radiation Density is given by:  $U(r, \theta, \phi) = \frac{r^2}{2\eta} \bar{E}_s(r, \theta, \phi)^2$ . By substituting and normalizing, we get the following equation:

$$U_n(\theta) = [\sin \theta]^2 \cdot \left[ \cos\left(\frac{\pi d}{2} \sin \theta + \frac{\beta}{2}\right) \right]^2 \quad (2.6)$$

### 2.1.3 N Element Linear Array Antennas (Uniform Amplitude and Spacing)

The linear array antenna is composed of N-identical elements with identical amplitudes and phases. Figure (2.3) depicts an example of N element array antenna. The output radiation pattern can be obtained by multiplying the field of a single element with the array factor of the isotropic elements. This is illustrated in Figure (2.4), where (a) represents the dipole pattern (EF), (b) represents the array factor pattern, and (c) represents the multiplication result.

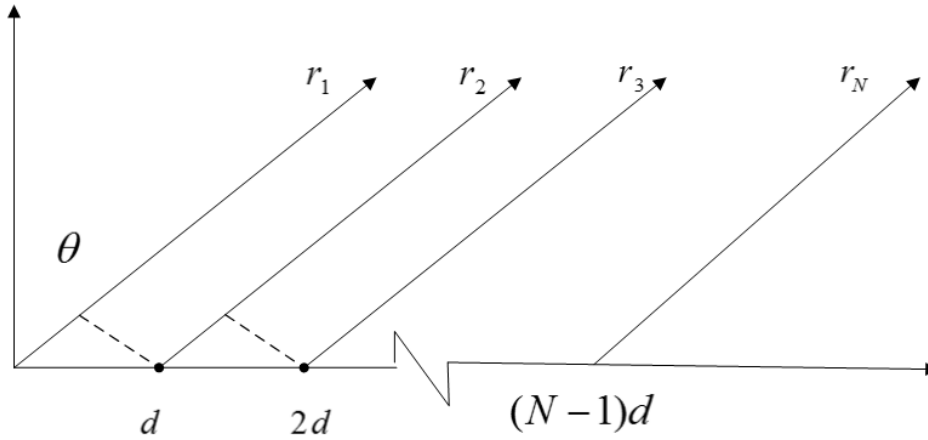


FIGURE 2.3: N elements antenna array

The array factor can be calculated as:

$$AF = 1 + e^{jkd \sin \theta + \beta} + e^{2jkd \sin \theta + \beta} + \dots + e^{j(N-1)kd \sin \theta + \beta} \quad (2.7)$$

$$AF = \sum_{n=1}^N e^{(n-1)\varphi} \quad (2.8)$$

where  $\varphi = kd \sin \theta + \beta$ . This can be further simplified and approximated as:

$$AF = \frac{\sin\left(\frac{N\varphi}{2}\right)}{\frac{N\varphi}{2}} \quad (2.9)$$

### 2.1.4 Smart Antennas

The smart antenna consists of antenna elements and digital signal processor. The purpose of smart antennas is to steer the antenna radiation pattern adaptively toward the desired direction. The capabilities of smart antennas are highly dependent on the implemented Digital

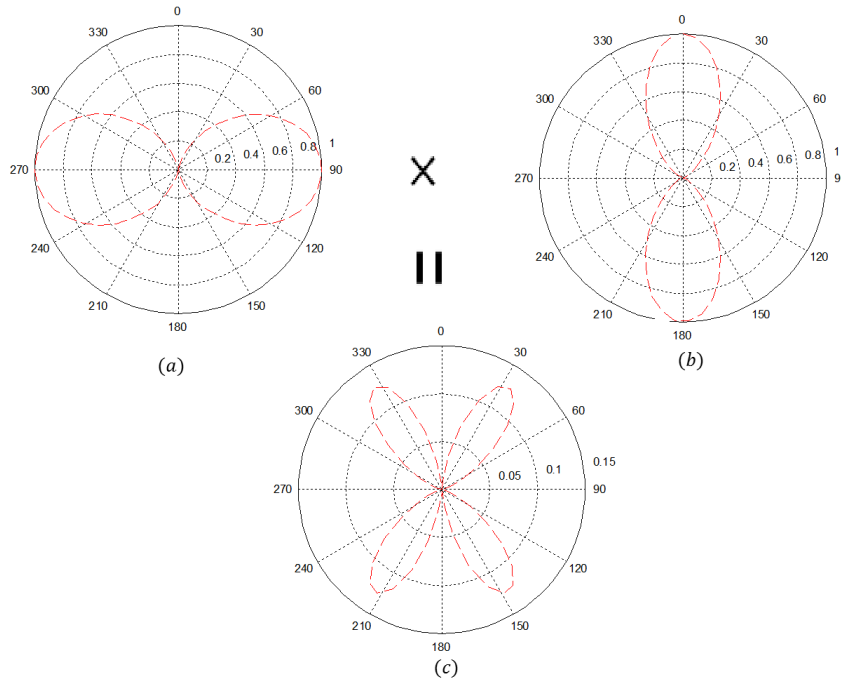


FIGURE 2.4: (a)Dipole Pattern,(b)Array Factor,(c)Multiplication Result

Signal Processing (DSP) algorithms. The smart antennas are designed to increase the radiation power in a certain direction while rejecting or nulling the signals that are coming from the undesired directions. This opportunity increases the overall wireless system capacity.

## 2.2 Digital Beamforming

The process of beamforming involves weighting of the input or output signals of the smart antenna in order to form the desired radiation pattern beam. This is done by down converting the signals into two baseband signals I and Q signals [71]. The forming of the beams is performed by adjusting the amplitudes and phases of I and Q signals. The adjustment is called the weighting process and the result is called the weighting vector. The digital beamformer is shown in Figure (2.5) where  $x(t)$  represents the input signal to be weighted,  $d(t)$  represents the training sequence,  $w$  represents the weighting vector, and  $y(t)$  is the desired output.

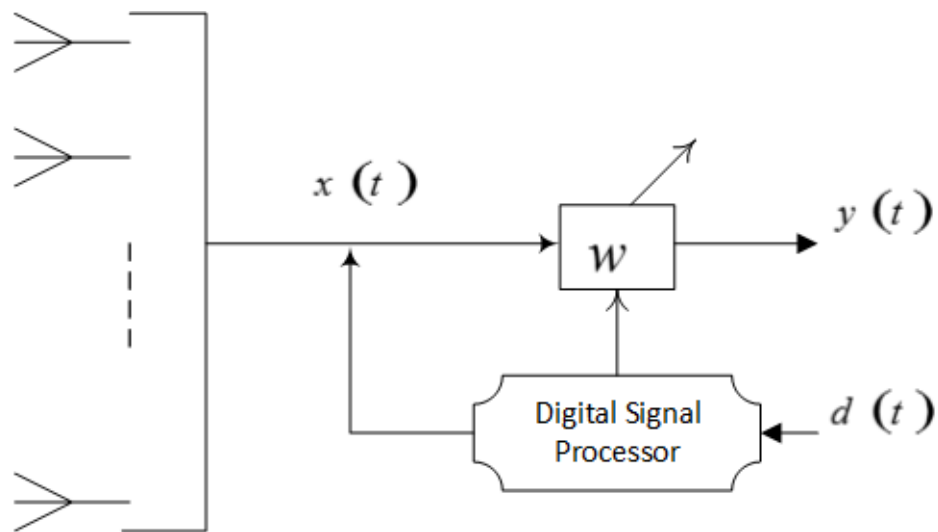


FIGURE 2.5: Digital Beamformer

The beamforming provides a great possibility to focus the signals toward the desired users. This gives the possibility of channels reuse in terms of the generated beams. Focusing the energy rises the SNR and significantly decreases the interference. In addition, the beamforming control is achieved via the DSP which means it is only software upgrade. This adds a large flexibility to the frequency reuse and much better efficiency to the scheduling procedures.

### 2.2.1 Switched Digital Beamforming

In this type of beamforming, there is a number of fixed predefined beams. The scheduling is done based on these beams. The beam's assignment is performed according to the user conditions. If the user conditions are changed, the system will assign the most appropriate available beam. This technique is relatively simple but it has some drawbacks. The first drawback is the existence of coverage gaps. This is shown in Figure(2.6).The second drawback is the large number of hand-offs that is required between beams during users movements.

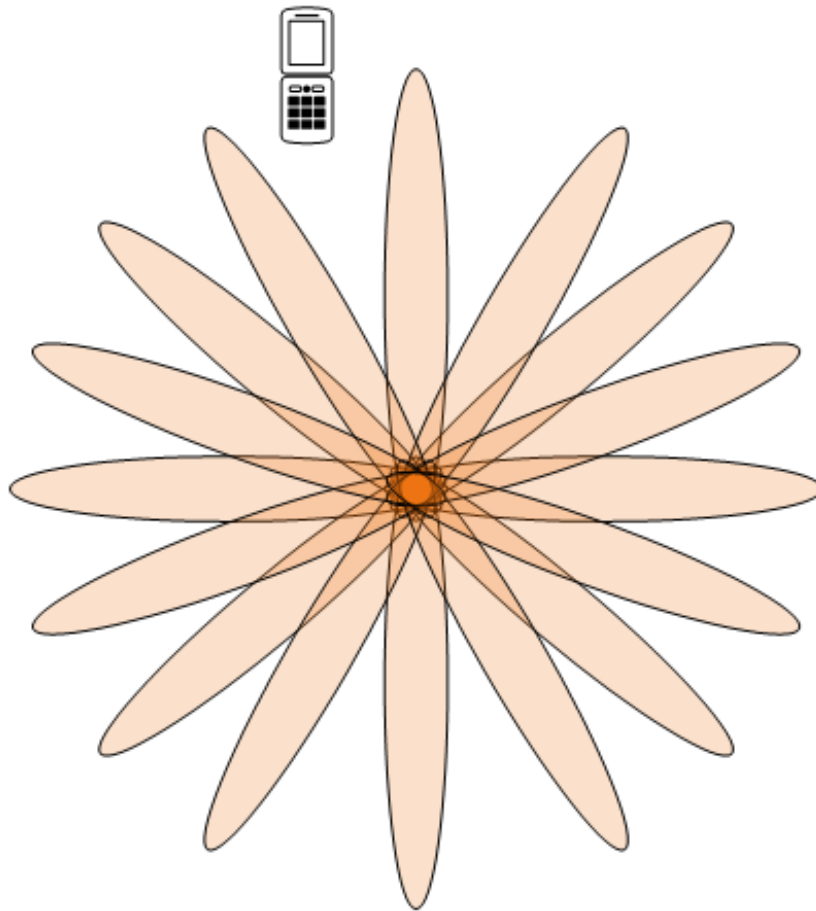


FIGURE 2.6: Switched Beamforming

### 2.2.2 Adaptive Digital Beamforming

In contrast to the switched beamforming, the adaptive beamforming generates the beams adaptively. This avoids the existence of uncovered areas. See Figure (2.7). Also, the adaptive beamforming does not require a large number of handovers. However, the efficiency of the adaptive beamforming is highly dependent on the implemented beamforming algorithms.

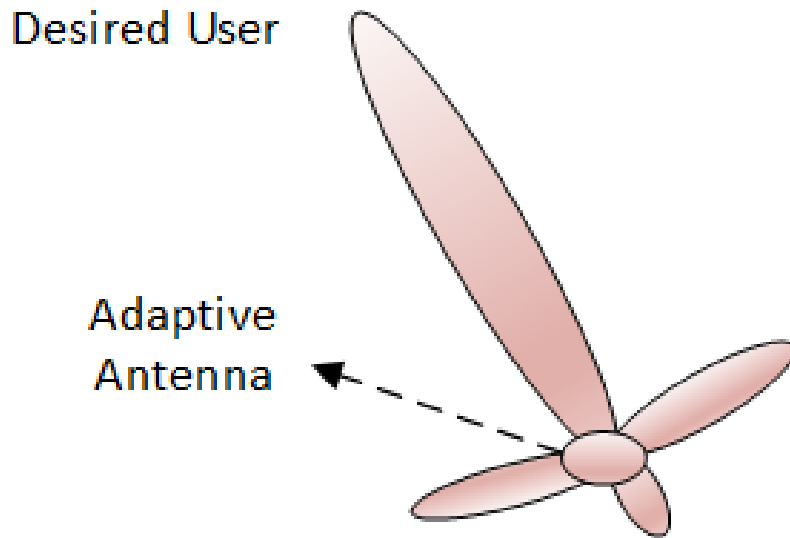


FIGURE 2.7: Adaptive Beamforming

## 2.3 Multiple Access in Frequency Domain

### 2.3.1 OFDM

OFDM stands for Orthogonal Frequency Division Multiplexing [72]. The working principle of OFDM is to break the higher data rate streams into several lower data streams. These lower data streams are transmitted concurrently over a number of subcarriers [73]. The term orthogonal means that, the subcarriers are orthogonal to each other. This gives the possibility to perfectly transmit and receive signals over a single channel without any interference. In other words, OFDM signals are sent in a way that the peak of one subcarrier occurs along with the nulls of the other subcarriers. Therefore, there will not be any interference between the subcarriers. The orthogonality concept is explained in Figure (2.8).

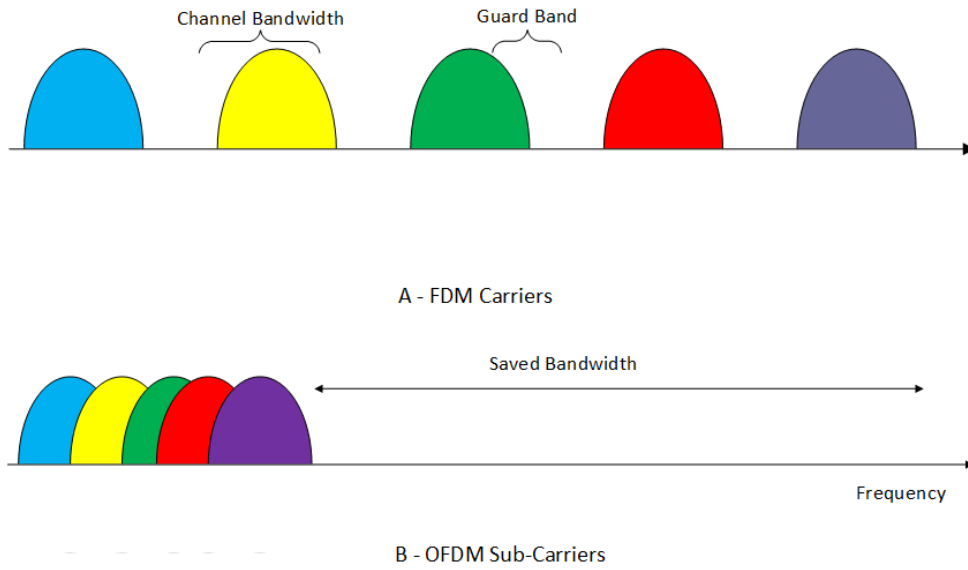


FIGURE 2.8: OFDM and FDMA Spectrum

The orthogonality principle can be expressed mathematically as:

$$\int_{-\infty}^{\infty} \varphi_i(t) \varphi_j(t) dt = 0 \quad (2.10)$$

where  $\varphi_i(t)$  and  $\varphi_j$  are any sub-carriers, and  $i$  and  $j$  are the sub-carrier numbers.

We consider only the period from 0 to  $T_s$ .

$$\int_0^{T_s} e^{2j\pi f_i t} e^{-2j\pi f_j t} dt = \int_0^{T_s} e^{-2j\pi(f_i - f_j)t} dt \quad (2.11)$$

$$\frac{e^{-2j\pi(f_i - f_j)t}}{-2j\pi(f_i - f_j)} \Big|_0^{T_s} = \frac{e^{-2j\pi(f_i - f_j)T_s} - 1}{-2j\pi(f_i - f_j)} \quad (2.12)$$

$$e^{-j\pi(f_i - f_j)T_s} \frac{\sin(\pi((f_i - f_j)T_s))}{\pi(f_i - f_j)} \quad (2.13)$$

Equation (2.13) is equal to zero if :

$$f_i - f_j = \frac{m}{T_s} \quad (2.14)$$

where  $m$  is any integer number, and  $f_i - f_j$  is the difference between any two subcarriers.

$$\Delta f = (f_i - f_j) = \frac{m}{T_s} \quad (2.15)$$

OFDM can be implemented using the block diagram shown in Figure (2.9).

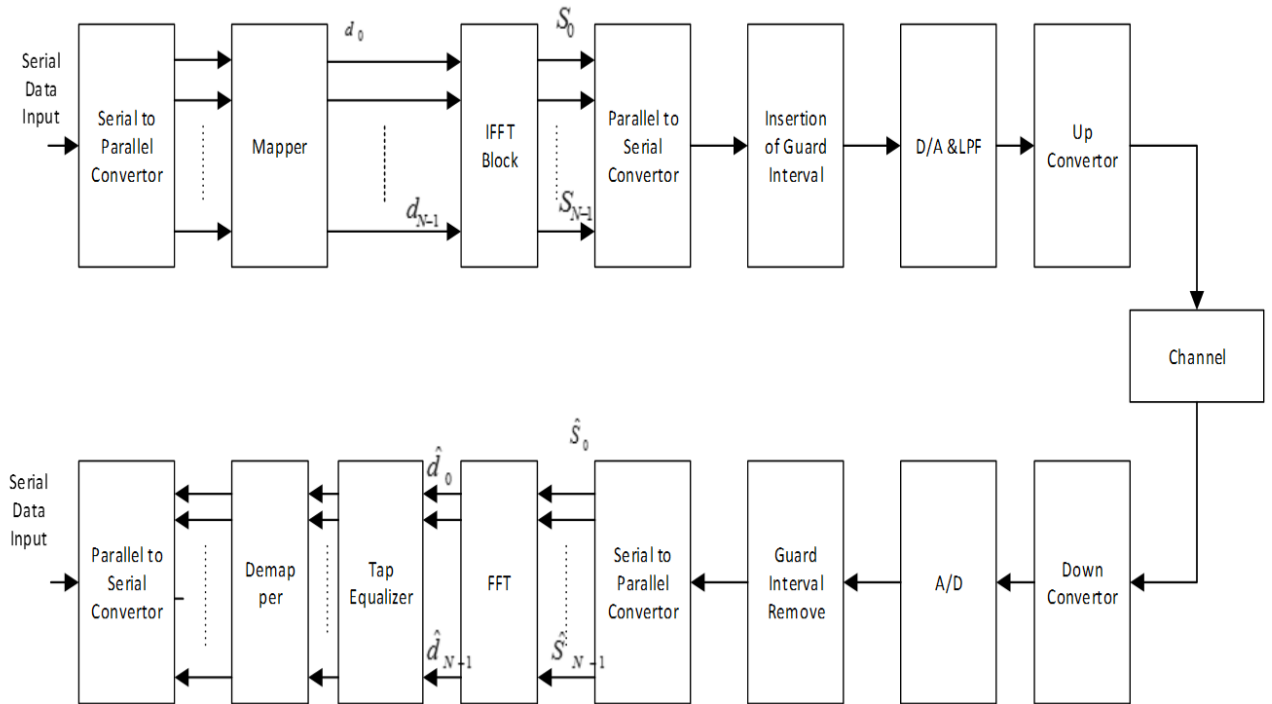


FIGURE 2.9: OFDM Block Diagram

There are two problems that appear during the transmission of signals through a dispersive channel. The first one is that, the channel dispersion eliminates the orthogonality between the subcarriers. This causes the inter carrier interference. The second one is the inter symbol interference between successive OFDM symbols. These two problems can be mitigated through the implementation of so called Cyclic Prefix (CP) insertion. The insertion of the CP is done by taking a copy of the last part of the OFDM symbol and insert it in the front part of the OFDM symbol. The CP duration is chosen to be greater than the estimated

maximum delay spread of the channel. This is shown in Figure (2.9).

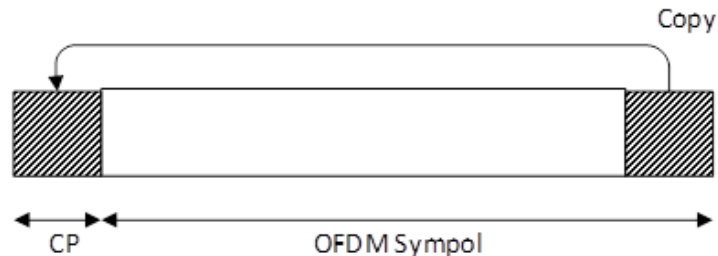


FIGURE 2.10: Cyclic Prefix Diagram

OFDM has several advantages over the other multiplexing techniques such as the improvement in spectral efficiency. This is gained because there is no need to insert a guard band between the subcarriers. In addition, OFDM is immune to the delay spread and multipath transmission. Furthermore, OFDM can resist the frequency selective fading, and it requires simple equalization. On the other hand, OFDM needs a high synchronization, it is sensitive to the carrier frequency offset, and the peak of the average power ratio is high [74].

### 2.3.2 OFDMA

OFDMA represents the multiuser version of the OFDM. It has been adopted by LTE as the 4G multiple access radio interface. OFDMA can be referred to as a combination of OFDM and TDMA.

In OFDMA, the available subcarriers are split into logical groups named as sub channels. Each logical group is composed of either contiguous or non-contiguous subcarriers. The allocation of the sub channels is done based on the channel conditions. OFDMA takes advantage of the multiuser diversity where different channels may have different conditions with different users. The channel diversity is shown in Figure (2.10). The allocation process is called scheduling. In contrast to the OFDM where one resource block is assigned to one

user, OFDMA allocates different sets of subcarriers to different users.

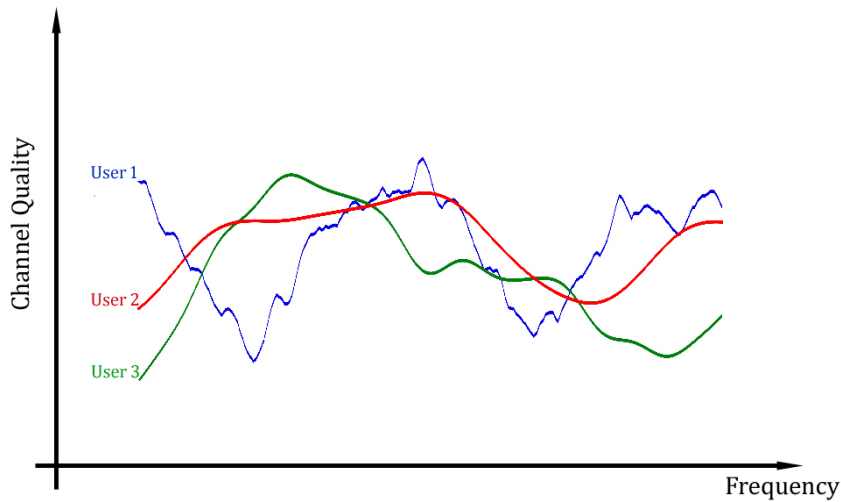


FIGURE 2.11: Users Diversity

The difference between OFDM and OFDMA is explained in Figures (2.11) and (2.12). These figures show that, the distribution of resource blocks is fixed in time for OFDM while it is varied in time in the case of OFDMA. Figure (2.13) clarifies that, in OFDMA, the distribution of the resource blocks is varied between the users in time.

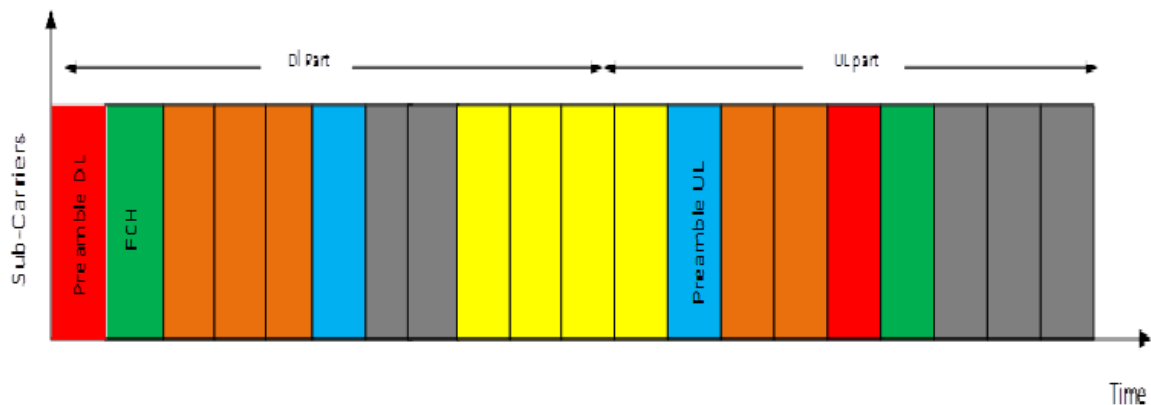


FIGURE 2.12: OFDM Resource Blocks

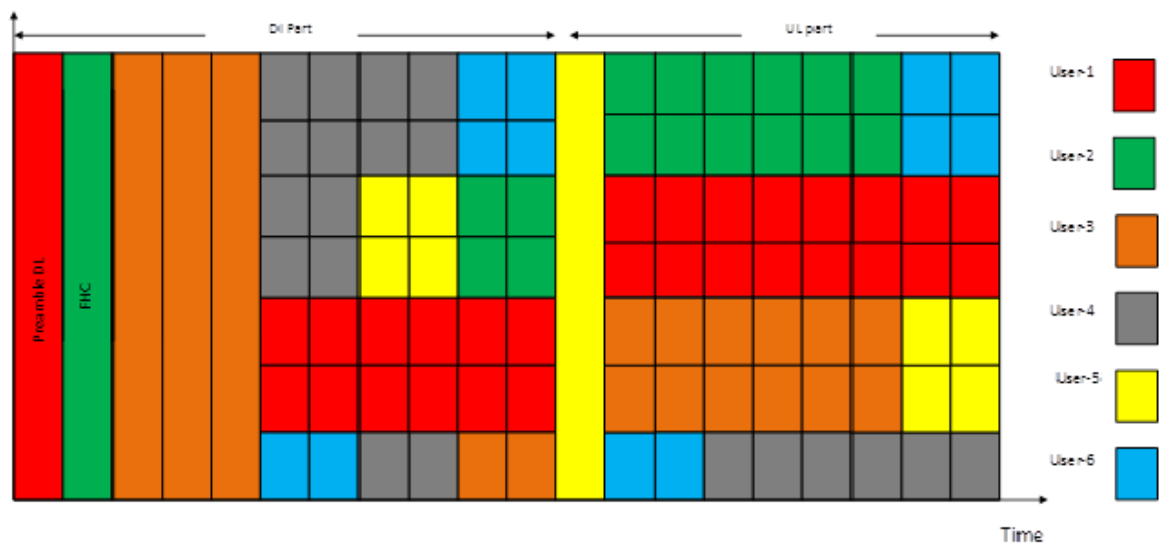


FIGURE 2.13: OFDMA Resource Blocks

OFDMA has some advantages over the other multiple access techniques. The first advantage is exploiting the frequency diversity through the allocation of distributed subcarriers to each user [75]. The second advantage is the implementation of the multiuser diversity. This is achieved by assigning a group of contiguous subcarriers that meet the best channel conditions of each user. The third advantage is the employment of the adaptive modulation and coding techniques. The last advantage is using simpler equalizers compared to the non-OFDM systems.

### 2.3.3 SC-FDMA

SC-FDMA is proposed by LTE as a multiple access technique in the uplink communication. It is suggested to overcome the drawbacks of OFDMA. The major drawback of OFDMA is the high Power Average Peak Ratio (PAPR) [76]. The PAPR appears due to the combination of several subcarriers together. This requires linear amplifiers at the transmitter. In the base station, it is possible to provide linear amplifiers. However, using these amplifiers at the

terminals leads to a shorter battery life due to the high power consumption. The block diagram of SC-FDMA is the same as the block diagram of OFDMA except there are two blocks that have been added [77]. These blocks are Discrete Fourier Transformer (DFT) and Inverse Discrete Fourier Transformer (IDFT) respectively. The first block distributes the time symbols over all the assigned subcarriers. DFT block spreads the information of each symbol between all the subcarriers before mapping them. This reduces the PAPR. At the receiver, the opposite process is applied where IDFT block is added right after SC-Demapping block.

# Chapter 3: Direction of Arrival

## Algorithms for User Identification for 5G

In this chapter, we introduce a mechanism to apply the DOA algorithms in the cellular mobile communication systems. Our proposed mechanism makes it possible to identify the direction of each user in the cell, track the users while they are moving in the cell, and consequently implement the SDMA optimally. This chapter includes signal model, proposed system model, simulation results, and the conclusion.

### 3.1 Direction of Arrival Algorithms

Consider Figure 3.1, if a source signal impinges on array element  $(i - 1)$  with angle of  $\theta$ , this signal will arrive at element  $i$  with delay equal to [78]:

$$\Theta_i = \frac{(i - 1)d \sin(\theta)}{c} \quad (3.1)$$

where  $c$  is the speed of light and  $d$  is the spacing between the antenna elements.

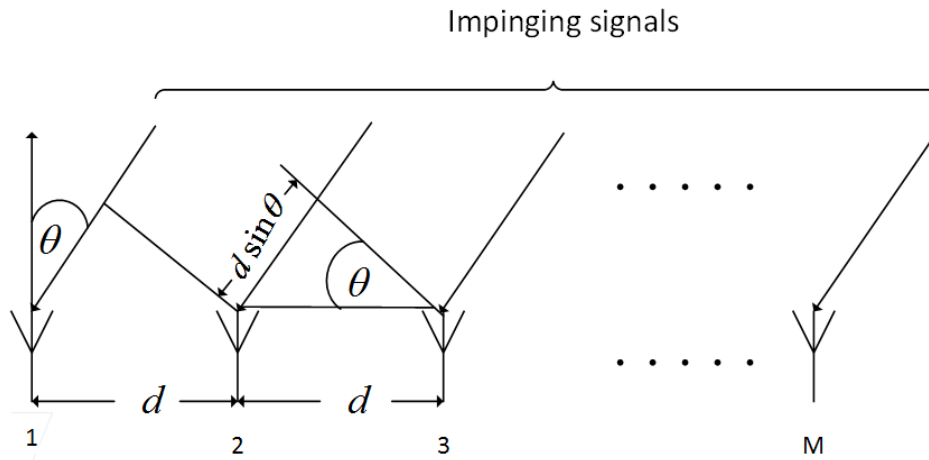


FIGURE 3.1: N Element Uniform Linear Antenna

Figure 3.2 shows a ULA composed of  $M$  elements. Consider  $D$  number of signals are arriving at the antenna. Assume each signal is taking as snapshots composed of  $K$  number of samples. The snapshots are taken at different instants of time  $t_1, t_2, \dots, t_M$ .

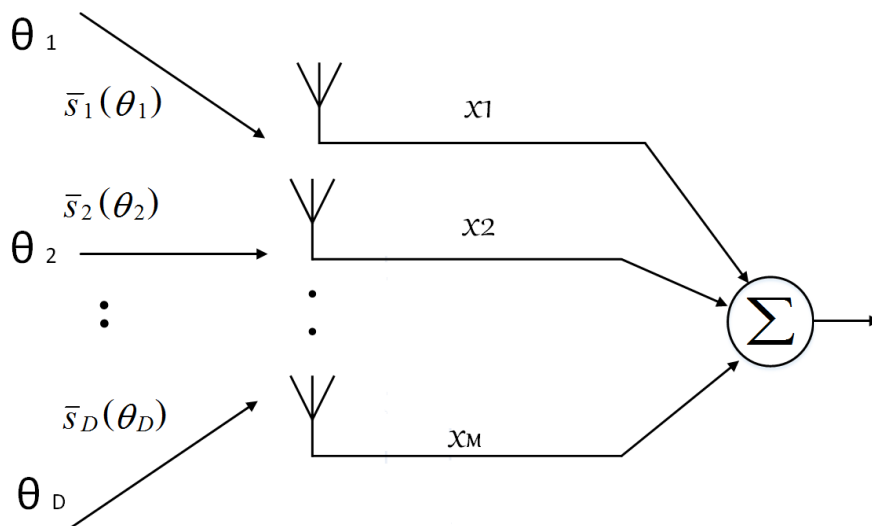


FIGURE 3.2: Antenna Receiver Model

The steering vector of the antenna can be expressed as:

$$\bar{a}(\theta) = [1 \ e^{-jkd \sin(\theta)} \ e^{-2jkd \sin(\theta)} \ \dots \ e^{-(M-1)jkd \sin(\theta)}] \quad (3.2)$$

where  $k$  is the wave number,  $d$  is the spacing between the antenna elements, and  $\theta$  is the incident angle. The signal received by the antenna can be expressed as:

$$\bar{x}(t) = \begin{bmatrix} \bar{x}_1(t) \\ \bar{x}_2(t) \\ \vdots \\ \bar{x}_D(t) \end{bmatrix} = [\bar{a}(\theta_1) \bar{a}(\theta_2) \dots \bar{a}(\theta_D)] \begin{bmatrix} \bar{s}_1(t) \\ \bar{s}_2(t) \\ \vdots \\ \bar{s}_M(t) \end{bmatrix} + \bar{n}(t) \quad (3.3)$$

where  $\bar{x}(t)$  is the received signal vector,  $\bar{s}(t)$  is the source signal vector, and  $\bar{n}(t)$  is the noise vector.

The steering vectors can be combined in one matrix named as  $\bar{A}$  matrix :

$$\bar{A} = [\bar{a}(\theta_1) \bar{a}(\theta_2) \dots \bar{a}(\theta_D)] \quad (3.4)$$

### 3.1.1 MUSIC Algorithm

The MUSIC algorithm is based on the decomposition of the covariance matrix into two subspaces. These subspaces are the signal subspace and the noise subspace. The covariance matrix of the received signal can be written as [79]:

$$\begin{aligned} \bar{R}_{xx} &= E \bar{x}\bar{x}^H = E (\bar{A}\bar{s} + \bar{n})(\bar{A}\bar{s} + \bar{n})^H \\ &= \bar{A}E \bar{s}\bar{s}^H \bar{A}^H + E \bar{n}\bar{n}^H \\ &= \bar{A}\bar{R}_{ss}\bar{A}^H + \bar{R}_{nn} \end{aligned} \quad (3.5)$$

where  $E$  denotes the expectation,  $(\cdot)^H$  denotes the Hermitian,  $\bar{R}_{ss}$  defines the correlation matrix of the source signal, and  $\bar{R}_{nn}$  denotes the correlation matrix of the noise. Consider  $(\lambda_1, \lambda_2, \dots, \lambda_M)$  are the eigenvalues of the correlation matrix  $\bar{R}_{xx}$ . There will be  $(e_1, e_2, \dots, e_M)$  eigenvectors correspond to these eigenvalues. By sorting the eigenvalues

of the correlation matrix in descending way, we get two subspaces  $\bar{E}_s$  and  $\bar{E}_N$ , where  $\bar{E}_s$  represents the signal subspace and  $\bar{E}_N$  represents the noise subspace. The components of  $\bar{E}_N$  are orthogonal to the steering vectors of the signal components at the arrival angles. This can be expressed as:  $\bar{a}^H(\theta) \bar{E}_N \bar{E}_N^H \bar{a}(\theta) = 0$ , at the angles  $\theta_1, \theta_2, \dots, \theta_D$ , the equation of the MUSIC spectrum is given by:

$$P_{MUSIC}(\theta) = \frac{1}{\bar{a}^H(\theta) \bar{E}_N \bar{E}_N^H \bar{a}(\theta)} \quad (3.6)$$

### 3.1.2 Root MUSIC Algorithm

The MUSIC algorithm gives the arriving angles as peaks on the power spectrum. This requires external interaction and exhaustive research to find out the corresponding angles. Root MUSIC represents another approach where the MUSIC spectral equation is simplified as [80]:

$$P_{MUSIC}(\theta) = \frac{1}{\bar{a}^H(\theta) \bar{E}_N \bar{E}_N^H \bar{a}(\theta)} = \frac{1}{\bar{a}^H(\theta) \bar{C} \bar{a}(\theta)} \quad (3.7)$$

where  $\bar{C} = \bar{E}_N \bar{E}_N^H$

The steering vector of the ULA can be written as:

$$\bar{a}_n(\theta) = e^{jkd(n-1)\sin\theta}, n = 1, 2, \dots, M \quad (3.8)$$

then,

$$\begin{aligned} \bar{a}^H(\theta) \bar{C} \bar{a}(\theta) &= \sum_{n=1}^{n=M} \sum_{m=1}^{m=M} e^{-jkd(n-1)\sin\theta} \bar{C}_{nm} e^{jkd(m-1)\sin\theta} \\ &= \sum_{r=M+1}^M \sum_{r=M+1}^1 c_r e^{jkd r \sin\theta} \end{aligned} \quad (3.9)$$

where  $c_r$  represents the summation of the diagonal elements of the matrix  $C$ . Equation (9) can be simplified as:

$$J(z) = \sum_{r=M+1}^{M-1} c_r z^r \quad (3.10)$$

where  $z = e^{jkd \sin \theta}$ . Due to the noise, the roots of the polynomial  $J(z)$  will be closed to the unit circle [81]. These roots can be used to find the angles of the incoming signals as:

$$\theta_j = \sin\left(\frac{\arg(z_j)}{kd}\right) \quad (3.11)$$

### 3.1.3 ESPRIT Algorithm

In contrast to the MUSIC algorithm, the ESPRIT does not apply exhaustive search over all the power spectrum to find out the peaks of the signals. This significantly reduces the computational complexity and the storage requirements [22]. Furthermore, the ESPRIT algorithm does not need a complete knowledge of the array manifold steering vectors.

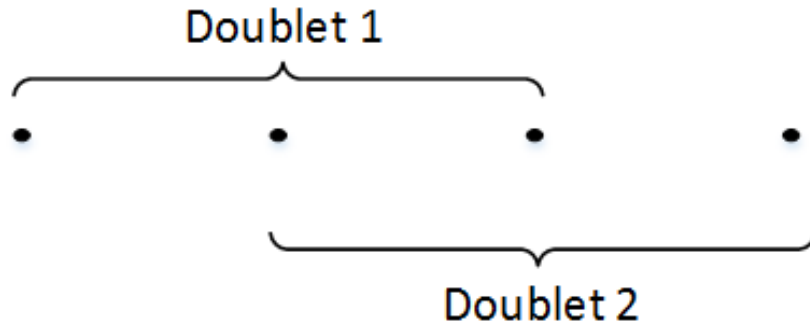


FIGURE 3.3: Two Identical Overlapped Sub-arrays

It assumes that the ULA is composed of two or more identical sub-arrays named as doublets. These doublets may overlap which means one element can be in more than one doublet. This is explained in Figure 3.3. The spacing between the ULA elements is  $d$ . The signals at

each doublet can be expressed as:

$$\begin{aligned} \bar{x}_1(t) &= [\bar{a}(\theta_1), \bar{a}(\theta_2), \dots, \bar{a}(\theta_D)] \begin{bmatrix} \bar{s}_1(t) \\ \bar{s}_2(t) \\ \vdots \\ \bar{s}_M(t) \end{bmatrix} + \bar{n}_1(t) \\ &= \bar{A}_1 \bar{s}(k) + \bar{n}_1(t) \end{aligned} \quad (3.12)$$

and

$$\begin{aligned} \bar{x}_2(k) &= [\bar{a}(\theta_1) \ \bar{a}(\theta_2) \ \dots \ \bar{a}(\theta_D)] \bar{s}(k) + \bar{n}_2(t) \\ &= \bar{A}_2 \bar{s}(t) + \bar{n}_1(t) = \bar{A}_1 \bar{\varphi} \bar{s}(t) + \bar{n}_2(t) \end{aligned} \quad (3.13)$$

where  $\bar{\varphi} = \text{diag} \ e^{jkd \sin \theta_1} \ e^{jkd \sin \theta_2} \ \dots, \ e^{jkd \sin \theta_D}$  is a

$D \times D$  diagonal unitary matrix that describes the relationship between the signals received by each doublet. The array output can be expressed as:

$$\bar{x}(k) = \begin{bmatrix} \bar{x}_1(t) \\ \bar{x}_2(t) \end{bmatrix} = \begin{bmatrix} \bar{A}_1 \\ \bar{A}_1 \cdot \bar{\varphi} \end{bmatrix} \cdot \bar{s}(t) + \begin{bmatrix} \bar{n}_1(t) \\ \bar{n}_2(t) \end{bmatrix} \quad (3.14)$$

the correlation matrix of the first doublet is given by:

$$\bar{R}_{11} = E \ \bar{x}_1 \cdot \bar{x}_1^H = \bar{A} \bar{R}_{ss} \bar{A}^H + \bar{R}_{nn} \quad (3.15)$$

and the correlation matrix of the second doublet can be expressed as:

$$\bar{R}_{22} = E \ \bar{x}_2 \cdot \bar{x}_2^H = \bar{A} \bar{\varphi} \bar{R}_{ss} \bar{\varphi}^H \bar{A}^H + \bar{R}_{nn} \quad (3.16)$$

The correlation matrix of the whole array is given by:

$$\bar{R}_{xx} = E \bar{x} \bar{x}^H = \bar{A} \bar{R}_{ss} \bar{A}^H + \bar{R}_{nn} \quad (3.17)$$

By finding the eigenvectors that correspond to  $D$  received signals, we can build the signal subspace of each doublet  $\bar{E}_1$  and  $\bar{E}_2$ . Since  $\bar{E}_1$  and  $\bar{E}_2$  are translationally related, there will be a unique non-singular transformation matrix  $\gamma$  that satisfies:

$$\bar{E}_1 \gamma = \bar{E}_2 \quad (3.18)$$

Furthermore, let  $\bar{T}$  be a unique nonsingular transformational matrix that satisfies:  $\bar{E}_1 = \bar{A} \bar{T}$  and  $\bar{E}_2 = \bar{A} \bar{\varphi} \bar{T}$  which leads to:

$$\bar{T} \gamma \bar{T}^{-1} = \bar{\varphi} \quad (3.19)$$

By obtaining the eigenvalues of  $\bar{\gamma}$  which are  $\lambda_1, \lambda_2, \dots, \lambda_D$ , the angles of arrival can be estimated as:

$$\theta_i = \sin^{-1} \left( \frac{\arg(\lambda_i)}{kd} \right) \quad (3.20)$$

## 3.2 System Model

Consider  $D$  signals  $\bar{s}_i$ ,  $i = 1, 2, \dots, D$  are transmitted at angles  $\theta_i$ . The steering vectors of the antenna can be expressed as:

$$\bar{a}(\theta_i) = [1 \ e^{jkd \sin \theta_i} \ e^{2jkd \sin \theta_i} \ \dots \ e^{(M-1)jkd \sin \theta_i}] \quad (3.21)$$

Due to the presence of noise and the effect of the Rayleigh fading channel, the signals received by the antenna elements will be corrupted so that the received signals can be expressed as:  $\bar{x}_i = \bar{a}^H(\theta_i) \bar{s}_i(\theta_i) + \bar{n}$ .

Furthermore, the angles will be deviated from the transmitted angles to a new angles, therefore , we will receive these signals at angles:  $\hat{\theta}_{est_i}, i = 1, 2, \dots, D$ . The estimated steering vectors according to these estimated angles are:

$$\bar{a}(\hat{\theta}_{est_i}) = [1 \ e^{-j d k \sin \hat{\theta}_{est_i}} \ e^{-2 j d k \sin \hat{\theta}_{est_i}} \dots \ e^{- (M - 1) j d k \sin \hat{\theta}_{est_i}} ] \quad (3.22)$$

where  $\bar{a}(\hat{\theta}_{est_i})$  are the new steering vectors according to the estimated DOAs of the MUSIC algorithm. Note that, there should be a threshold set to limit the number of the resultant peaks that will be considered. This is applied only for the MUSIC algorithm but there is no need to apply it for the Root MUSIC and ESPRIT algorithms. We use these steering vectors to get more accurate signals which means the received signals will be  $:\bar{x}_1, \bar{x}_2, \dots, \bar{x}_D$ .

Now, we need to distinguish the desired signal user from the other signals at the estimated angles.

The data received by the array antenna elements form a single output is expressed as:

$$y(t) = \bar{w}^H \bar{x}(t) \quad (3.23)$$

where  $\bar{w}$  represents the  $M - 1$  complex weighting vector which is needed to steer the array response to the direction of the incoming signals. The array steering is performed by adjusting the elements weights  $\bar{w}$ .

Let ,

$$\bar{w} = \bar{a}(\hat{\theta}_{est_i}) = [1 \ e^{-j d k \sin \hat{\theta}_{est_i}} \ e^{-2 j d k \sin \hat{\theta}_{est_i}} \dots \ e^{- (M - 1) j d k \sin \hat{\theta}_{est_i}} ] \quad (3.24)$$

and

$$y(t) = \bar{a}^H(\hat{\theta}_{est_i}) \bar{x}(t) \quad (3.25)$$

where  $y(t) = [y_1(t) y_2(t)] \dots y_D(t)]^H$ ,  $\bar{a}^H(\hat{\theta}_{est_i}) = [\bar{a}^H(\hat{\theta}_{est_1}), \bar{a}^H(\hat{\theta}_{est_2}) \dots \bar{a}^H(\hat{\theta}_{est_{(M)}})]$ , and  $\bar{x}(t) = [\bar{x}_1(t), \bar{x}_2(t) \dots \bar{x}_D(t)]^H$ , then, we can construct the transmitted signals as:

$$\hat{s}_i(t) = \sum_{i=1}^D \bar{a}^{-1}(\hat{\theta}_{est_i}) y_i(t) \quad (3.26)$$

where  $\hat{s}_i(t)$  represents the transmitted signals at the estimated directions obtained from the peaks resultant from the MUSIC algorithm. Then, we take the correlation between these estimated signals and the reference signal to identify the direction of the desired user. The correlation can be written as:

$$z_i(t) = \int_{-\infty}^{\infty} d^*(t) \hat{s}_i(t + \tau) dt \quad (3.27)$$

where  $d^*(t)$  denotes the complex conjugate of  $d$ , which is the reference signal and  $\tau$  is the lag. By using the cross correlation, we can estimate how much the estimated transmitted signal  $\hat{s}_i(t)$  and the reference signal are correlated, and from that we get :

$$\max(\text{corr}(i)) = \max(z_i(\tau)) \quad (3.28)$$

As a result the signal which has largest correlation with the reference signal will be the desired signal and it's steering vector will express the user direction.

### 3.3 Accuracy Enhancement

The APA algorithm is an adaptive filter algorithm that utilizes the gradient based method [82]. This method employs the error vector instead of a scalar error which is used in LMS algorithm to adjust the variable step size. The system model of the Affine adaptive beamforming system is shown in Figure 3.4.

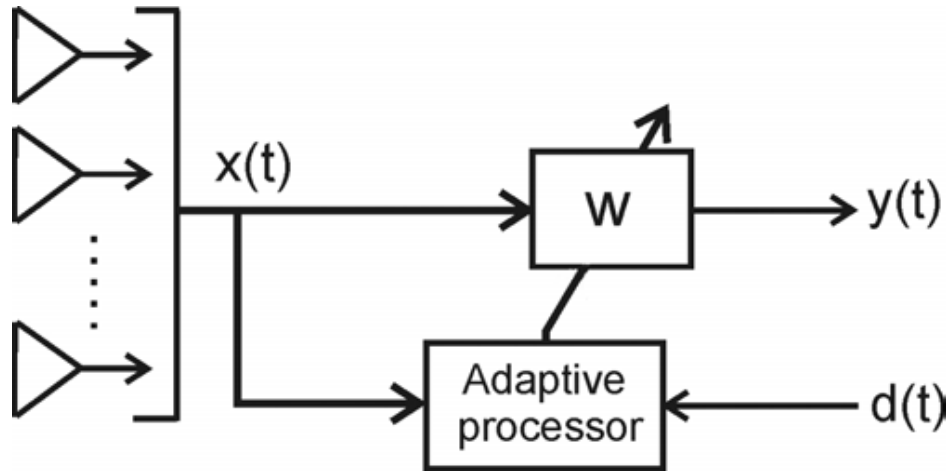


FIGURE 3.4: Affine Adaptive Beamforming System

Consider the Wiener filter:

$$\hat{d}(n) = \sum_{k=0}^P w(k) x(n-k) \quad (3.29)$$

where  $w(k)$  is the unit sample response of the finite impulse response (FIR) Wiener filter that process  $d(n), x(n)$  then the error is estimated as:

$$e(n) = d(n) - \hat{d}(n) = d(n) - \sum_{k=0}^P w(k) x(n-k) \quad (3.30)$$

where  $e(n)$  is the error between the desired and actual outputs . The coefficients of the filter are obtained by minimizing the mean square error (MSE) where

$$E e(n)^2 = E \left[ d(n) - \sum_{k=0}^P w(k) x(n-k) \right]^2 \quad (3.31)$$

then by solving the Wiener-Hopf, we get:

$$\bar{R}_{xx} \bar{w} = \bar{r}_{xd} \quad (3.32)$$

where  $\bar{R}_{xx}$  is the covariance matrix of the input data matrix to the filter and  $r_{xd}$  is the cross-correlation vector between the input data vector  $x(k)$  and the training sequence  $d(k)$  result after using the filter coefficients to converge the data to their describe values then, the coefficient vector recursion is given by

$$w(n+1) = w(n) + \mu(n)x(n)(x^T(n)x(n) + \sigma_1 I)^{-1} \quad (3.33)$$

where  $\sigma_1$  is a small positive number,  $I$  is a unit matrix of size  $M \times M$ , and  $\bar{x}(n)$  is the received signal, then the variable step size  $\mu(n)$  is obtained by:

$$\mu(n) = \mu_{max} \frac{P(n)^2}{P(n)^2 + \sigma_2} \quad (3.34)$$

where  $\sigma_2$  is a positive number proportional to  $M$  and inversely proportional to  $SNR$ ,  $\mu_{max}$  is a positive number, and  $P(n)$  is an  $M \times 1$  vector recursively can be estimated by time averaging as:

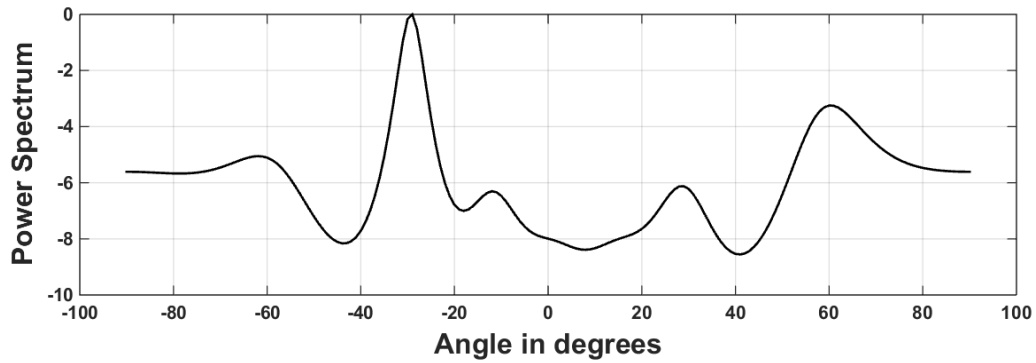
$$P(n) = \Psi P(n+1) + (1 - \Psi) x(n) (x(n)^T x(n) + \sigma_1 I)^{-1} e(n) \quad (3.35)$$

where  $\Psi$  is a smoothing factor  $0 < \Psi < 1$

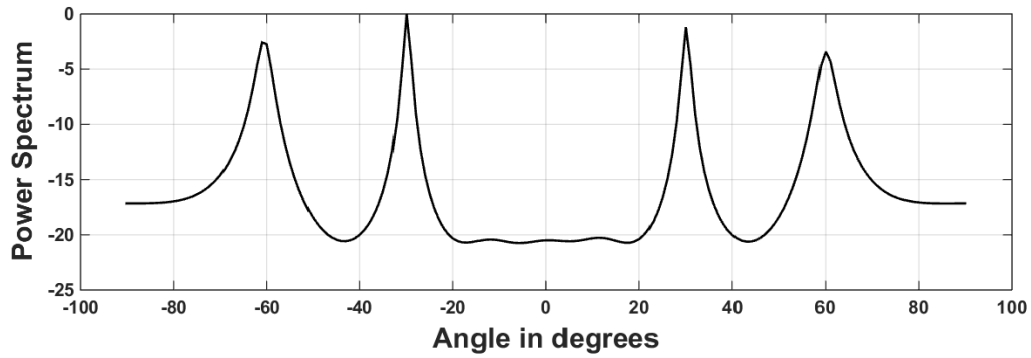
### 3.4 Simulation Results

We have considered ULA composed of ten elements. The inter spacing between the antenna elements is  $d = 0.5\lambda$ . We use Binary Phase Shift Keying (BPSK) modulated snapshots composed of 1024 samples each. The first procedure is to experience the ability of the MUSIC algorithm to find the direction of the desired user in terms of the reference signal. We have considered four signals impinging on the antenna array at  $[-60^\circ \quad -30^\circ \quad 30^\circ \quad 60^\circ]$ .

Figure 3.5 shows how the MUSIC algorithm scans the angle  $\theta$  over the angular region of the interest for the ULA from  $-90^\circ$  to  $+90^\circ$  degrees, and measures the output power



(a)



(b)

FIGURE 3.5: DOA Estimation using MUSIC Algorithm for 10 Elements ULA at (a)  $SNR = 10dB$  and (b)  $SNR = 0dB$

of the steered array to find out the peaks of the incoming signal at  $SNR = 10dB$  and  $SNR = 0dB$  values. The simulation results show that, at values less than  $0dB$ , the performance of the MUSIC algorithm is degraded causing accuracy error of the measured angles of the incoming signals. Table 3.1 (a) and (b) shows the obtained estimated angles at  $SNR = 10dB$  and  $0dB$ , respectively.

(a) at  $SNR = 10dB$ 

Transmitted angle $\theta$	$60^\circ$	$30^\circ$	$30^\circ$	$60^\circ$
Estimated angle $\hat{\theta}_{est}$	$65^\circ$	$27^\circ$	$33^\circ$	$58^\circ$

(b) at  $SNR = 0dB$ 

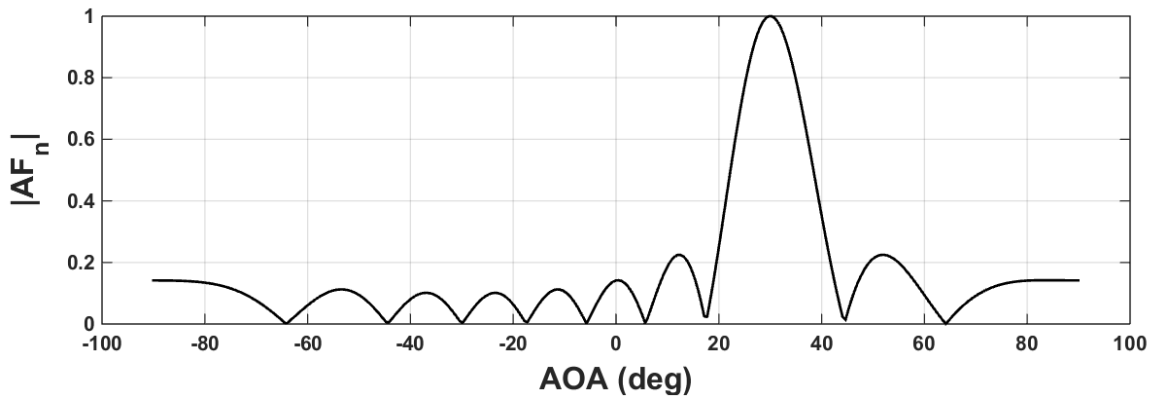
Transmitted angle $\theta$	$60^\circ$	$30^\circ$	$30^\circ$	$60^\circ$
Estimated angle $\hat{\theta}_{est}$	$57^\circ$	$29^\circ$	$28^\circ$	$59^\circ$

TABLE 3.1: MUSIC Algorithm Results

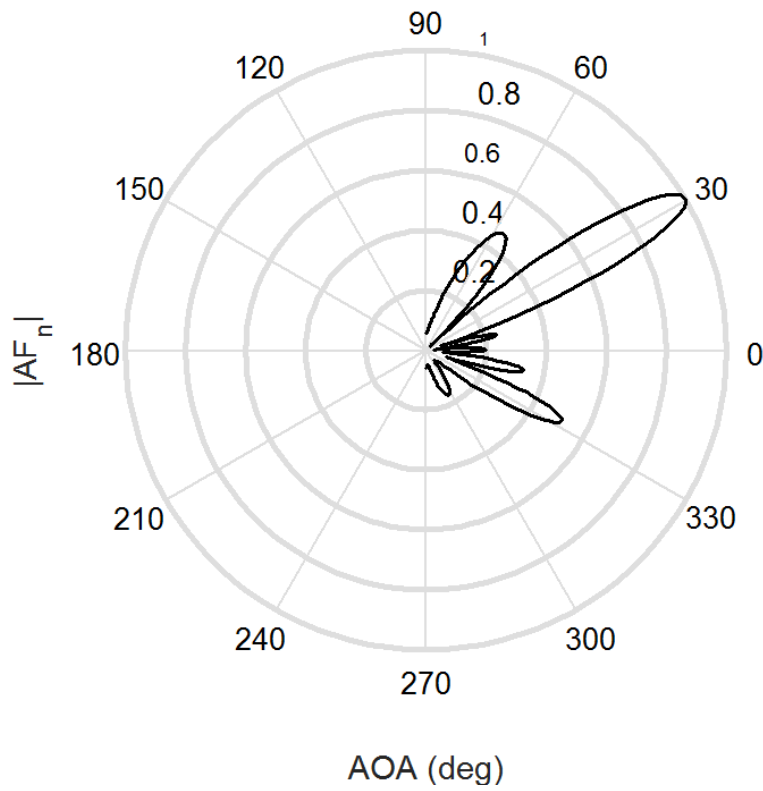
The second step is to generate a new steering vectors according to the estimated DOAs. Then, by applying the cross correlation between the detected signals and the reference signal, we find that the desired user is located at the direction of  $+33^\circ$ . Now, we feed this information (the steering vector at the obtained direction) as initial weights to the APA algorithm to enhance the accuracy, and generate a beam in the direction of the desired user and nulls towards the interferers.

We have considered antenna composed of ten elements. These elements need to be optimally weighted in order to steer the antenna towards the desired direction. From the simulations, we can show that the APA algorithm gets to the optimum weights after less than 100 iterations. This is due to the reduction of the error between the output signal and the reference signal to the minimum.

The APA algorithm improves the DOA accuracy by adjusting the weights of the antenna elements. Figure 3.6 (a) and (b) shows how the APA algorithm forms the main beam towards the desired user and nulls toward the interferes in Cartesian and Polar coordinates respectively.



(a)

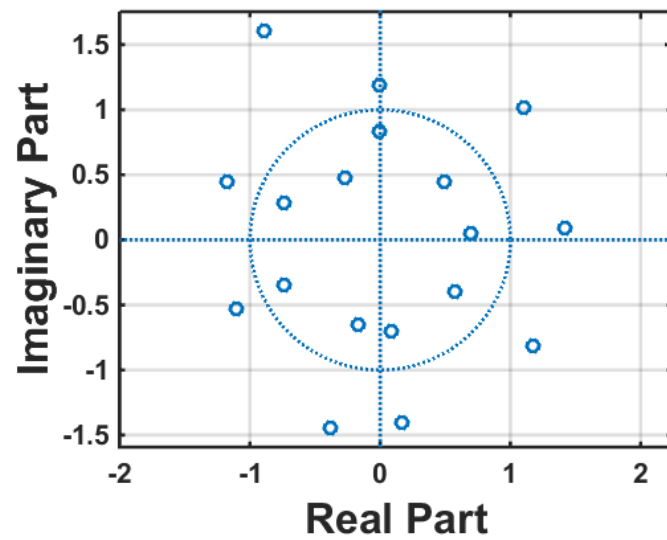


(b)

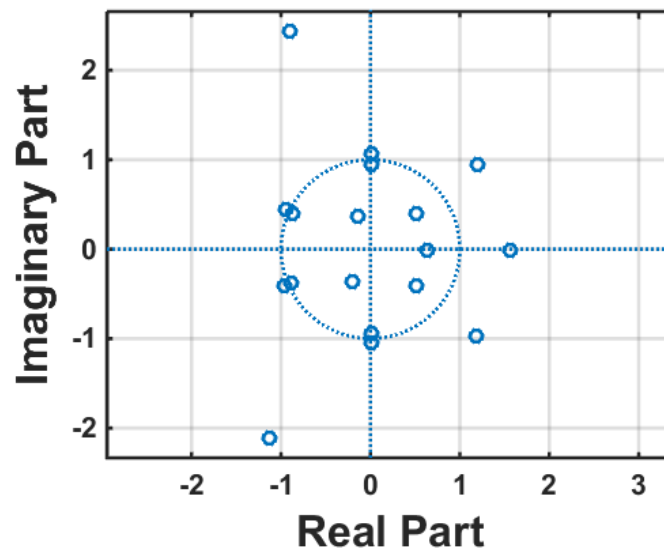
FIGURE 3.6: Generate a Beam towards the Desired User and Nulls towards the Interferes in (a) Cartesian coordinates (b) Polar coordinates

Figure 3.7 depicts the behavior of the Root MUSIC algorithm at  $SNR = 10 \text{ dB}$  and

0 dB, respectively. The Root MUSIC algorithm figures out the estimated signals by examining the roots of the spectrum polynomial.



(a)



(b)

FIGURE 3.7: the Angles Associated with the Root Music Algorithm (a) at  $SNR = 10dB$  and (b)  $SNR = 0dB$

Assume the desired user is located at  $\theta = 30^\circ$ . Table 3.2 (a) shows the obtained estimated DOAs in form of eighteen roots, then by applying the cross correlation function, we figure out that the estimated direction of the desired user is  $\hat{\theta}_{est} = 23.030^\circ$  in case of  $SINR = 10dB$ , and at  $\hat{\theta}_{est} = 29.817^\circ$  in case of  $SINR = 0dB$ . This is explained in Tables 3.2 (a) and 3.2 (b), respectively.

(a)  $\hat{\theta}_{est}$  at  $SINR = 10dB$

$23.030^\circ$	$42.319^\circ$	$14.298^\circ$	$38.126^\circ$	$1.076^\circ$	$10.993^\circ$
$27.891^\circ$	$59.872^\circ$	$60.4534^\circ$	$60.4534^\circ$	$55.1776^\circ$	$27.891^\circ$
$42.319^\circ$	$10.993^\circ$	$1.076^\circ$	$38.126^\circ$	$14.298^\circ$	$23.030^\circ$

(b)  $\hat{\theta}_{est}$  at  $SINR = 0dB$

$37.496^\circ$	$39.439^\circ$	$12.044^\circ$	$0.238^\circ$	$12.765^\circ$	$29.817^\circ$
$29.817^\circ$	$60.194^\circ$	$60.194^\circ$	$60.946^\circ$	$60.946^\circ$	$30.202^\circ$
$30.202^\circ$	$12.044^\circ$	$0.238^\circ$	$12.765^\circ$	$37.496^\circ$	$39.439^\circ$

Table 3.2: The obtained DOAs using Root MUSIC algorithm

The same procedure is repeated for the ESPRIT algorithm at  $SINR = 0dB$  and  $SINR = 10dB$ . Table 3.3 shows the obtained estimated angles.

(a) at  $SINR = 10 dB$

Transmitted angle $\theta$	$60^\circ$	$30^\circ$	$30^\circ$	$60^\circ$
Estimated angle $\hat{\theta}_{est}$	$56.518^\circ$	$24.044^\circ$	$27.938^\circ$	$55.816^\circ$

(b) at  $SINR = 0 dB$

Transmitted angle $\theta$	$60^\circ$	$30^\circ$	$30^\circ$	$60^\circ$
Estimated angle $\hat{\theta}_{est}$	$58.900^\circ$	$28.969^\circ$	$28.688^\circ$	$58.982^\circ$

Table 3.3: The obtained DOAs using ESPRIT algorithm

The user position was found at  $\hat{\theta}_{est} = 27.938^\circ$  in case of  $SINR = 10dB$ , and at  $\hat{\theta}_{est} = 28.688^\circ$  in case of  $SINR = 0dB$ . By applying the APA algorithm, the accuracy is improved and the corrected direction is at  $\hat{\theta}_{est} = 29.5^\circ$ . Note that, the accuracy of the MUSIC, ROOT MUSIC, and the ESPERIT algorithms is very high when  $SINR = 0dB$ .

### **3.5 Conclusion**

In this chapter, we have introduced a method to identify the desired user from the interferers by applying the cross correlation between the received signals and the reference signal which is known by the transmitter and receiver. Also, by implementing a fast adaptive processor unit such APA which has a fast convergence rate with minimum square error, we have improved the accuracy of the obtained DOA of the desired user by determining the optimum complex weights. This maximizes the signal to the interference ratio via suppressing the signal from the interference sources. Then, the beamforming technique is used to generate a beam towards the desired user and nulls in the directions of the interferers. Simulation results show that after applying the fast adaptive APA algorithm, the performance of the DOA algorithms are significantly improved in case of low SINR values.

# Chapter 4: Adaptive Beamforming for 5G

In this chapter we introduce an algorithm which is a combination of the MUSIC and LMS algorithms named as MLMS. The MUSIC algorithm is combined with the correlator which we named as User Identifier (UI) to find the direction of the desired user, then we feed the LMS algorithm with the initial estimation of the desired user direction and signal. This makes the difference between the reference signal and the ULA output smaller from the early iterations. This makes the convergence to occur faster and gives the LMS algorithm the capability to work even at hard conditions such as very low SINR value.

## 4.1 Adaptive Beamforming Algorithms

The efficiency of the adaptive beamforming is highly dependent on the implemented beamforming algorithms. The beamforming algorithms can be classified into two classes [83]. The first class is blind algorithms. Blind algorithms do not utilize reference or training signals in calculating the weighting vectors and generating the beams. The reference signals are signals sent by the transmitter and known by the receiver. The blind algorithms perform their calculations based on the estimation of the DOA of the desired and interfering signals,

structural characteristics of the signal, and the knowledge of the previous symbols nature. The second class is non blind algorithms. These algorithms use reference signals in calculating the weighting vectors and generating beams. This class is appropriate for wireless communications because the transmission of reference signals has been adopted by most of the wireless networks such as WiMAX and LTE [84]. The LMS and RLS are examples of blind algorithms. These classes are shown in Figure (4.1).

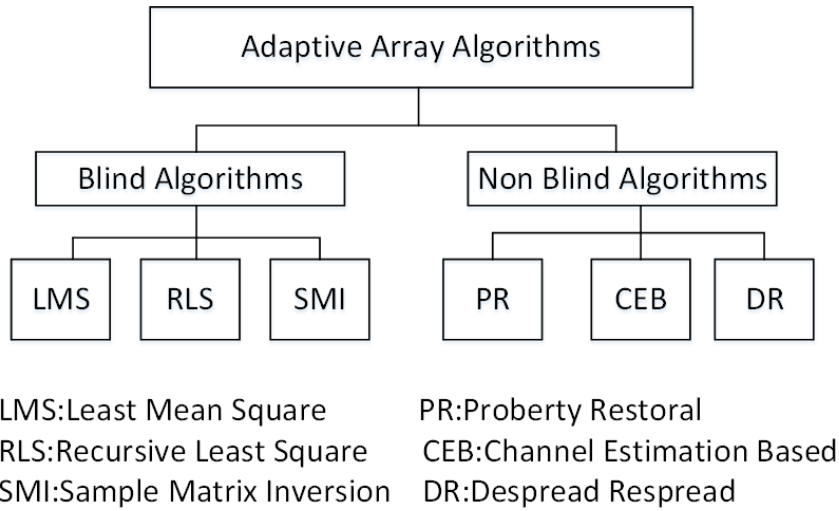


FIGURE 4.1: The Classes of Beamforming Algorithms

## 4.2 Wiener Solution

Consider Figure (4.2) where the input signals are fed to be weighted . The output will be the sum of the inputs multiplied by their weights.

The error signal can be expressed as:

$$e(k) = d(k) - y(k) \quad (4.1)$$

and  $y(k)$  can be expressed as:

$$y(k) = w^H x(k) \quad (4.2)$$

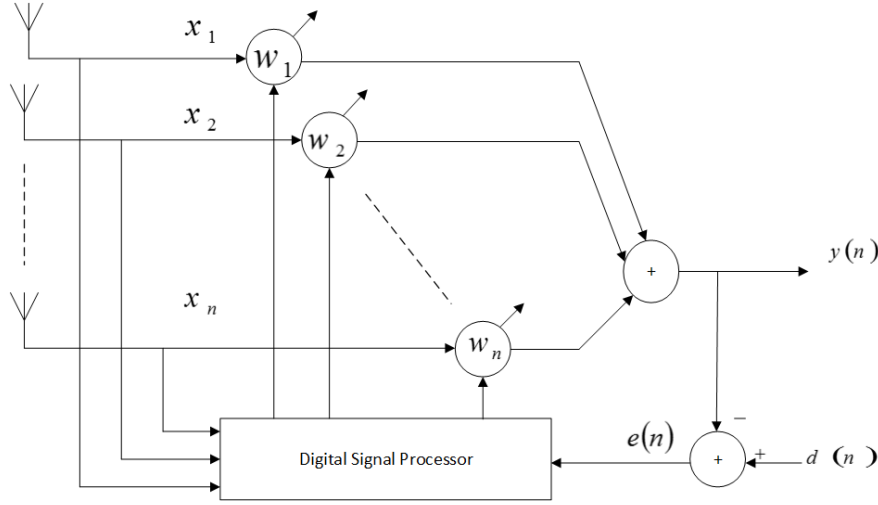


FIGURE 4.2: Adaptive Beamformer

where  $w^H$  represents the Hermitian transpose of the weighting vector,  $w = [w_1, w_2, w_3, \dots, w_N]$  and  $d(k)$  represents the training sequence or the reference signal that is sent by the transmitter and known by the receiver.

By applying the Minimum Square Error method and taking the expectation, we get:

$$\begin{aligned}
 E[ e(k)^2 ] &= E[ d(k) \quad y(k) \quad d(k) \quad y(k) ] \\
 &= E[ d(k) \quad \bar{x}(k) \quad d(k) \quad \bar{w}^H \bar{x}(k) ] \\
 &= E[ d(k)^2 \quad d(k) \bar{x}^H(k) \bar{w} \quad \bar{w}^H \bar{x}(k) d(k) + \bar{w}^H(k) \bar{w} ] \\
 &= E[ d(k)^2 \quad \bar{r}_{xd} \bar{w} \quad \bar{w}^H \bar{r}_{xd} + \bar{w}^H \bar{R}_{xx} \bar{w} ]
 \end{aligned} \tag{4.3}$$

where  $\bar{R}_{xx} = E[\bar{x}(k) \bar{x}^H(k)]$  is  $N \times N$  covariance matrix of the input data vector  $\bar{x}(k)$ , and  $\bar{r}_{xd} = E[\bar{x}(k) d(k)]$  is the  $N \times 1$  cross-correlation vector between the input vector  $\bar{x}(k)$  and the training sequence  $d(k)$ .

By rewriting the obtained equation, we get:

$$E[ e(k)^2 ] = E[ d^2(k) \quad 2\bar{w}^H \bar{r}_{xd} + \bar{w}^H \bar{R}_{xx} \bar{w} ] \tag{4.4}$$

This equation is a quadratic function. It has a unique minimum which can be obtained by taking its derivative with respect to  $\bar{w}$ .

$$(E[e(k)^2]) = \frac{\partial}{\partial \bar{w}} E[e(k)^2] \quad (4.5)$$

This leads to :  $2\bar{r}_{xd} + 2\bar{R}_{xx}\bar{w}_{opt} = 0$

$$\bar{w}_{opt} = \bar{R}_{xx}^{-1} \bar{r}_{xd} \quad (4.6)$$

This solution is called the Wiener solution. The problem with this solution is that it requires the entire knowledge of  $\bar{R}_{xx}$  and  $\bar{r}_{xd}$  to get to the optimum solution. Another problem is the difficulty of calculating  $\bar{R}_{xx}^{-1}$  and in some cases  $\bar{R}_{xx}$  has no inverse.

### 4.3 Steepest Descent Method

The basic idea of this method is to find the gradient. Then go back and forth by subtracting or adding a small amount called the step size [71]. This continues until we get to the optimum solution. This operation can be expressed mathematically as in equation 4.7. Equation 4.7 is called the updating equation.

$$w(i+1) = w(i) - \frac{\mu}{2} \frac{\partial \epsilon}{\partial w} \Big|_{w=w(i)} \quad (4.7)$$

where  $\mu$  is the step size which is the most important parameter. This method does not include the calculation of  $R_{xx}^{-1}$ . However, we still need to know  $\bar{p}$  and  $\bar{R}$ . Furthermore, this method works off line.

## 4.4 Least Mean Square

LMS is the adaptive version of the Steepest Descent algorithm. It is the most popular adaptive algorithm. LMS gains its popularity due to its simplicity and the ease of implementation. There are many versions of LMS algorithm that have been proposed such as LMS-LMS, LLMS and BLMS. In LMS, the correlation matrix  $\bar{R}_{xx}$  and the cross correlation vector  $\bar{r}_{xd}$  are replaced by their momentarily values as following [85]:

$$\bar{R}_{xx} = \bar{x}(n)\bar{x}^H(n) \quad (4.8)$$

$$\bar{r}_{xd} = \bar{x}(n)d(n) \quad (4.9)$$

The LMS algorithm can be summarized in the following steps:

$w(0)$  initial (usually initiated with zero vector)

*for*  $n = 0$  *to* *final*

$$y(n) = \bar{w}^H \bar{x}(n)$$

$$e(k) = d(k) - y(k)$$

then use the following updating equation:

$$w(n+1) = w(n) + \mu \bar{x}(n)e(n) \quad (4.10)$$

where  $\mu$  is the step size and is limited by:

$$0 < \mu < \frac{2}{\lambda_{max}} \quad (4.11)$$

## 4.5 Proposed Tracking Model

This scenario combines the MUSIC and LMS algorithms in one algorithm named as MLMS algorithm. MLMS starts with determining the position of the user in the cell. We achieve this using the MUSIC algorithm due to its high resolution. Then, we use the LMS algorithm to generate a beam in the direction of the desired user and nulls in the directions of the interferers, and keep tracking of the desired user. Consider  $D$  signals are transmitted

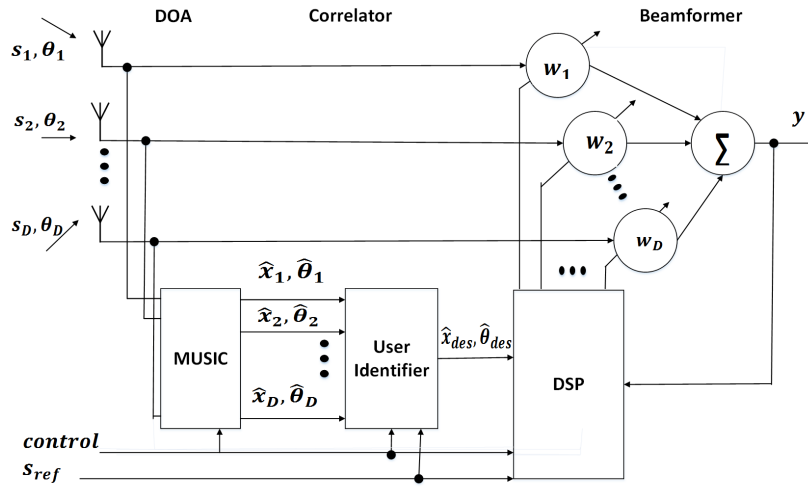


FIGURE 4.3: MLMS Algorithm

at angles  $\theta_1, \theta_2, \dots, \theta_D$  as shown in Figure (4.3). The steering vectors that correspond to these angles can be expressed as:

$$\bar{a}(\theta_i) = [1 \ e^{jkd \sin(\theta_i)} \ e^{j2kd \sin(\theta_i)} \ \dots \ e^{j(M-1)kd \sin(\theta_i)}]^T \quad (4.12)$$

The output of the ULA can be written as:

$$\bar{\mathbf{x}}(k) = \begin{bmatrix} \bar{x}_1(k) \\ \bar{x}_2(k) \\ \vdots \\ \bar{x}_D(k) \end{bmatrix} = [\bar{a}(\theta_1) \bar{a}(\theta_2) \dots \bar{a}(\theta_D)] \begin{bmatrix} \bar{s}_1(k) \\ \bar{s}_2(k) \\ \vdots \\ \bar{s}_M(k) \end{bmatrix} + \bar{\mathbf{n}}(k) \quad (4.13)$$

The MUSIC algorithm will give us estimated values of the transmitted angles at  $\hat{\theta}_1, \hat{\theta}_2 \dots \hat{\theta}_D$ .

Therefore, the actual output of the MUSIC algorithm can be expressed as:

$$\hat{\mathbf{x}}(k) = \begin{bmatrix} \hat{x}_1(k) \\ \hat{x}_2(k) \\ \vdots \\ \hat{x}_D(k) \end{bmatrix} = [\bar{a}(\hat{\theta}_1) \bar{a}(\hat{\theta}_2) \dots \bar{a}(\hat{\theta}_D)] \begin{bmatrix} \bar{s}_1(k) \\ \bar{s}_2(k) \\ \vdots \\ \bar{s}_M(k) \end{bmatrix} + \bar{\mathbf{n}}(k) \quad (4.14)$$

where  $(\hat{\cdot})$  represents an estimation of the original value. Using the MUSIC algorithm with a proper threshold, we get peaks on the power spectrum at  $\hat{\theta}_1, \hat{\theta}_2 \dots \hat{\theta}_D$ . By applying the cross correlation function concept between the reference signal and the incoming signals which we have already proposed in [69], we can estimate the desired user signal and the desired user direction. The UI will separate the desired signal from the interference. The operation of the system has two cycles. In the first cycle, the DOA and the UI parts operate while keeping the beamforming part OFF. In the second cycle, beamforming part operates while DOA and UI parts are OFF. Therefore, the output signal of the UI can be expressed as:

$$\mathbf{y}_{UI}(k) = \bar{a}(\hat{\theta}_{des})^H \hat{\mathbf{x}}_{des} \quad (4.15)$$

where  $\hat{x}_{des}$  is the estimated version of the  $\bar{x}_{des}$ , and  $\hat{\theta}_{des}$  is the obtained direction of the desired user. At the first iteration, the reference signal will be compared with the output of the UI. This means that, instead of comparing the reference signal with the ULA output which leads to slow convergence and weak tracking capabilities as it is in the conventional LMS, we feed the LMS with initial estimation of the desired user signal and direction. Therefore, the error at time  $t$  can be expressed as:

$$e_{(t)}(k) = s_{ref}(k) - y_{(UI)}(k) = s_{ref}(k) - \bar{a}^H(\hat{\theta}_{des}) \hat{x}_{des}(k) \quad (4.16)$$

Note that, we have expressed  $e_{(t)}$  as a function of time because our model will keep comparing with the re-transmitted reference signal every  $0.5 \text{ ms}$ . We have chosen the time  $0.5 \text{ ms}$  because it is the shortest time adapted by LTE for sending the reference signals. By taking the square of the Equation (4.16) and taking the expectation of it, we get:

$$E \{ e_{(t)}(k)^2 \} = E \{ (s_{ref}(k) - y_{(UI)}(k))(s_{ref}(k) - y_{(UI)}(k))^H \} \quad (4.17)$$

In addition, it is worth to note that  $y_{(t)}$  is an estimation of the desired user signal, therefore, the error from the start will be small. Equation (4.17) is a quadratic equation with one minimum. By taking the derivative with respect to  $\bar{w}$  and solving, we get:

$$\bar{w}_{MLMS_{opt}} = \bar{R}_{x_{des}x_{des}}^{-1} \bar{r}_{new} \quad (4.18)$$

where  $\bar{w}_{MLMS_{opt}}$  represents the optimum weights obtained by the algorithm,  $\bar{R}_{x_{des}x_{des}}^{-1}$  and  $\bar{r}_{new}$  are the proposed versions of  $R_{xx}$  and  $\bar{r}$  respectively. They are given by:

$$\bar{R}_{x_{des}x_{des}} = \bar{x}_{des}(k) \bar{x}_{des}^H(k) \quad (4.19)$$

and

$$\bar{r}_{new} = s_{ref}(k) \bar{x}_{des}(k) \quad (4.20)$$

The updating equation of the beamformer is given by:

$$\bar{w}(k+1) = \bar{w}(k) - \mu [\bar{R}_{x_{des}x_{des}} \bar{w} - \bar{r}_{rd}] \quad (4.21)$$

where  $\mu$  represents the step size and Its limited by:

$$0 < \mu < \frac{1}{2\lambda_{max}} \quad (4.22)$$

where  $\lambda_{max}$  indicates the largest eigenvalue of  $\bar{R}_{x_{des}x_{des}}$ .

After the first iteration and finding the optimum weights, the LMS part and the reference signal will be compared with the ULA output in the tracking procedure. If the user is moved to a new point, the difference between the reference signal and the array output will be increased which means the MLMS will adjust the antenna weights to redirect the antenna to the new direction. We will use the Equation (4.21) to update the ULA weights. Note that, the conventional LMS algorithm is not capable to work at large amount of interference. Feeding the LMS algorithm with the estimation of the desired signal and the direction of the desired user makes the convergence faster, and the tracking process is applicable. We implement the LMS algorithm to enhance the DOA accuracy of the obtained estimated angle, generate a beam towards the desired user and nulls toward the interferers. These steps are explained in algorithm 1. The array factor (AF) is sketched to obtain the beam parameters  $\theta_+$  and  $\theta_-$ . These angles are the angles that correspond to the two HPBW points of the maximum power of each beam.

---

**1 Algorithm 1: MLMS algorithm steps**

---

- Step 1:** gather the data from the antenna elements  
**Step 2:** estimate the correlation matrix  $\bar{R}_{xx}$   
**Step 3:** calculate the eigenvalues of  $\bar{R}_{xx}$   
**Step 4:** obtain the noise eigenvectors  $[\bar{v}_{D+1} \bar{v}_2 \dots \bar{v}_M]$   
**Step 5:** draw the power spectrum  $P_{MUSIC}(\theta)$   
**Step 6:** find out the largest peaks on the power spectrum  
**Step 7:** find out the angles that correspond to these peaks  
**Step 8:** apply the correlation concept proposed in Yousefi to find out the direction of the desired user  $\hat{\theta}_{des}$   
**Step 9:** feed this information to LMS algorithm  
**Step 10:**

for  $k = 0$  to  $\text{final}$   
     $\Rightarrow$  calculate  $y(k) = \bar{w}^H(k) \hat{x}_{des}(k)$   
     $\Rightarrow$  calculate the error signal  
         $e(k) = s_{ref(t)}(k) - y(k)$   
     $\Rightarrow$  update  $\bar{w}(k+1) = \bar{w}(k) + \mu e^*(k) \hat{x}_{des}(k)$   
end for

- Step 11:** calculate the array factor at the desired angle according to the following equation:

$$AF(\theta_{des}) = \sum_{m=1}^M w_m e^{-j(m-1)d\beta \sin(\theta_{des})} \quad (4.23)$$

- Step 12:** if the user moves, go back to step 10 and update Equation (4.21)
- 

## 4.6 Simulation Results

We have considered a uniform linear SA composed of 10 elements with inter-element spacing equal to  $0.5 \lambda$ . The results are obtained using snapshots of 1024 samples. These samples are modulated using Binary Phase Shift Keying (BPSK) in the presence of AWGN at  $SNR = -10 \text{ dB}$  and the presence of four interfering signals. The simulation is performed using MATLAB R2015 a. Figure (4.4) shows a comparison between the proposed algorithm MLMS and the conventional LMS in terms of the convergence. It shows that, MLMS gets to the convergence after 13 iterations while the conventional LMS needs 85 iterations to reach to the convergence.

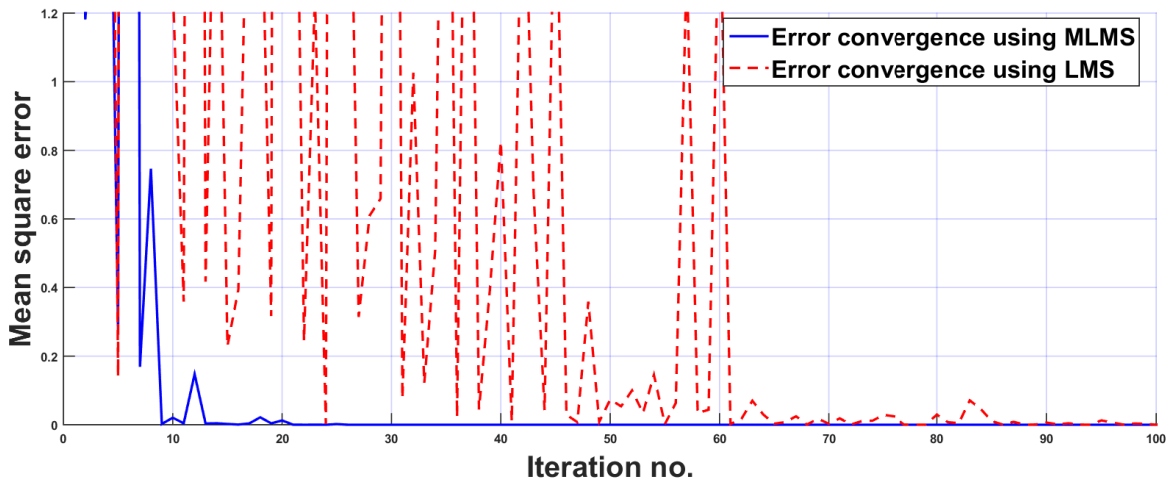


FIGURE 4.4: Convergence of MLMS and LMS Algorithms

In addition, Figure (4.5) shows a comparison between the two algorithms in terms of the capability of tracking of the desired user signal. We have chosen 50 iterations zooming to declare the tracking results. Figure (4.5) explains that, MLMS can completely follow the desired user signal after 13 iterations. On the other hand, it clarifies that LMS needs 85 iterations to track the desired user signal. This provides 84.7% improvement compared with the LMS.

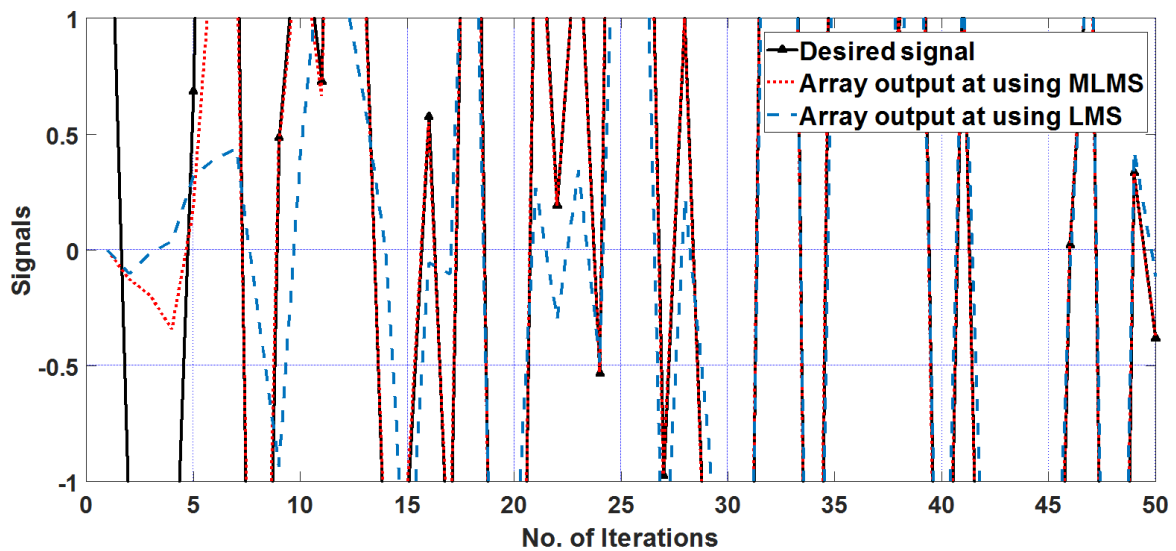


FIGURE 4.5: Tracking Capability of MLMS and LMS Algorithms

## 4.7 Conclusion

In this chapter, an algorithm for adaptive beamforming is proposed. In this algorithm, the MUSIC and LMS algorithms are combined to find the directions of the users in the cell, then generating beams toward the desired users and nulls in the directions of the interferers. Furthermore, we have put a mechanism to track the users while they are moving inside the cell. Our simulation results confirm that our proposed algorithm is very efficient in terms of the convergence and the capability of tracking. We have improved the convergence and the tracking of the desired users signals to occur after 13 iterations instead of 85 which is the number of iterations given by the conventional LMS algorithm. This means an improvement of 84.7 %.

Our proposed algorithm shows powerful efforts to converge and fully track the desired users signals much faster than the traditional LMS algorithm. Using this algorithm, the space diversity can be introduced to the existing mobile systems which already have the time and frequency diversities. The addition of the space diversity will significantly improve the system capacity due to the improved scheduling.

# **Chapter 5: Scheduling Based on Beamforming**

The scheduling is about managing the available resources such that no channel will be left idle. This is achieved according to certain rules that take into account the channel, user, and space diversities. In this chapter, we introduce a practical scheduling scheme for the next generations of the mobile communication systems. In this chapter, we take the advantage of knowing the users locations to build up an optimum scheduling scheme. Furthermore, we consider two services which are DS and NDS services. We optimally divide the available bandwidth between these services using the utility function concept.

## **5.1 Scheduling in LTE**

To implement scheduling in the frequency domain in LTE, eNodeB requires information about the concurrent status of each sub-carrier with every user. This information is obtained from the feedback sent by each user. However, sending feedback about all sub-carriers consumes a great amount of up link resources. There is always some balance that has to be set between the transmitted feedback and the utilized resources. There are numerous techniques

that have been suggested to reduce the amount of required feedback. In [86], user devices transmit CSI of all sub-carriers that have exceeded a predetermined threshold. In [87], user devices send CSI of sub-carriers with the best gains. In [88], the same mechanism in [86] is applied. However, the feedback is one bit. LTE applies a practical combination of all previously mentioned techniques [89]. In LTE, the transmitted CSI is quantized into 4-bit value. This value is known as QCI which is explained in Table 5.1[90]. In addition to all, LTE reports the average CSI of large sets of sub-carriers.

CQI Index	Modulation	Code Rate 1024	Efficiency	Bits per RB Per sub frame
0	<i>outofrange</i>			
1	QPSK	78	0.5123	21.931
2	QPSK	120	0.2344	33.754
3	QPSK	193	0.377	54.288
4	QPSK	308	0.6016	86.63
5	QPSK	449	0.877	126.288
6	QPSK	602	1.1758	169.288
7	16QAM	378	1.4766	212.63
8	16QAM	490	1.9141	275.63
9	16QAM	616	2.4063	346.507
10	64QAM	466	2.7305	393.192
11	64QAM	567	3.3223	478.411
12	64QAM	666	3.9023	561.931
13	64QAM	772	4.5234	651.37
14	64QAM	873	5.1152	736.589
15	64QAM	948	5.5547	799.877

Table 5.1: Parameters of CQI

## 5.2 Modelling DS and NDS calls

In this work, we consider two QoS classes. These classes are DS and NDS. The DS class represents the real time applications which might be video conferencing, video calls, etc. The NDS class represents the non real time applications class such as the email transmission where the delay can be tolerated. Both DS and NDS creates two Poisson streams with arriving

rates  $\lambda_1$  and  $\lambda_2$  respectively. The service duration follows an exponential distribution with  $\mu_1$  and  $\mu_2$  factors. The system provides traffics of [91]:

$$A_1 = \frac{\lambda_1}{\mu_1}$$

and

$$A_2 = \frac{\lambda_2}{\mu_2}$$

(5.1)

where  $A_1$  and  $A_2$  represent the total traffic for the DS and NDS services respectively.

The framework of the system follows a Markov chain with two dimensions and continuous time. The channels which are utilized by the DS class are defined by  $k_1(t)$ .

On the other hand, the channels utilized by NDS class are defined by  $k_2(t)$  where  $0 \leq k_1(t) + k_2(t) \leq K$ .

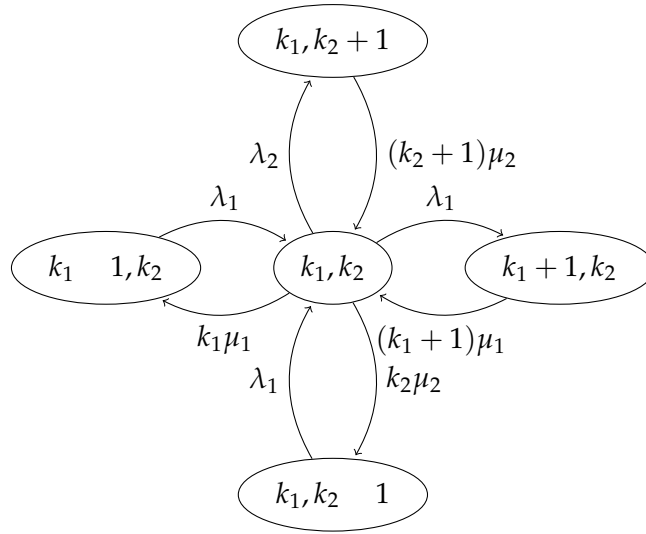


FIGURE 5.1: Two Dimensional Markov Chain

Figure (5.1) shows the representation of the four possible Markov states. At the state  $0,0$ , all the channels are vacant. This can be mathematically expressed as,

$$(\lambda_1 + \lambda_2) [p_{0,0}]_K = \mu_1 [p_{1,0}]_K + \mu_2 [p_{0,1}]_K \text{ for } k_1 = k_2 = 0 \quad (5.2)$$

Further, at state  $(k_1, k_2)$ ,  $k_1$  channels are serving calls of class 1, and  $k_2$  channels are serving calls of class 2. This can be written as:

$$\begin{aligned} (\lambda_1 + \lambda_2 + k_1 \mu_1 + k_2 \mu_2) [p_{k_1, k_2}]_K &= \lambda_1 [p_{k_1-1, k_2}]_K + \\ \lambda_2 [p_{k_1, k_2-1}]_K + (k_1 + 1) \mu_1 [p_{k_1+1, k_2}]_K + & \quad (5.3) \\ (k_2 + 1) \mu_2 [p_{k_1, k_2+1}]_K & \quad \text{for } (k_1 + k_2) < K \end{aligned}$$

at the state  $k_1 + k_2 = K$ :

$$(k_1 \mu_1 + k_2 \mu_2) [p_{k_1, k_2}]_K = \lambda_1 [p_{k_1-1, k_2}]_K + \lambda_2 [p_{k_1, k_2-1}]_K \quad (5.4)$$

which leads to :

$$[p(k_1, k_2)]_K = \frac{\frac{A_1^{k_1}}{k_1!} \frac{A_2^{k_2}}{k_2!}}{\sum_{i=0}^k \sum_{j=0}^{k-1} \frac{A_i}{i!} \frac{A_j}{j!}} \quad (5.5)$$

and the blocking probability is given by:

$$B = \frac{\sum_{Q(K)} \frac{A_1^{k_1}}{k_1!} \frac{A_2^{k_2}}{k_2!}}{\sum_{i=0}^k \sum_{j=0}^{k-1} \frac{A_i}{i!} \frac{A_j}{j!}} \quad (5.6)$$

where  $Q(K) = \{k_1, k_2 : k_1 + k_2 = K\}$

### 5.3 Resource Allocation Formula in OFDM System

Consider  $K$  number of sub-carriers to be allocated on  $J$  uniformly distributed users in a circular cell. Further, assume there are  $I$  number of beams generated using algorithm 1. The users are considered to be in the same beam if they are located in the area limited by  $\theta_i$  and  $\theta_{i+1}$ . Let  $k = 1, 2, \dots, K$ ,  $j = 1, 2, \dots, J$  and  $i = 1, 2, \dots, I$  are the sets of

the sub-carriers, users, and beams respectively. Our objective is to maximize the total aggregated data rate of the system using the scheduling based on beamforming. We achieve this through maximizing the data rate of each user. The bit rate of the  $j_{th}$  user is given by [92]:

$$R_j = \frac{B}{K} \sum_{k=1}^K \alpha_{i,j,k} \log_2(1 + SNR_{i,j,k}) \quad i \quad (5.7)$$

where  $B$  is the total bandwidth, and  $\alpha_{i,j,k}$  is an index showing the sub-carrier assignment. It takes the value of 1 if the sub-carrier  $k$  is assigned to the user  $j$  in the beam  $i$  and 0 otherwise. This can be expressed mathematically as:

$$\alpha_{i,j,k} = \begin{cases} 1 & \text{if sub-carrier } k \text{ is allocated to user } j \text{ in beam } i \\ 0 & \text{otherwise} \end{cases} \quad (5.8)$$

The bandwidth of each sub-channel is defined in terms of the Orthogonal Frequency Division Multiplexing (OFDM) symbol duration  $T$  as,  $B = K/T$ . Moreover,  $SNR_{i,j,k}$  refers to the signal to the noise ratio for the sub-channel  $k$  with the user  $j$  in beam  $i$ . It can be expressed as:

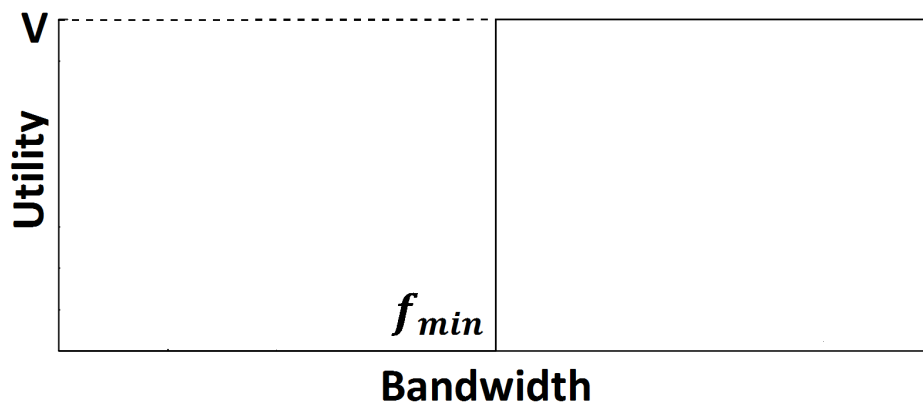
$$SNR_{i,j,k} = \frac{pw_{i,j,k} h_{i,j,k}^2}{N_0 \frac{B}{K}} \quad (5.9)$$

where  $pw_{i,j,k}$  shows the received power of the sub-channel  $k$  with the user  $j$  in beam  $i$ ,  $h_{i,j,k}$  represents the channel gain, and  $N_0$  represents the spectral density of the Additive White Gaussian Noise (AWGN) channel. Based on equation (5.7), the total data rate of the system can be expressed as:

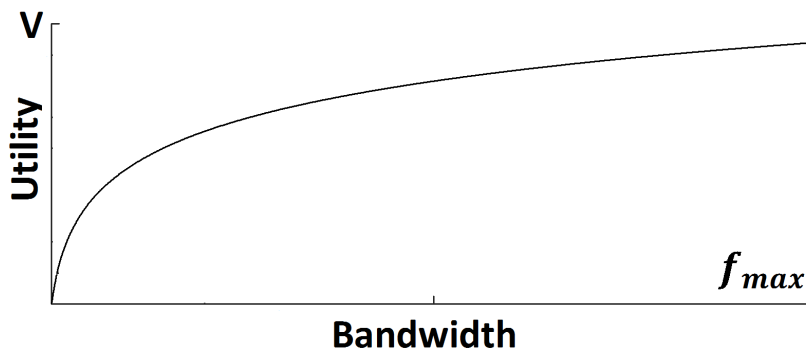
$$R_T = \frac{B}{K} \sum_{i=1}^I \sum_{j=1}^J \sum_{k=1}^K \alpha_{i,j,k} \log_2\left(1 + \frac{pw_{i,j,k} h_{i,j,k}^2}{N_0 \frac{B}{K}}\right) \quad (5.10)$$

## 5.4 Modeling the utility function of the requested services

The fairness among different users might be satisfied relatively via the satisfaction of their QoS requirements. In this paper, we implement two classes of services. The first class is the delay sensitive services and the second is the non-delay sensitive services. The DS can be described by Figure 5.2(a) [46], [93], [94].



(a)



(b)

FIGURE 5.2: Utility Function of (a) DS and (b) NDS Applications

The DS applications include the real time applications. These applications are extremely sensitive to the delays and the degradation in the bandwidth requirements. The DS class can

be expressed mathematically as:

$$u_1(f_{ds}) = V \frac{\text{sgn}(f_{ds} - f_{min}) + 1}{2} \quad (5.11)$$

where  $f_{ds}$  is the allocated bandwidth in case of the DS services,  $f_{min}$  represents the minimal bandwidth requirements for the DS class,  $V$  is a utility scale, and  $\text{sgn}$  is a sign function.

On the other hand, the NDS applications are the services which can tolerate the delays and the degradation in the bandwidth requirements. The email and the file transfer services are examples of these services. The behavior of the NDS services are described in Figure 5(b).

Furthermore, they might be expressed mathematically as:

$$u_2(f_{nds}) = V \frac{\log(f_{nds} + 1)}{\log(f_{max} + 1)} \quad (5.12)$$

where  $f_{nds}$  is the allocated bandwidth in case of the NDS services and  $f_{max}$  defines the maximal required bandwidth of the NDS applications.

Let the utility function of the system be,

$$U = u_1(f_{ds}) + u_2(f_{nds}) \quad (5.13)$$

Let  $p_1$  and  $p_2$  represent two assigned bandwidth proportions in the case of the two traffic classes. They satisfy :  $p_1 + p_2 = 1$ . The objective function can be expressed as following:

$$\text{objective function: } \max_{RB_{i,j,k}, pw_{i,j,k}} U$$

subject to:

$$\begin{aligned} \text{C1: } & p_1 f_{ds} + p_2 f_{nds} \leq B \\ \text{C2: } & \alpha_{i,j,k} \in \{0, 1\} \\ \text{C3: } & \sum_{k=1}^K \alpha_{i,j,k} = 1, \quad i, j \\ \text{C4: } & \sum pw_{i,j,k} \leq P_{max}, \quad i, j, k \\ \text{C5: } & \sum_{j=1}^J \sum_{k=1}^K \alpha_{i,j,k} pw_{i,j,k} \leq P_{max}, \quad i \end{aligned} \tag{5.14}$$

where  $B$  is the available bandwidth,  $pw_{i,j,k}$  represents the power of the sub-carrier  $k$  with user  $j$  in the beam  $i$ , and  $P_{max}$  represents the maximum power allowed for each user. The constraints C2 and C3 are to emphasize that each sub-channel is allocated to one user in one beam. The constraints C4 and C5 denote the power constraint. First we solve the equation (3.6) according to the constraint number one (C1) to obtain the optimum values of  $p_1$  and  $p_2$ , then we check the validity of our solution according to the other constraints.

Put Equation (5.13) in the Lagrange form and take the derivatives of  $\mathcal{L}_{u_1}$ ,  $\mathcal{L}_{u_2}$  and  $\lambda_l$  with

respect to  $f_{ds}, f_{nds}$ , and  $\lambda_l$  respectively, we get:

$$\begin{aligned}
\max(\mathcal{L}) &= u_1(f_{ds}) + u_2(f_{nds}) + \lambda_l [B - p_1 f_{ds} - p_2 f_{nds}] \\
\mathcal{L}_{u_1} &= \frac{\partial \mathcal{L}}{\partial f_{ds}} = \frac{\partial}{\partial f_{ds}} \left( V \frac{\text{sgn}(f_{ds} - f_{min}) + 1}{2} \right) + \\
&\quad \frac{\partial}{\partial f_{ds}} [B - p_1 f_{ds} - p_2 f_{nds}] = 0 \quad f_{ds} = 0 \\
\mathcal{L}_{u_2} &= \frac{\partial \mathcal{L}}{\partial f_{nds}} = \frac{\partial}{\partial f_{nds}} \left( V \frac{\log(1 + f_{nds})}{\log(1 + f_{max})} \right) + \\
&\quad \frac{\partial}{\partial f_{nds}} [B - p_1 f_{ds} - p_2 f_{nds}] = 0 \quad f_{nds} = 0 \\
\mathcal{L}_\lambda &= \frac{\partial \mathcal{L}}{\partial \lambda} = B - p_1 f_{ds} - p_2 f_{nds} = 0 \quad \lambda = 0
\end{aligned} \tag{5.15}$$

where  $\lambda_l$  is the Lagrange multiplier. Going further in the solution, we get the following results:

$$\begin{aligned}
\mathcal{L}_{u_1} &= \frac{2 p_1 V \delta(f_{min})}{2} - \lambda p_1 = 0, \text{ which leads to :} \\
\lambda &= \frac{V}{p_1}
\end{aligned} \tag{5.16}$$

$$\begin{aligned}
\mathcal{L}_{u_2} &= \frac{\partial \mathcal{L}}{\partial f_{nds}} = \frac{V}{\log(1 + f_{max})} \frac{1}{1 + f_{nds}} - \lambda p_2 = 0, \text{ which gives:} \\
\lambda &= \frac{V}{p_2 \log(1 + f_{max})}
\end{aligned} \tag{5.17}$$

$$\mathcal{L}_\lambda = B - p_1 f_{ds} - p_2 f_{nds} = 0$$

By solving Equations (5.17) and (3.9), we get  $\frac{VC}{p_1} = \frac{V}{p_2 \log(1 + f_{max})}$ , which leads to :

$$\frac{p_1}{p_2} = \log(1 + f_{max}) \tag{5.18}$$

Let  $f_{min} = 64 \text{ kb/s}$  which is a proper value for the DS applications, this means  $f_{max} = 2 \cdot 64 \text{ kb/s}$ , which gives  $p_1 = 4.8 p_2$ . This means the bandwidth of the DS services will

be about five times the bandwidth for the NDS services. This means 80% of the available bandwidth will be assigned to the DS applications while 20% will be assigned to the NDS applications. Finally, the total data rate of the system is given by:

$$R_T = \sum_{i=1}^I \sum_{j=1}^J \sum_{k=1}^K \alpha_{i,j,k} RB_{i,j,k} \log_2 \left( 1 + \frac{pw_{i,j,k} h_{i,j,k}^2}{N_0 \frac{B}{N}} \right) \quad (5.19)$$

where  $RB_{i,j,k}$  represents the assigned resource blocks. Each resource block contains a certain number of sub-carriers.

## 5.5 Scheduling Procedure

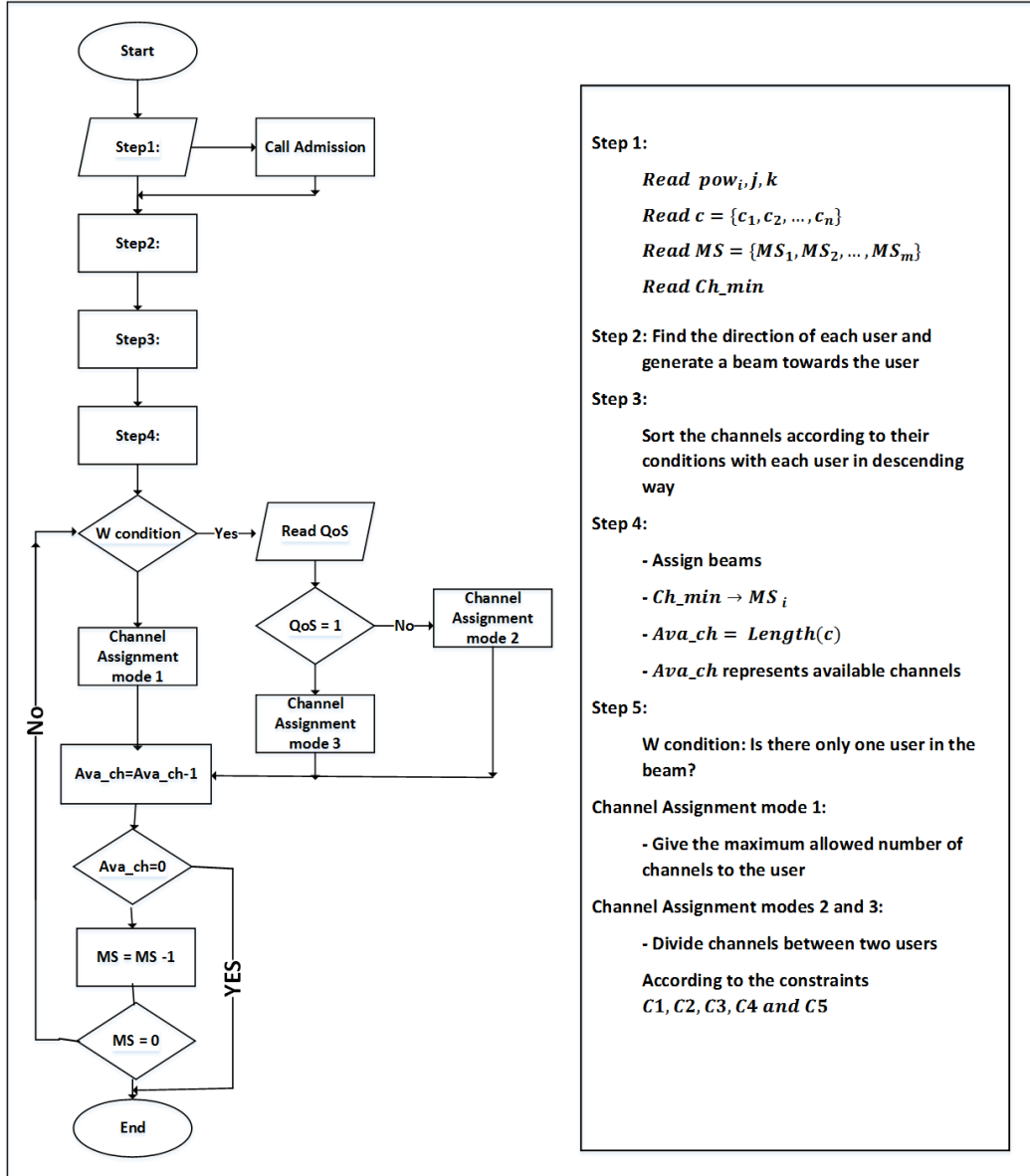


FIGURE 5.3: Scheduler Flowchart

Figure (5.3) shows the flowchart of the proposed scheduling algorithm. In the first step, the scheduler reads the power of each channel with each user  $pw_{i,j,k}$ , the available channels, the users who are asking for calls( we consider the calls are arriving according to the model described in section (III)), and the minimum number of channels that should be assigned

to each user. The second step includes finding the directions of the users in the cell as explained in algorithm 1. The third step contains the implementation of the frequency and the time diversities by sorting the channels in descending way according to the associated received power of each channel with each user. In the fourth step, the scheduler will assign the minimum required number of sub-channels to each user. The scheduler will choose the best sub-channels for each user. Then, the scheduler will find out if there is more than one user in the beam or not. This leads to step five where channel modes 1 2, and 3 represent the constraints two, three, four, and five.

## 5.6 Simulation Results

In this simulation, we fed our proposed scheduler with the results of our proposed algorithm MLMS. By knowing these results, the scheduler will be able to recognize the location of each user. In this simulation, we have used the same version of MATLAB, we have considered 100 sub-channels, each has 15 *kHz* bandwidth.

Moreover, we have considered 80 channels as the maximum allowed number of sub-channels to each QoS class according to Equation (5.18). Moreover, the minimum assigned bandwidth is also calculated according the same equation. In addition, the scheduler has always kept checking the validity of the power constraint according to the constraint  $C5$  in Equation (5.14).

Figure (5.4) depicts the relationship between the total aggregated data rate and the number of active users at different beam sizes. It shows that, as the beam size decreases, the total aggregated data rate will be increased. Note that, at a small number of users, the total aggregated data rates of the system is almost the same. However, when the number of users is increased, the total aggregated data rates of the system are significantly increased.

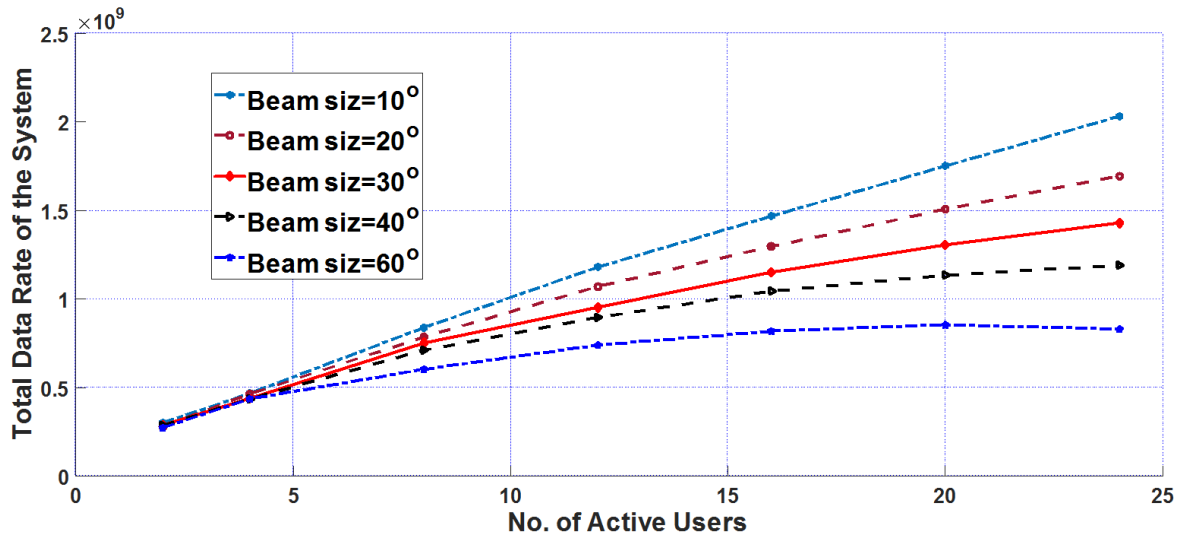


FIGURE 5.4: Total aggregated Data Rate at different beam sizes

Figure (5.5) depicts the same results in terms of the number of the occupied sub-channels at different beam sizes.

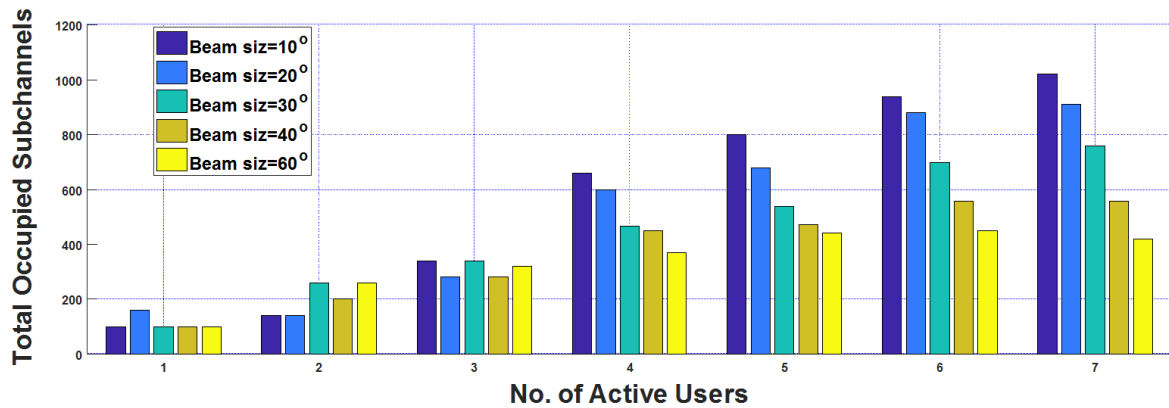


FIGURE 5.5: Total Occupied Subchannels at Different Beam Sizes

Table (5.2) explains the total aggregated data gain according to the decrease in the beam sizes. We have taken these results at 24 active number of users. Note that, the total aggregated throughput gain will be increased by increasing the number of the active users.

Beam size decrements	60°	40°	40°	30	30°	20	20°	10°
Total aggregated throughput Gain	30.3 %		16.67 %		15.64 %		16.64 %	

Table 5.2: Total aggregated throughput Gain

## 5.7 Conclusion

In this chapter , we have proposed a scheduling algorithm based on beamforming for 5G. Our scheduling scheme implements the scheduling based on the knowledge of the direction of the desired users. We use the utility function concept in order to optimally divide the available bandwidth between the DS and NDS services. Our simulation results shows that total aggregated data rates of the system have been improved by around 15% for each 10% decrease in the beam size.

# Chapter 6: Frequency Reuse Based on Beamforming for 5G

In this chapter, we present an approach for Frequency Reuse (FR) based on beamforming for 5G. This work is a continuation of the work in chapters three and four where we proposed a practical algorithm for finding the directions of the users in the cell and keep tracking them. In addition, we used the beamformer to produce a beam towards the desired direction and nulls toward the interferers. In this chapter, we introduce the implementation of the synthesizing techniques to smartly form the desired beam shape and make the nulls deeper. We use the features of the smart antenna (SA), beamforming efforts, and the radiation pattern (RP) synthesizing techniques to develop a FR plan for 5G. Further more, we have developed a formula for calculating the Signal to Interference and Noise Ratio (SINR) as a function of the desired and the interferers directions. Our condition is to keep the SINR at the lowest levels required by LTE. We started by dividing each standard hexagonal cell into six beams. Each beam is of size  $60^\circ$  width. After that based on the calculated SINR, we increase the number of beams from 6 to 12 beams and achieve a 36-beam cell plan.

## 6.1 The Concept of Transmit Beamforming

The beamforming process involves adjusting the weights of the antenna elements to receive and transmit from a certain direction. It increases the gain of the antenna in the desired direction. Furthermore, it creates nulls at the directions of the intereferers.

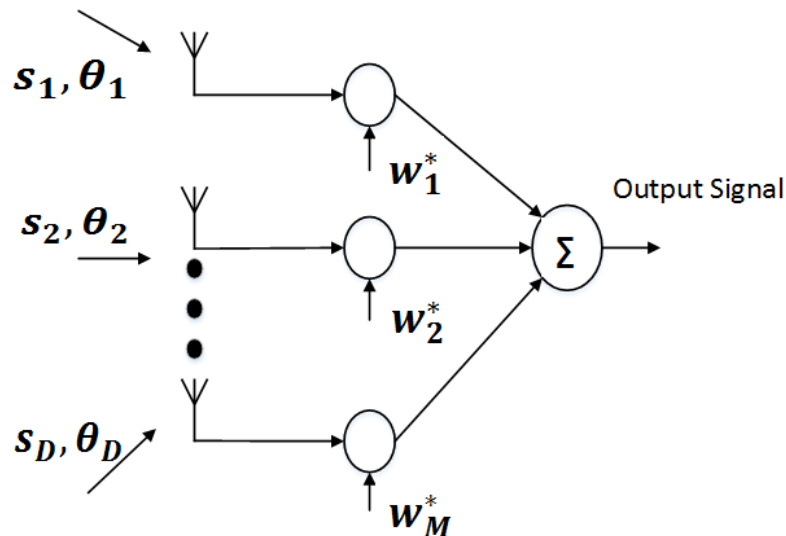


FIGURE 6.1: A General Beamforming System

Figure 6.1 explains the receive beamforming concept. The signal impinging on the antenna elements will be multiplied by the complex conjugate of the antenna elements weights  $w_m$ , where  $(\cdot)$  represents the complex conjugate of the antenna element weights. The output signal of the beamformer at any time  $n$ ,  $y_n(\theta)$ , is a linear combination of the signal at the  $M$  antenna elements. This is expressed as:

$$y_n(\theta) = \sum_{m=1}^M w_m \bar{x}_m(n), n = 1, 2, \dots, N \quad (6.1)$$

where  $\bar{x}_m(n)$  represents the received signal vector of length  $M$  at time  $n$ . Equation 6.1 can be written in the vector form as [71]:

$$y_n(\theta) = \bar{w}^H \bar{x}(n) \quad (6.2)$$

where  $^H$  represents the Hermitian transpose,  $\bar{w}$  represents the antenna weighting vector of length  $M$ , i.e.,  $\bar{w}^H = [w_1, w_2, \dots, w_M]$  of length  $M$  at time  $n$ . The received signal  $\bar{x}(n)$  is composed of the source signal and the noise. It is given by:

$$\bar{x}(n) = \bar{s}(n) + \bar{v}(n) \quad (6.3)$$

where  $\bar{s}(n)$  represents the source signal and  $\bar{v}(n)$  represents the AWGN at the same source. Both  $\bar{s}(n)$  and  $\bar{v}(n)$  are vectors of length  $N$ .  $N$  indicates the number of the received samples, i.e.,  $n = 1, 2, \dots, N$ . Since  $(\bar{A} \bar{B})^H = \bar{B}^H \bar{A}^H$ , where  $\bar{A}$  and  $\bar{B}$  are matrices, the beamformer output can be written as:

$$y_n(\theta) = \bar{x}^H(n) \bar{w} \quad (6.4)$$

In the case of transmit beamforming, the output of the beamformer can be expressed as:

$$y_n(\theta) = \bar{x}_t^H(n) \bar{w} \quad (6.5)$$

where  $\bar{x}_t(n)$  represents the signal to be transmitted. Equation 6.5 represents the output of the transmit beamformer. We assume that, the weighting vectors of all beamformers which are considered in our system model are optimum at the desired directions.

## 6.2 Radiation Pattern Shaping

The RP shaping or synthesizing is used to smartly shape the beam RP towards the desired direction, making deep nulls toward the interferers, and minimizing the Side-Lobe Levels (SLL). This can be achieved by finding the optimum weights of the antenna elements for a given beam-width, array elements positions, individual antenna RPs, and desired and interferers directions. This problem can be considered as a convex problem [91]. The procedure is to choose the weights in Equation (6.1) to achieve the desired pattern, therefore we would like

to maximize  $y(\theta_i)$  in the range  $\theta_i \in [\theta_{des} - \alpha, \theta_{des} + \alpha]$  where  $\alpha$  represents the HPBW,  $\theta_i$  represents the angle of the RP range, and  $\theta_{des}$  represents the angle of the desired direction. Also, we want to minimize the gain out of this range, i.e.  $y(\theta_i) \leq \tau$  for  $\theta_i \notin [\theta_{des} - \alpha, \theta_{des} + \alpha]$ . Our concern on minimizing the SLL. This is formulated as:

$$\begin{aligned} & \text{minimize } \max_i y(\theta_i) \\ & \text{subject to } y(\theta_{des}) = 1 \end{aligned} \tag{6.6}$$

By introducing a new variable  $\tau$ , Equation (6.6) is expressed as a convex formula as following:

$$\begin{aligned} & \text{minimize } \tau \\ & \text{subject to } y(\theta_i) \leq \tau \\ & \quad y(\theta_{des}) = 1 \end{aligned} \tag{6.7}$$

This represents a convex problem which can be solved using the interior point methods [91]. In the subsequent section, we use the DOA, beamforming concept, and the RP shaping to introduce the proposed FR mechanism.

### 6.3 Proposed Frequency Reuse Mechanism

In this Section, we present the proposed FR mechanism. We start by developing formulas for calculating the SINR based on the knowledge of the desired users and the interferers directions. Then, we introduce the proposed FR plan based on beamforming. After that, we set up the scenario and the formulas of the worst case analysis.

### 6.3.1 SINR Calculation

Assume that, the location of any user can be found [69]. Let the desired user be located at the point  $P(r, \theta_1)$ , where  $r$  represents the distance and  $\theta_1$  represents the direction of the mobile user. Moreover, suppose that the travel of the users from a beam to another can be tracked [70]. Furthermore, assume four beamformers are located at the center of a circular cell as shown in Figure 6.2. Each transmitted signal will be multiplied by the weighting vector of the beamformer.

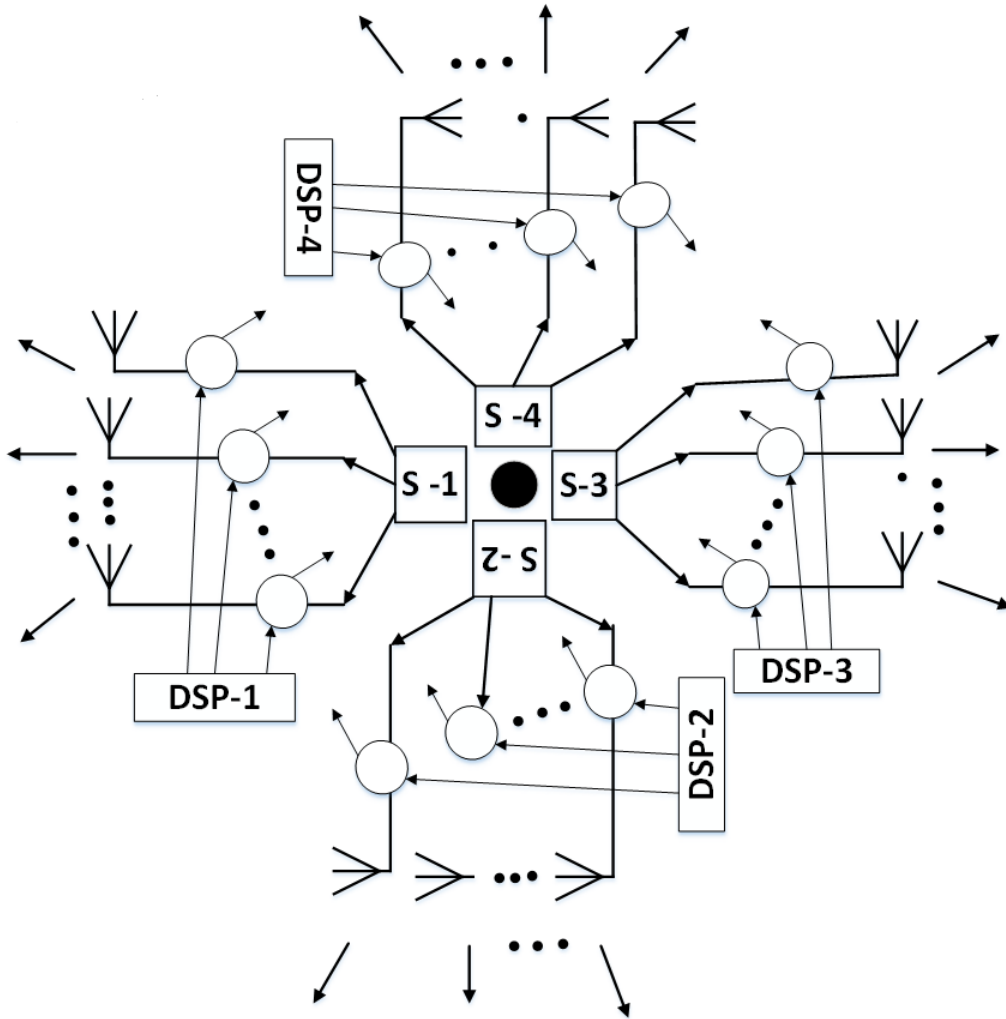


FIGURE 6.2: Four Beamformers Located at the Cell Center

Let  $S_i, i = 1, \dots, 4$  represent the information source of the beamformer  $i$ . Each beamformer is composed of  $M$  antenna elements. The surrounding conditions such as the path loss and the shadowing factor are the same for all the beamformers. Assume DSP- $i, i = 1, \dots, 4$  are digital signal processors used to optimally steer the beamformers toward the desired directions. The output signal of each beamformer at time  $n$  is given by:

$$y_{n_i}(\theta) = \bar{x}_i^H(n) \bar{w}_{i_{\theta_i}} \quad (6.8)$$

where  $\bar{w}_{i_{\theta_i}}, i = 1, \dots, 4$  represents the weighting vector of the beamformer  $i$  which generates a beam RP centered at  $\theta_i$ , and  $\bar{x}_i(n)$  represents the input signal of the beamformer  $i$ . Fig.6.3 shows a mobile antenna placed at the point  $P(r, \theta_1)$  which is located in the coverage area of the first beamformer.

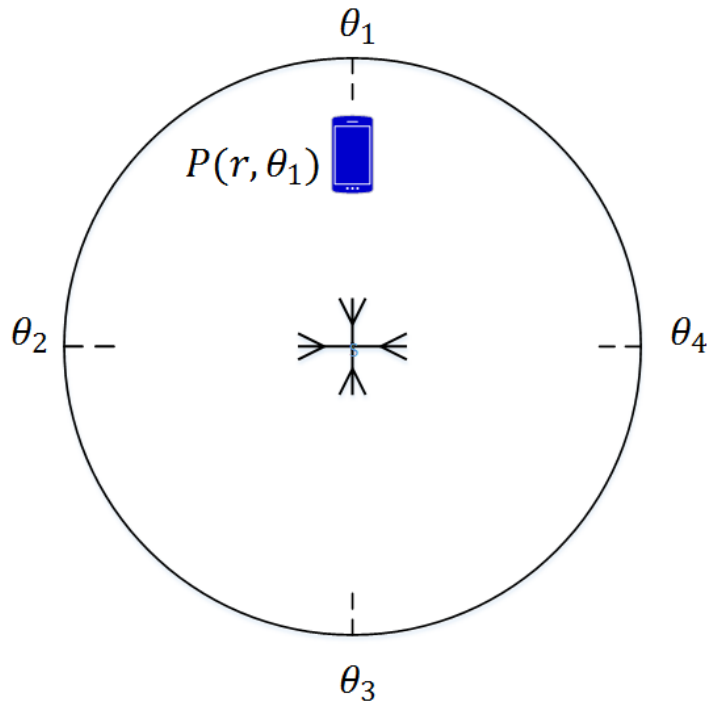


FIGURE 6.3: Four beamformers at the center and mobile placed at  $P(r, \theta_1)$ .

Since we assume that the direction of any user in the cell is known, therefore, the mobile

will adjust the weights of its antenna elements to transmit and receive from the first beamformer. This means, both, the beamformer and the mobile will use compatible weighting vectors to maximize their gain. For simplicity, we consider that, they use the same weighting vectors. Based on this, we may express the average power of the desired signal received by the mobile as:

$$S_{des} = \frac{\sum_{n=1}^N \sum_{m=1}^M y_{n_1}(\theta_1) w_{1\theta_{1m}}^2}{Nr^p} \quad (6.9)$$

where  $\bar{w}_{1\theta_1}$  represents the weighting vector of the first beamformer at  $\theta_1$ ,

i.e.,  $\bar{w}_{1\theta_1}^H = [w_{1\theta_{1_1}}, w_{1\theta_{1_2}}, \dots, w_{1\theta_{1_M}}]$ .

On the other hand, the signals which are coming from the other beamformers are considered as interfering signals. They will be multiplied by the weighting vector of the mobile which is different from them. The interfering signals are originally sent at the angles  $\theta_2$ ,  $\theta_3$ , and  $\theta_4$ . However, due to the reflections and the diffractions during their path toward the mobile, they will be received at the mobile at the angles  $\hat{\theta}_2$ ,  $\hat{\theta}_3$ , and  $\hat{\theta}_4$ , where  $(\hat{\cdot})$  represents an estimation of the original value. Therefore, the interfering signals are expressed as:

$$S_{interf} = \frac{\sum_{n=1}^N \sum_{m=1}^M y_{n_2}(\theta_2) w_{1\theta_{1m}}^2}{Nr^p} + \frac{\sum_{n=1}^N \sum_{m=1}^M y_{n_3}(\theta_3) w_{1\theta_{1m}}^2}{Nr^p} + \frac{\sum_{n=1}^N \sum_{m=1}^M y_{n_4}(\theta_4) w_{1\theta_{1m}}^2}{Nr^p} \quad (6.10)$$

and the  $SINR$  can be written as :

$$SINR = \frac{S_{des}}{S_{interf}} \quad (6.11)$$

The generalized formula of the  $SINR$  at a beamformer  $k$  can be written as:

$$SINR_{at\ k} = \frac{\sum_{n=1}^N \sum_{m=1}^M y_{n_k}(\theta_k) w_{k\theta_{km}}^2}{\sum_{i=1, i \neq k}^K (\sum_{n=1}^N \sum_{m=1}^M y_{n_i}(\theta_i) w_{k\theta_{km}}^2)} \quad (6.12)$$

where  $K$  represents the number of the beamformers. Note that, since we know the directions of the interferers, we can send deep nulls towards them. We will use this fact in calculating the SINR value.

### 6.3.2 Frequency Reuse Plan

We use the triangular shape as an approximation of the beam RP. The triangular shape represents the cells in the proposed system model. These cells are described by the triangle that connects between the center of the cell and the two HPBW power points at the RP. These two points can be defined in terms of their corresponding angles in the polar coordinates  $\theta_+$  and  $\theta_-$ . In addition, each two triangular cells represent a mini-cluster in our proposed model. Figure 6.4 shows the graphical representation of the proposed triangular beam cells. Also, it explains how we combine two beam cells in one mini-cluster.

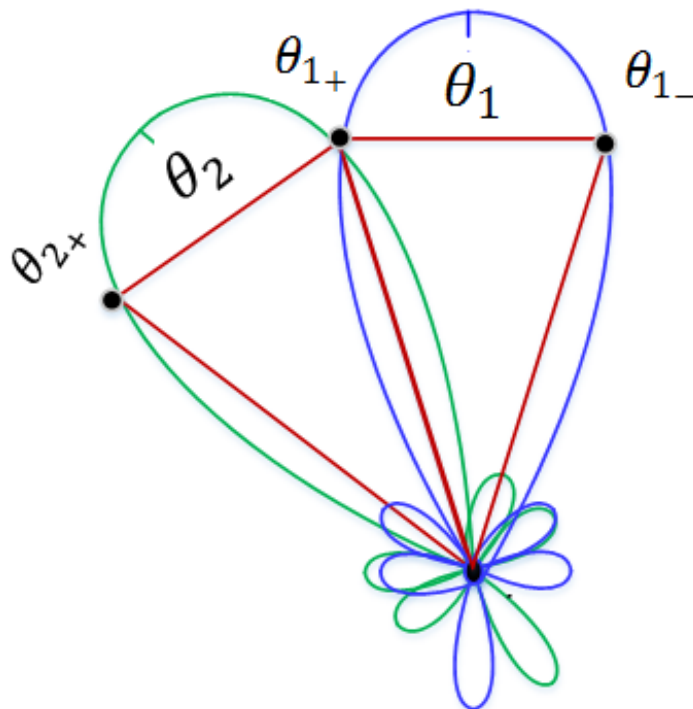


FIGURE 6.4: A mini-cluster composed of two cells

Furthermore, we use the hexagonal shape to approximate the clusters of our proposed model. Figure 6.5 shows the combination of our mini-clusters in one cluster, where A's and B's represent two sets of frequencies to be reused per each mini-cluster.

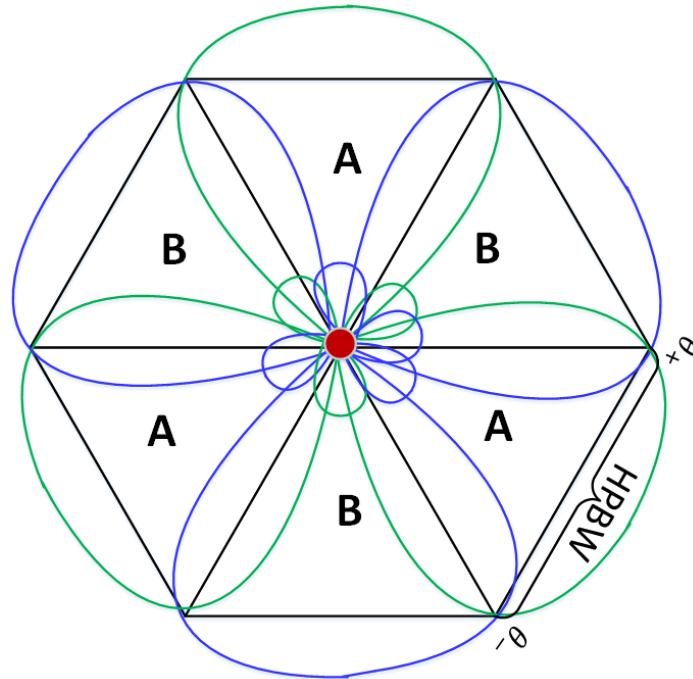


FIGURE 6.5: Cluster of six cells

To avoid the interference that might result from combining the clusters together, we choose A's such that they do not face other A's from the other clusters. Fig.6.6 shows how we combine the proposed mini-clusters and clusters in one FR plan. This combination is used to cover the whole intended coverage area.

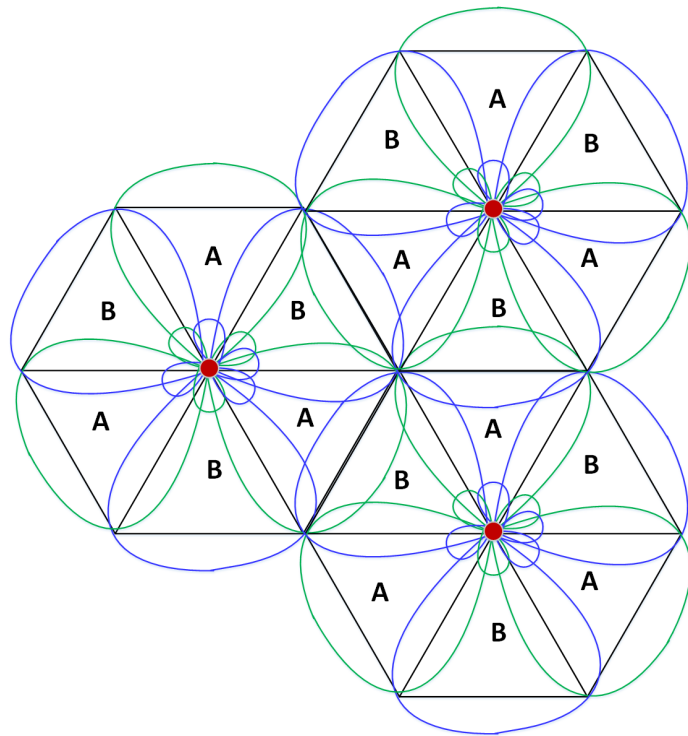


FIGURE 6.6: A combination of mini-clusters and clusters in one FR plan

Our goal is to move from one large beam cell to smaller while the required SINR is satisfied. This means going from Figure 6.7 (a) to 6.7 (b), 6.7 (c), and 6.7 (d).

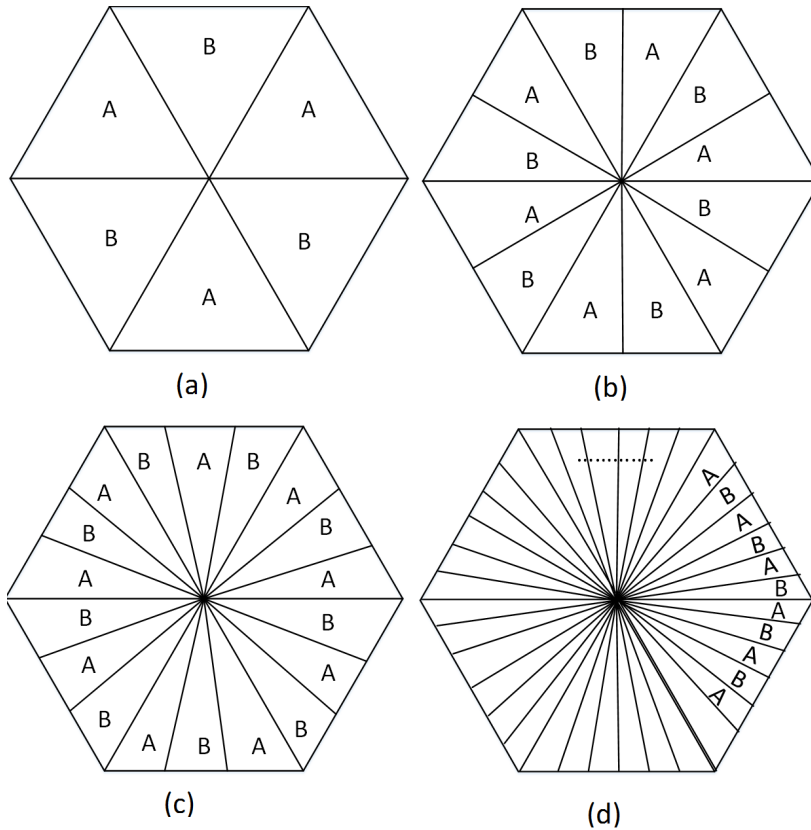


FIGURE 6.7: (a) Cluster of 6, (b) 12, (c) 18, and 36 cells

## 6.4 Worst Case Scenario Calculations

For the worst case scenario, consider a Base Station (BS) provided with the Smart Antenna (SA) capabilities located at the center of a standard cell. We call this BS as  $BS_1$ .  $BS_1$  has a beam RP centered at  $\theta_1$ . This is illustrated in Figure 6.8. The boundaries of the  $BS_1$ 's beam RP are described by  $\theta_{1+}$  and  $\theta_1$ . Consider a mobile located at one edge of the two beam RP edges of  $BS_1$ , let it be  $\theta_{1+}$ . The mobile is also provided with the SA capabilities. Since the directions of  $BS_1$  and the mobile are known, the mobile will adjust its SA in order to maximize its SINR and keep its gain maximum.

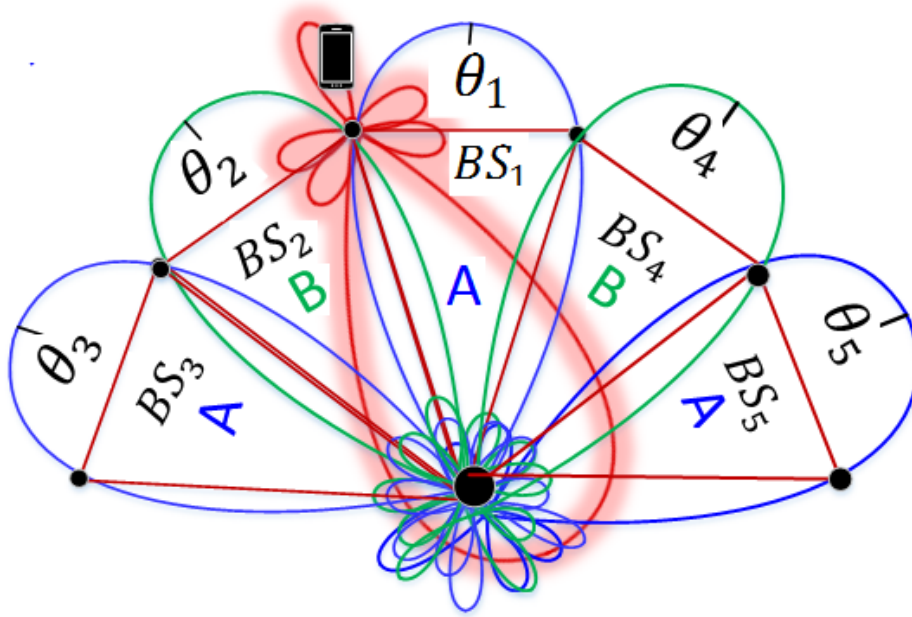


FIGURE 6.8: Worst Case Scenario

The mobile can maximize its gain by steering its beam radiation pattern to be centered at  $\theta_{1+}$ .  $\theta_{1+}$  represents the angle between the mobile and  $BS_1$ . The received signal at the mobile is expressed as:

$$S_{des} = \frac{\sum_{n=1}^N \sum_{m=1}^M y_{n_1(\theta_1)} w_{1_{\theta_{1+m}}}^2}{Nr^p} \quad (6.13)$$

Furthermore, consider additional four base stations located at the center of the cell. Let them be  $BS_2$ ,  $BS_3$ ,  $BS_4$ , and  $BS_5$ . Assume that they have beam RPs centered at  $\theta_2$ ,  $\theta_3$ ,  $\theta_4$ , and  $\theta_5$ , respectively. Due to the path reflections and diffractions, the signals which are transmitted by  $BS_2$ ,  $BS_3$ ,  $BS_4$ , and  $BS_5$  will be received at the mobile at the angles  $\hat{\theta}_2$ ,  $\hat{\theta}_3$ ,  $\hat{\theta}_4$ , and  $\hat{\theta}_5$ , respectively. The received signals from  $BS_3$  and  $BS_5$  represent interference for  $BS_1$  since they use the set of frequencies. The received signals from  $BS_3$  and  $BS_5$  will be

multiplied by the weighting vector of the mobile at  $\theta_{1+}$ . This is expressed as:

$$S_{interf} = \frac{\sum_{n=1}^N \sum_{m=1}^M y_{n_3(\theta_3)} w_{1\theta_{+m}}^2}{Nr^p} + \frac{\sum_{n=1}^N \sum_{m=1}^M y_{n_5(\theta_5)} w_{1\theta_{+m}}^2}{Nr^p} \quad (6.14)$$

and the SINR is written as:

$$SINR_{at\ Mobile} = \frac{\sum_{n=1}^N \sum_{m=1}^M y_{n_1(\theta_1)} w_{1\theta_{+m}}^2}{\sum_{i=1,5} (\sum_{n=1}^N \sum_{m=1}^M y_{n_i(\theta_i)} w_{1\theta_{+m}}^2)} \quad (6.15)$$

$$SINR_{at\ BS_1} = \frac{S_{des}}{S_{interf}} = \frac{\sum_{m=1}^M y_{n_1(\theta_1)} w_{1\theta_{+m}}^2}{\sum_{m=1}^M y_{n_3(\theta_3)} w_{1\theta_{+m}}^2 + \sum_{m=1}^M y_{n_5(\theta_5)} w_{1\theta_{+m}}^2} \quad (6.16)$$

### 6.4.1 Detailed Procedure

Figure 6.9 shows the proposed configuration for implementing the FR based on beamforming in 5G. This configuration is composed of DOA, correlator, adaptive beamforming, and synthesizer. We use the DOA and the correlator to find the users directions in the cell. Then, we use the adaptive beamforming process to produce a beam towards the desired user, nulls in the directions of the main beams of the interferers, and keep tracking the users. After that, we implement the synthesizer to make the radiation beam more focused towards the desired user and the nulls are deeper toward the interferers. This means, we apply a window that passes the desired user signal and significantly removes the interference coming from the interferers.

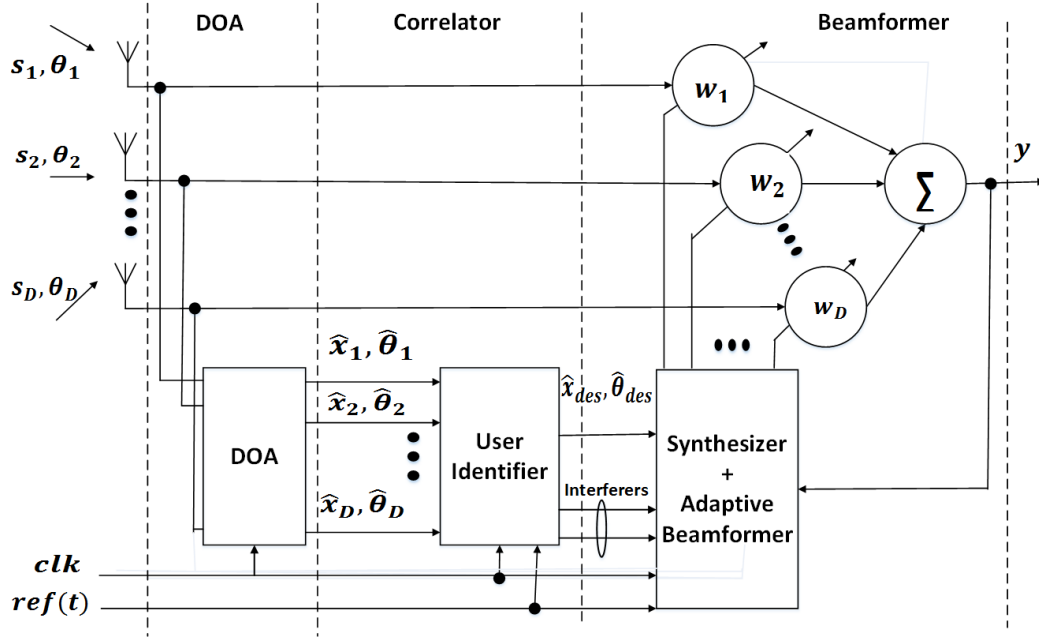


FIGURE 6.9: The proposed Configuration

Consider  $D$  signals are transmitted at angles  $\theta_1, \theta_2, \dots, \theta_D$  as shown in Figure 6.9. The steering vectors that correspond to these angles can be expressed as:

$$\bar{a}(\theta_i) = [1 \ e \ jkd \sin(\theta_i) \ e \ j2kd \sin(\theta_i) \ \dots \ e \ j(M-1)kd \sin(\theta_i)]^T \quad (6.17)$$

The output of the ULA can be written as:

$$\bar{x}(k) = \begin{bmatrix} \bar{x}_1(k) \\ \bar{x}_2(k) \\ \vdots \\ \bar{x}_D(k) \end{bmatrix} = [\bar{a}(\theta_1) \ \bar{a}(\theta_2) \ \dots \ \bar{a}(\theta_D)] \begin{bmatrix} \bar{s}_1(k) \\ \bar{s}_2(k) \\ \vdots \\ \bar{s}_M(k) \end{bmatrix} + \bar{n}(k) \quad (6.18)$$

The DOA part will give us estimated values of the transmitted angles at  $\hat{\theta}_1, \hat{\theta}_2 \dots \hat{\theta}_D$ . Therefore, the actual output of the DOA part is written as:

$$\hat{\mathbf{x}}(k) = \begin{bmatrix} \hat{x}_1(k) \\ \hat{x}_2(k) \\ \vdots \\ \hat{x}_D(k) \end{bmatrix} = [\bar{a}(\hat{\theta}_1) \bar{a}(\hat{\theta}_2) \dots \bar{a}(\hat{\theta}_D)] \begin{bmatrix} \bar{s}_1(k) \\ \bar{s}_2(k) \\ \vdots \\ \bar{s}_M(k) \end{bmatrix} + \bar{n}(k) \quad (6.19)$$

where  $\hat{(\cdot)}$  represents an estimation of the original value. Using the DOA part, we get peaks on the power spectrum at  $\hat{\theta}_1, \hat{\theta}_2 \dots \hat{\theta}_D$ . By applying the cross correlation between the Reference Signal (RS) and the incoming signals, we estimate the desired user signal and direction [69]. The correlation process is included in the User Identifier (UI) part. The UI separates the desired signal and the interference. The output signal of the UI is given by:

$$y_{UI}(k) = \bar{a}(\hat{\theta}_{des})^H \hat{x}_{des} \quad (6.20)$$

where  $\hat{x}_{des}$  and  $\hat{\theta}_{des}$  represent the estimated values of the desired user signal and direction, respectively. In the first cycle, the RS is compared with the output of the UI. This means, instead of comparing the RS with the ULA output which leads to a slow convergence and weak tracking capabilities, we provide the beamforming part with initial estimations of the desired user signal and direction. Therefore, the error at time  $t$  is written as:

$$e_{(t)}(k) = s_{ref}(k) - y_{(UI)}(k) = s_{ref}(k) - \bar{a}^H(\hat{\theta}_{des}) \hat{x}_{des}(k) \quad (6.21)$$

It should be noted, we have expressed  $e_{(t)}$  as a function of time because our model will keep comparing with the re-transmitted RS every small period of time. This is done for the tracking purpose. By taking the square of the Equation (6.21) and taking the expectation of

it, we get:

$$E \{ e_t(k)^2 \} = E \{ (s_{ref}(k) - y_{(UI)}(k))(s_{ref}(k) - y_{(UI)}(k))^H \} \quad (6.22)$$

It should be pointed out that  $y_{(t)}$  is an estimation of the desired user signal, therefore, the error from the beginning will be small. Equation (6.22) is a quadratic equation with a unique minimum. By taking the derivative with respect to  $\bar{w}$  and solving, we get:

$$\bar{w}_{opt} = \bar{R}_{x_{des}x_{des}}^{-1} \bar{r}_{rd} \quad (6.23)$$

where  $\bar{w}_{opt}$  expresses the optimum weights obtained by our algorithm,  $\bar{R}_{x_{des}x_{des}}^{-1}$  and  $\bar{r}_{rd}$  are given by:

$$\begin{aligned} \bar{R}_{x_{des}x_{des}} &= \bar{x}_{des}(k) \bar{x}_{des}^H(k) \\ \bar{r}_{rd} &= s_{ref}(k) \bar{x}_{des}(k) \end{aligned} \quad (6.24)$$

The updating equation of the beamformer is given by:

$$\bar{w}(k+1) = \bar{w}(k) + \mu [\bar{R}_{x_{des}x_{des}} \bar{w} - \bar{r}_{rd}] \quad (6.25)$$

where  $\mu$  represents the step size and its limited by:

$$0 < \mu < \frac{1}{2\lambda_{max}} \quad (6.26)$$

After the first cycle and obtaining the optimum weights, the *clk* will turn ON only the adaptive beamforming and the synthesizer parts. This means, the RS will be compared with the ULA output during the tracking process. If the user travels to a new place, the difference

between the RS and the ULA output will be increased which means the adaptive beamforming and the synthesizer parts will modify the antenna weights to redirect the antenna to the new direction. It is worth to note that, the classical adaptive beamforming algorithms can not work at large amount of interference. Providing the adaptive beamforming algorithms with the estimation of the desired signal and direction speeds up the convergence and makes the tracking process is possible. We apply the adaptive beamforming part to emphasize the DOA accuracy, produce beam towards the desired user and nulls in the directions of the interferers. In addition, we use the synthesizer to specifically control the antenna RP. This control includes forming a beam that passes signals from the desired directions, producing nulls in the directions of the interferers, and controlling the SLLs.

## 6.5 Simulation Results

In this section we have developed a simulation model to evaluate the performance of our proposed FR plan. We have used the Matlab R2017b to obtain our simulation results. Our simulation model uses the Convex Optimization method to perform the synthesizing process, and to calculate the minimum required number of antenna elements at each specified beam size at different SINR values. As an example, Figure 6.10 shows a scenario of cluster composed of 24 beams and mobile placed at a beam boundary. Each beam has size of  $15^\circ$  width measured at the two HPBW points. A and B represent a set of frequencies to be reused inside the cluster. The boundaries of the beams are also shown in the same figure. We consider a mobile placed at the boundary between two beams at angle  $90^\circ$  which is the worst case scenario.

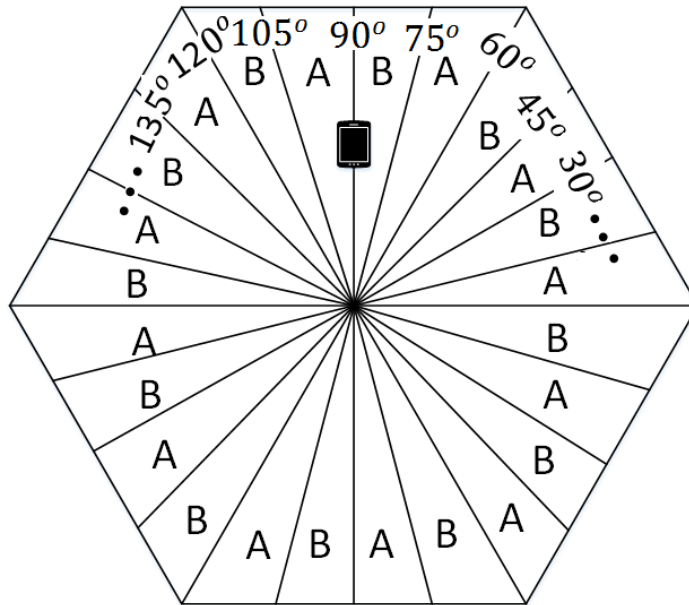


FIGURE 6.10: Cluster of 24 beams and mobile placed at a beam boundary.

We assume the mobile detects the interfering signals coming at the angles  $60^\circ$  and  $120^\circ$ . Using the combination of the beamformer and the synthesizer, the mobile should place the nulls at the angles  $60^\circ$ ,  $120^\circ$ . We present Figure 6.11 to illustrate how we can get the desired beam shape and place the nulls at the desired directions. Figure 6.11 shows a beam centered at  $90^\circ$  with beam-width of  $15^\circ$  measured at the two  $-3\text{dB}$  points. In this figure, SLL in  $\text{dB}$  is drawn versus the looking angle.

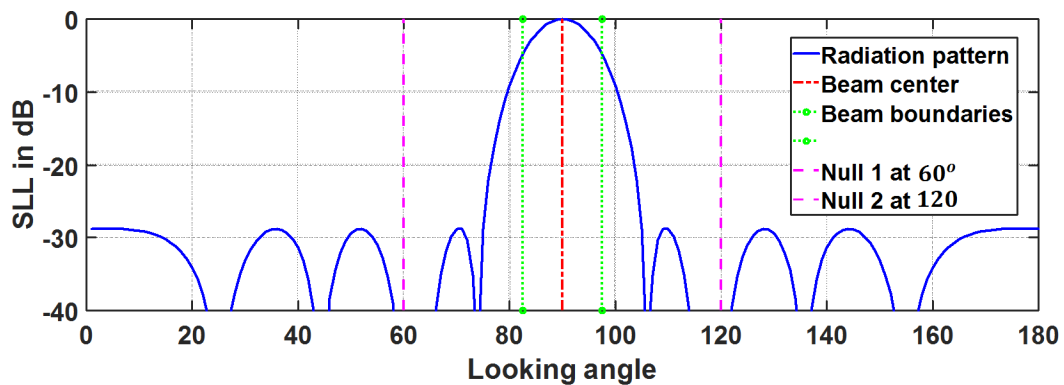


FIGURE 6.11: Beam shape in the Cartesian coordinates with  $HPBW = 15^\circ$  centered at  $90^\circ$ .

Figure 6.12 sketches the same results in the polar coordinates. It shows the RP, SLL value, beam boundaries, and the nulls placements

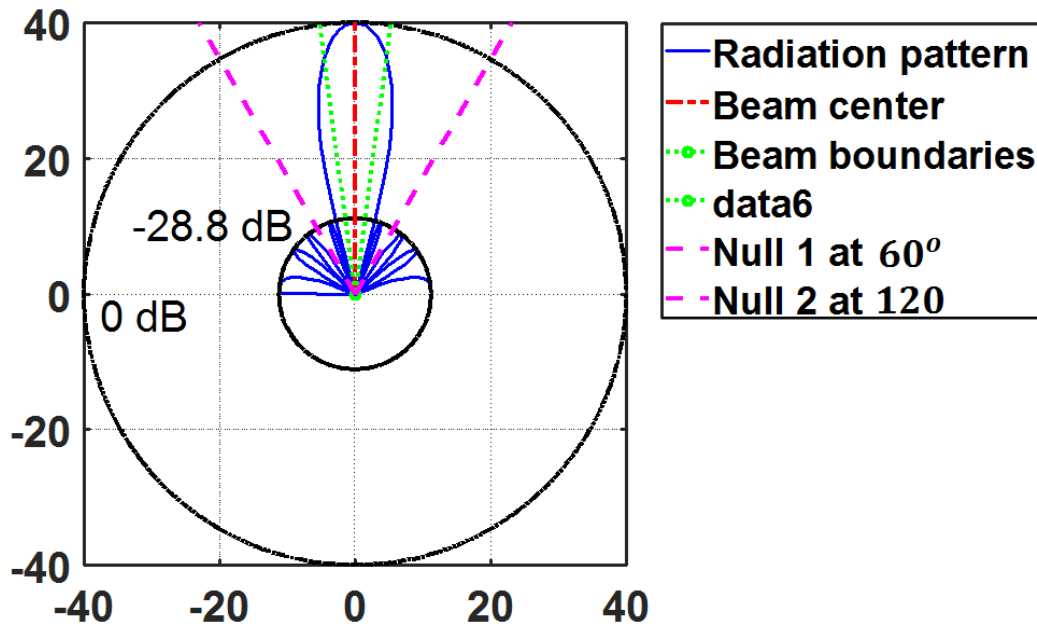


FIGURE 6.12: Beam shape in the Polar coordinates with  $HPBW = 15^\circ$  centered at  $90^\circ$  and  $SLL = -28.7\text{ dB}$ .

As an additional example, Figure 6.13 and Figure 6.14 depict a beam radiation pattern of  $10^\circ$  width in the Cartesian and Polar coordinates, respectively. Here, we assume the mobile detects the interfering signals coming at the angles  $10^\circ$ , and  $70^\circ$ . The dashed lines show the nulls placements.

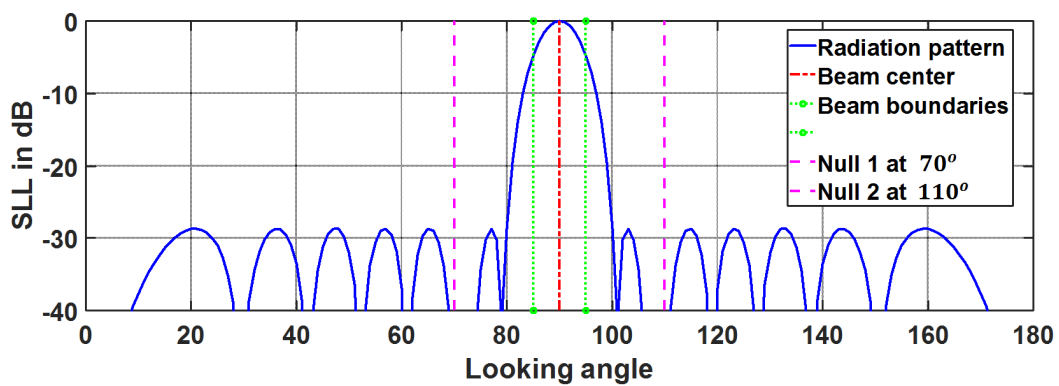


FIGURE 6.13: Beam shape in the Cartesian coordinates with  $HPBW = 10^\circ$  centered at  $90^\circ$ .

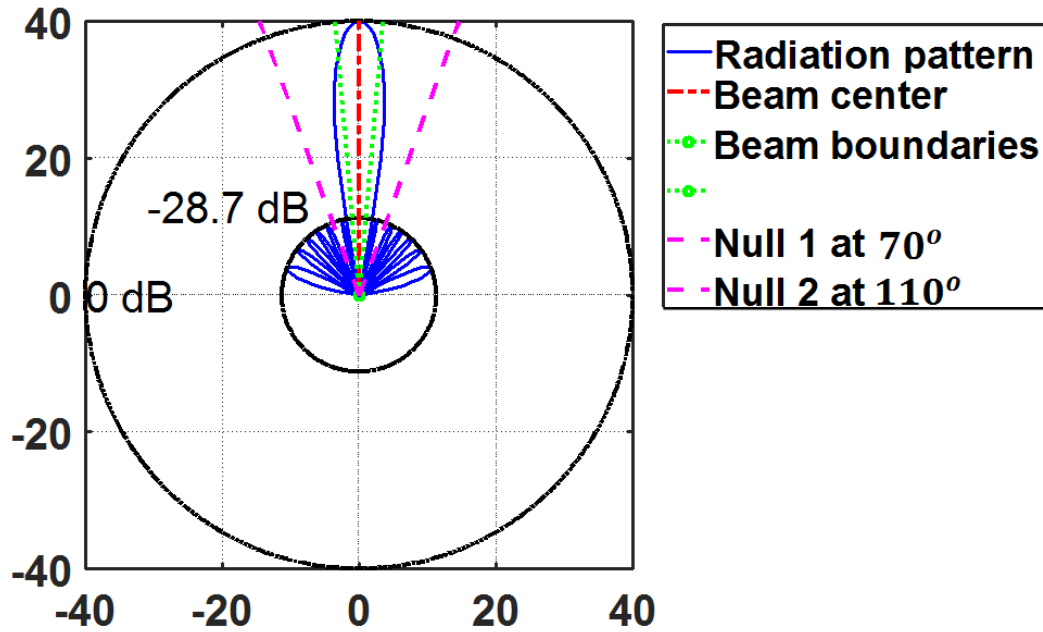


FIGURE 6.14: Beam shape in the Polar coordinates with  $HPBW = 10^\circ$  centered at  $90^\circ$  and  $SLL = -28.8\text{ dB}$ .

Furthermore, we present Figure 6.15 to show that we can realize a FR plane based on small size beams, and small number of antenna elements while keeping the SINR at acceptable levels. Figure 6.15 shows the relationship between the required number of antenna elements and the proposed beam sizes. For instant, to build up a FR plan based on beams of size  $60^\circ$  width, we need a SA composed of about 4 elements to provide  $SINR = 28\text{ dB}$ . Also, we need a SA composed of 2 elements to provide  $SINR = 21\text{ dB}$  for the same frequency reuse plan. Note that,  $SINR = 21\text{ dB}$  provides a very acceptable LTE data calls.

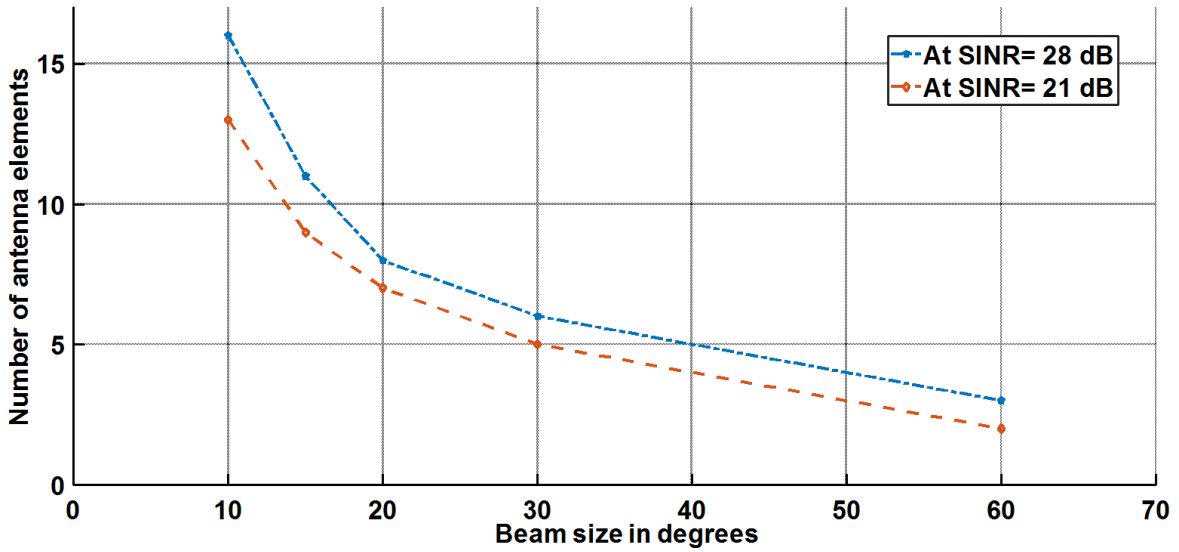


FIGURE 6.15: Beam size with number of antenna elements.

## 6.6 Conclusion

We have introduced a very efficient mechanism for a FR scheme based on beamforming for 5G. The proposed mechanism starts with implementing the DOA and the correlator to find the directions of the users and the interferers in the cell. Then, we have introduced the usage of the beamformers to enhance the accuracy of the obtained DOAs, tracking the users while they are moving, producing a beam towards the desired user direction and nulls toward the interferers. The third part of the proposed FR mechanism includes the implementation of the synthesizer. We implement the synthesizer to perfectly form the beam RPs, and to make the nulls deeper. The fourth part of the proposed FR mechanism includes the use of the knowledge of the users and interferers directions, and the capability of tracking in a very efficient FR scheme. We have built up the FR scheme based on the proposed system capabilities. Also, we have presented SINR formula that calculates the SINR in terms of the desired and interferers directions. The simulation results verify that, using a ULA of 11 elements, we can achieve the preferable SINR values using beams of  $10^\circ$  width. This will significantly increase the FR factor from 1 to 18 and multiplies the number of mobile users by 18 times.

# Chapter 7: Conclusion and Future Work

## 7.1 Conclusion

The implementation of SDMA is the key element to meet the exponentially increasing demand on the limited resources in mobile communications. Knowing the direction of the users provides the possibility of using scheduling and frequency reuse techniques in an efficient way. In this research, we have introduced a method to identify the desired user from the interferences by applying the cross correlation between the received signals and the RF signal which is known by the transmitter and receiver. Also, by implementing an adaptive processor algorithm such APA which has a fast convergence rate, we have improved the accuracy of the obtained DOA of the desired user by determining the optimum complex weights.

Moreover, we have proposed a novel algorithm for adaptive beamforming. In this algorithm, the MUSIC and LMS algorithms are combined to find the direction of the users then directing the antenna beams toward them. The results confirm that the proposed algorithm MLMS algorithm is very efficient in terms of convergence and the capability to track the desired user signal. We have improved the tracking of the desired signal and the mean square error convergence to occur after 13 iterations instead of 85 which means 84.7 % improvement. The proposed algorithm shows powerful efforts to track the desired signal and offers

much faster convergence than the traditional LMS algorithm. Furthermore, we have introduced the concept of scheduling based on performing using the adaptively generated beams which we have generated by MLMS. The total aggregated throughput of the system has been improved by 15% for each  $10^0$  decrease in the beam size.

In addition, we have introduced a very powerful mechanism of constructing an optimum FR scheme based on beamforming for 5G. The proposed system model begins with applying the DOA plus the correlator in order to figure out the directions of the users in the cell. Then, we have introduced the implementation of the beamformers to enhance the accuracy of the obtained DOAs, tracking the users movements, generating a beam towards the desired direction and nulls towards the interferers. The third component of the proposed system model involves the implementation of the synthesizer. We use the synthesizer to perfectly form the shape of the beam RPs and to make the nulls deeper. The fourth component of the proposed system includes the use of the knowledge of the users and interferers directions and the capability of tracking in a very efficient FR scheme. We have built up the FR scheme based on the proposed system capabilities. Also, we have presented SINR formula that calculates the SINR in terms of the desired and interferers directions. The simulation results show that we might have large SINR values along with implementing very small beam sizes in the standard cells. This will significantly increase the available bandwidth for the coming generations of the mobile communication systems.

## **7.2 Future Work**

There are several directions that might be pursued based on this thesis. We present below some directions for the possible extensions:

### **7.2.1 Compare between the LMS, RLS, and APA adaptive beamforming algorithms in the presence of the correlator**

In this direction, the tracking model might be expanded to cover the other adaptive beamforming algorithms such as NLMS and RLS. This includes giving the mathematical and performance analysis. The study should contain an analytical comparison between the LMS, RLS, and APA adaptive beamforming algorithms in the presence of the adaptive transmission of reference signal. This comparison should be performed in terms of the tracking capabilities, error convergence speed, execution time, and the complexity.

### **7.2.2 Calculating the system capacity based on the proposed frequency reuse and beamforming**

It is significant and interesting to calculate the system capacity that we get after applying the proposed frequency reuse based on beamforming scheme. The resultant capacity should be calculated in the presence of the DS and NDS services. This can be done by developing a three dimensional Markov chain. The dimensions are the arriving rate of the DS calls, the arriving rate of the NDS calls, and the probability of users moving from beam to an other beam at different beam sizes. Moreover, it should be calculated in terms of the available channels, and in terms of the acceptable blocking probability value.

### **7.2.3 Analyze the performance of the proposed scheduling and frequency reuse schemes in the presence of more than two QoS classes**

Our scheduling and FR schemes were built based on the existence of two QoS classes. In this direction, the study can be expanded to include three, four, and five QoS classes. The goal

is to study the improvement in the total aggregated throughput of the system while keeping eye on the complexity increase.

#### **7.2.4 Designing the best antenna for the proposed frequency reuse based on beamforming**

In this direction, there is a possibility to work on studying different possible antenna structures and find out the design that can be compatible with our proposed frequency reuse based on beamforming scheme. The study should include considering different synthesizing algorithms such as the convex synthesizing, genetic algorithm, and particle swarm optimization. The performance should be analyzed in terms of the number of the required antenna elements, and side lobe reduction levels.

# Bibliography

- [1] R. Rummmler, A. D. Gluhak, and H. Aghvami, *Multicast in Third-Generation Mobile Networks: Services, Mechanisms and Performance*. Wiley Publishing, 2009.
- [2] L. Korowajczuk, *ImmLTE, WiMAX and WLAN Network Design, Optimization and Performance Analysis*. John Wiley & Sons, 2011.
- [3] E. Dahlman, S. Parkvall, J. Skold, and P. Beming, *3G Evolution: HSPA and LTE for Mobile Broadband*. Academic press, 2010.
- [4] V. Garg, *Wireless Communications & Networking*. Elsevier, 2010.
- [5] T. Halonen, J. Romero, and J. Melero, *GSM, GPRS and EDGE Performance: Evolution Towards 3G/UMTS*. John Wiley & Sons, 2004.
- [6] H. Kaaranen, A. Ahtiainen, L. Laitinen, S. Naghian, and V. Niemi, *UMTS Networks: Architecture, Mobility and Services*. John Wiley & Sons, 2005.
- [7] Y. Rao, W.-C. Yeung, and A. Kripalani, Third-generation (3g) radio access standards , IEEE Communication Technology Proceedings, 2000. WCC-ICCT 2000, vol. 2, 2000, pp. 1017 1023.
- [8] J. Korhonen, *Introduction to 3G Mobile Communications*. Artech House, 2003.
- [9] A. Ghosh, J. Zhang, J. G. Andrews, and R. Muhamed, *Fundamentals of LTE*. Pearson Education, 2010.
- [10] H. Holma and A. Toskala, *HSDPA/HSUPA for UMTS: High Speed Radio Access for Mobile Communications*. John Wiley & Sons, 2007.

- [11] H. Holma and A. Toskala, *WCDMA for Umts: HSPA Evolution & LTE*. Wiley, 2007.
- [12] H. Holma and A. Toskala, *LTE Advanced: 3GPP Solution for IMT-Advanced*. John Wiley & Sons, 2012.
- [13] A. Ghosh, R. Ratasuk, B. Mondal, N. Mangalvedhe, and T. Thomas, Lte-advanced: Next-generation wireless broadband technology , *IEEE wireless communications*, vol. 17, no. 3, 2010.
- [14] P. Phunchongharn, E. Hossain, and D. I. Kim, Resource allocation for device-to-device communications underlying lte-advanced networks , *IEEE Wireless Communications*, vol. 20, no. 4, pp. 91–100, 2013.
- [15] J. Lee, Y. Kim, H. Lee, B. L. Ng, D. Mazzaresse, J. Liu, W. Xiao, and Y. Zhou, Coordinated multipoint transmission and reception in lte-advanced systems , *IEEE Communications Magazine*, vol. 50, no. 11, 2012.
- [16] D. Astely, E. Dahlman, G. Fodor, S. Parkvall, and J. Sachs, Lte release 12 and beyond [accepted from open call] , *IEEE Communications Magazine*, vol. 51, no. 7, pp. 154–160, 2013.
- [17] J. Lee, Y. Kim, Y. Kwak, J. Zhang, A. Papasakellariou, T. Novlan, C. Sun, and Y. Li, Lte-advanced in 3gpp rel-13/14: An evolution toward 5g , *"IEEE Communications Magazine"*, vol. 54, no. 3, pp. 36–42, 2016.
- [18] C. Hoymann, D. Astely, M. Stattin, G. Wikstrom, J.-F. Cheng, A. Hoglund, M. Frenne, R. Blasco, J. Huschke, and F. Gunnarsson, Lte release 14 outlook , *IEEE Communications Magazine*, vol. 54, no. 6, pp. 44–49, 2016.
- [19] A. B. Constantine *et al.*, *Antenna theory: Analysis and design* , *MICROSTRIP ANTENNAS, third edition*, John Wiley & Sons, 2005.
- [20] J. C. Liberti and T. S. Rappaport, *Smart Antennas for Wireless Communications: IS-95 and Third Generation CDMA Applications*. Prentice Hall PTR, 1999.

- [21] R. Schmidt, Multiple emitter location and signal parameter estimation , *IEEE transactions on antennas and propagation*, vol. 34, no. 3, pp. 276–280, 1986.
- [22] R. Roy, A. Paulraj, and T. Kailath, Estimation of signal parameters via rotational invariance techniques-esprit , *IEEE MILCOM 1986 - IEEE Military Communications Conference: Communications-Computers: Teamed for the 90's*, 1985, pp. 83–89.
- [23] K. A. Midfa, G. V. Tsoulos, and A. Nix, Performance evaluation of direction-of-arrival (doa) estimation algorithms for mobile communication systems , *IEEE 51st VTC 2000-Spring Tokyo.*, vol. 2, pp. 1055–1059.
- [24] R. J. Weber and Y. Huang, Analysis for capon and music doa estimation algorithms , *IEEE Antennas and Propagation Society International Symposium APSURSI'.*, 2009, pp. 1–4.
- [25] Z. Ye, J. Dai, X. Xu, and X. Wu, Doa estimation for uniform linear array with mutual coupling , *IEEE Transactions on Aerospace and Electronic Systems*, vol. 45, no. 1, pp. 280–288, 2009.
- [26] G. Bartoli, R. Fantacci, D. Marabissi, and M. Pucci, Lte-a femto-cell interference mitigation with music doa estimation and null steering in an actual indoor environment , *IEEE International Conference on Communications (ICC)*, 2013, pp. 2707–2711.
- [27] C. Gentner and T. Jost, Indoor positioning using time difference of arrival between multipath components , *IEEE International Conference on Indoor Positioning and Indoor Navigation*, 2013, pp. 1–10.
- [28] U. Hamid and S. A. Abbas, Application of high resolution direction finding algorithms in mobile communications , *IEEE International Conference on Intelligent Systems Engineering (ICISE)*, 2016.

- [29] C. Cox, *An Introduction to LTE: LTE, LTE-advanced, SAE and 4G Mobile Communications*. John Wiley & Sons, 2012.
- [30] N Sonbolestan and S. Hadei, A fast affine projection algorithm based on matching pursuit in adaptive noise cancellation for speech enhancement , *IEEE Intelligent Systems, Modelling and Simulation (ISMS)*, 2010, pp. 193–198.
- [31] S. G. Sankaran and A. L. Beex, Convergence behavior of affine projection algorithms , *IEEE Transactions on Signal Processing*, vol. 48, no. 4, pp. 1086–1096, 2000.
- [32] J. Srar and K.-S. Chung, Adaptive rlms algorithm for antenna array beamforming , *Proceedings of IEEE TENCON 2009*, pp. 1–6, 2009.
- [33] J. A. Srar and K.-S. Chung, Performance of rlms algorithm in adaptive array beamforming , *IEEE Communication Systems ICCS 2008. 11th Singapore International Conference on*, 2008, pp. 493–498.
- [34] J. A. Srar and K.-S. Chung, Rlms algorithm for fixed or adaptive beamforming , *IEEE 9th Malaysia International Conference on Communications (MICC)*, 2009, pp. 163–167.
- [35] J. A. Srar, K.-S. Chung, and A. Mansour, Analysis of the rlms adaptive beamforming algorithm implemented with finite precision , *IEEE 16th Asia-Pacific Conference on Communications (APCC)*, 2010, pp. 231–236.
- [36] J. A. Srar, K. Chung, and A. Mansour, A new llms algorithm for antenna array beamforming , *IEEE Wireless Communication and Networking Conference*, 2010, pp. 1–5.
- [37] J. A. Srar, K.-S. Chung, and A. Mansour, Adaptive array beamforming using a combined lms-lms algorithm , *IEEE Transactions on Antennas and Propagation*, vol. 58, no. 11, pp. 3545–3557, 2010.

- [38] J. A. Srar, K.-S. Chung, and A. Mansour, Performance of an llms beamformer in the presence of element gain and spacing variations , IEEE The 17th Asia Pacific Conference on Communications, 2011, pp. 593 598.
- [39] J. A. Srar, K. Chung, and A. Mansour, Analysis of the rlms adaptive beamforming algorithm implemented with finite precision , IEEE 16th Asia-Pacific Conference on Communications (APCC), 2010, pp. 231 236.
- [40] R. de Francisco, M. Kountouris, D. T. Slock, and D. Gesbert, Orthogonal linear beamforming in mimo broadcast channels , IEEE Wireless Communications and Networking Conference WCNC, 2007, pp. 1210 1215.
- [41] P. Svedman, S. K. Wilson, L. J. Cimini, and B. Ottersten, Opportunistic beamforming and scheduling for ofdma systems , *IEEE Transactions on Communications*, vol. 55, no. 5, pp. 941 952, 2007.
- [42] W. Yu, T. Kwon, and C. Shin, Multicell coordination via joint scheduling, beamforming, and power spectrum adaptation , *IEEE Transactions on Wireless Communications*, vol. 12, no. 7, pp. 1 14, 2013.
- [43] M. Yazdanpanah, C. Assi, and Y. Shayan, Cross-layer optimization for wireless mesh networks with smart antennas , *Computer Communications*, vol. 34, no. 16, pp. 1894 1911, Elsevier 2011.
- [44] M. Yazdanpanah, C. Assi, and Y. Shayan, Optimal joint routing and scheduling in wireless mesh networks with smart antennas , IEEE International Symposium on "A World of Wireless, Mobile and Multimedia Networks" (WoWMoM), 2010, pp. 1 7.
- [45] M. Yazdanpanah, S. Sebbah, C. Assi, and Y. Shayan, Impact of successive interference cancellation on the capacity of wireless networks: Joint optimal link scheduling and power control , IEEE International Conference on Communications (ICC), 2013, pp. 1582 1587.

- [46] C. Liu, L. Shi, and B. Liu, Utility-based bandwidth allocation for triple-play services , *IEEE Fourth European Conference on Universal Multiservice Networks*, vol. 2, 2007, pp. 327–336.
- [47] A. Gohil, H. Modi, and S. K. Patel, 5g technology of mobile communication: A survey , *IEEE International Conference on Intelligent Systems and Signal Processing (ISSP)*, 2013, pp. 288–292.
- [48] G. J. Mullett, *Wireless Telecommunications Systems and Networks*. Cengage Learning, 2005.
- [49] J. Javaudin, J. Lainé, D. Lacroix, and O. Seller, On inter-cell interference in ofdma wireless systems , *IEEE 13th European Signal Processing Conference*, 2005, pp. 1–4.
- [50] H. Holma and A. Toskala, *LTE for UMTS: OFDMA and SC-FDMA Based Radio Access*. John Wiley & Sons, 2009.
- [51] T. D. Novlan, R. K. Ganti, A. Ghosh, and J. G. Andrews, Analytical evaluation of fractional frequency reuse for ofdma cellular networks , *IEEE Transactions on wireless communications*, vol. 10, no. 12, pp. 4294–4305, 2011.
- [52] H. E.E.O. M. Elfadil, M. A. I. Ali, and M. Abas, Fractional frequency reuse in lte networks , *IEEE 2nd World Symposium on Web Applications and Networking (WSWAN)*, 2015, pp. 1–6.
- [53] N. Saquib, E. Hossain, and D. I. Kim, Fractional frequency reuse for interference management in lte-advanced hetnets , *IEEE Wireless Communications*, vol. 20, no. 2, pp. 113–122, 2013.
- [54] S. M. Razavizadeh, M. Ahn, and I. Lee, Three-dimensional beamforming: A new enabling technology for 5g wireless networks , *IEEE Signal Processing Magazine*, vol. 31, no. 6, pp. 94–101, 2014.

- [55] A. Nordrum and K. Clark, Everything you need to know about 5g , *IEEE Spectrum*, 2017.
- [56] A. L. Swindlehurst, E. Ayanoglu, P. Heydari, and F. Capolino, Millimeter-wave massive mimo: The next wireless revolution? , *IEEE Communications Magazine*, vol. 52, no. 9, pp. 56–62, 2014.
- [57] F. Boccardi, R. W. Heath, A. Lozano, T. L. Marzetta, and P. Popovski, Five disruptive technology directions for 5g , *IEEE Communications Magazine*, vol. 52, no. 2, pp. 74–80, 2014.
- [58] B. Debaillie, B. van Liempd, B. Hershberg, J. Craninckx, K. Rikkinen, D. J. van den Broek, E. A. M. Klumperink, and B. Nauta, In-band full-duplex transceiver technology for 5g mobile networks , *IEEE ESSCIRC Conference 2015 - 41st European Solid-State Circuits Conference (ESSCIRC)*, 2015, pp. 84–87.
- [59] Q. C. Li, H. Niu, A. T. Papathanassiou, and G. Wu, 5g network capacity: Key elements and technologies , *IEEE Vehicular Technology Magazine*, vol. 9, no. 1, pp. 71–78, 2014.
- [60] F. Haider, C. Wang, H. Haas, D. Yuan, H. Wang, X. Gao, X.-H. You, and E. Hepsaydir, Spectral efficiency analysis of mobile femtocell based cellular systems , *IEEE 13th International Conference on Communication Technology*, vol. 11, 2011, pp. 347–51.
- [61] C.-X. Wang, F. Haider, X. Gao, X.-H. You, Y. Yang, D. Yuan, H. Aggoune, H. Haas, S. Fletcher, and E. Hepsaydir, Cellular architecture and key technologies for 5g wireless communication networks , *IEEE Communications Magazine*, vol. 52, no. 2, pp. 122–130, 2014.
- [62] N. Al-Falahy and O. Y. K. Alani, Design considerations of ultra dense 5g network in millimetre wave band , *IEEE Ninth International Conference on Ubiquitous and Future Networks (ICUFN)*, 2017, pp. 141–146.

- [63] I. Ahmed, H. Khammari, A. Shahid, A. Musa, K. S. Kim, E. De Poorter, and I. Mörner, A survey on hybrid beamforming techniques in 5g: Architecture and system model perspectives , *IEEE Communications Surveys & Tutorials*, vol. 20, no. 4, pp. 3060–3097, 2018.
- [64] W. Lee, S.-R. Lee, H.-B. Kong, and I. Lee, 3d beamforming designs for single user mimo systems , *IEEE Global Communications Conference*, 2013, pp. 3914–3919.
- [65] J. Jang, M. Chung, S. C. Hwang, Y.-G. Lim, H.-j. Yoon, T. Oh, B.-W. Min, Y. Lee, K. S. Kim, C.-B. Chae, *et al.*, Smart small cell with hybrid beamforming for 5g: Theoretical feasibility and prototype results , *IEEE Wireless Communications*, vol. 23, no. 6, pp. 124–131, 2016.
- [66] X. Yang, A multilevel soft frequency reuse technique for wireless communication systems , *IEEE Communications Letters*, vol. 18, no. 11, pp. 1983–1986, 2014.
- [67] R. K. Saha and C. Aswakul, A novel clustering, frequency reuse and allocation technique for 2d regular grid-based dense urban femtocell deployment for 5g mobile networks , *Proc. 2017 International Conference on Electronics, Information, and communication (ICEIC)*, 2017, pp. 220–223.
- [68] M. S. Hossain, F. Tariq, G. A. Safdar, N. H. Mahmood, and M. R. A. Khandaker, Multi-layer soft frequency reuse scheme for 5g heterogeneous cellular networks , *IEEE Globecom Workshops (GC Wkshps)*, 2017, pp. 1–6.
- [69] Y. A. Abohamra, A. A. Amin, M. R. Solymani, and Y. R. S. , Direction of arrival algorithms for user identification in cellular networks , *IEEE 7th Annual Information Technology, Electronics and Mobile Communication Conference (IEMCON)*, 2016 , pp. 1–7 .
- [70] Y. A. Abohamra, M. R. Solymani, and Y. R. Shayan, Optimum scheduling based

- on beamforming for the fifth generation of mobile communication systems , IEEE 8th IEEE Annual Information Technology, Electronics and Mobile Communication Conference (IEMCON), 2017, pp. 332 339.
- [71] J. Litva and T. K. Lo, *Digital Beamforming in Wireless Communications*, 1st. Artech House, Inc., 1996.
- [72] A. B. Narasimhamurthy, M. K. Banavar, and C. Tepedelenliouglu, *OFDM Systems for Wireless Communications*. Morgan & Claypool Publishers, 2010.
- [73] K. Kale, *Advances in Computer Vision and Information Technology*. IK International Pvt Ltd, 2008.
- [74] S. C. Yang, *OFDMA System Analysis and Design*. Artech House, 2010.
- [75] H. Yin and S. Alamouti, *Ofdma: A broadband wireless access technology* , IEEE Sarnoff Symposium, 2006, pp. 1 4.
- [76] F. E. A. El-Samie, F. S. Al-Kamali, A. Y. Al-nahari, and M. I. Dessouky, *SC-FDMA for Mobile Communications*, 3rd. CRC press, 2016.
- [77] J. T. Penttinen, *The Telecommunications Handbook: Engineering Guidelines for Fixed, Mobile and Satellite Systems*. John Wiley & Sons, 2015.
- [78] Z. Chen, G. Gokeda, and Y. Yu, *Introduction to Direction-of-arrival Estimation*. Artech House, 2010.
- [79] I. Nicolaescu and D. Stoica, *Smart antennas for wireless communications systems* , IEEE Conference Proceedings ICECom, 20th International Conference on Applied Electromagnetics and Communications, 2010, pp. 1 4.
- [80] A. Barabell, *Improving the resolution performance of eigenstructure-based direction-finding algorithms* , IEEE ICASSP '83. IEEE International Conference on Acoustics, Speech, and Signal Processing, vol. 8, 1983, pp. 336 339.

- [81] J. Foutz, A. Spanias, and M. Banavar, *Narrowband Direction of Arrival Estimation for Antenna Arrays*. Morgan & Claypool, 2008.
- [82] M. Samir, E. M. Shaheen, and A. A. E. Wahab, Performance analysis of ds-cdma system using fast adaptive filtering under different jamming techniques , IEEE International Conference on Engineering and Technology (ICET), 2012, pp. 1 - 6.
- [83] B. Allen and M. Ghavami, *Adaptive Array Systems: Fundamentals and Applications*. John Wiley & Sons, 2006.
- [84] M. Rumney *et al.*, *LTE and the Evolution to 4G Wireless: Design and Measurement Challenges*. John Wiley & Sons, 2013.
- [85] B. G. Frank, *Smart Antennas for Wireless Communications With MATLAB*. 2005.
- [86] D. Gesbert and M. Alouini, How much feedback is multi-user diversity really worth? , IEEE International Conference on Communications (IEEE Cat. No.04CH37577), vol. 1, 2004, pp. 234 - 238.
- [87] S. Sanayei and A. Nosratinia, Opportunistic downlink transmission with limited feedback , *IEEE Transactions on Information Theory*, vol. 53, no. 11, pp. 4363 - 4372, 2007.
- [88] J. Chen, R. A. Berry, and M. L. Honig, Limited feedback schemes for downlink ofdma based on sub-channel groups , *IEEE Journal on Selected Areas in Communications*, vol. 26, no. 8, 2008.
- [89] S. N. Donthi and N. B. Mehta, Performance analysis of user selected subband channel quality indicator feedback scheme of lte , IEEE Global Telecommunications Conference GLOBECOM 2010, 2010, pp. 1 - 6.
- [90] F. Kuo, H. Wang, K. Ting, C. Tseng, and P. Liu, Robust lte uplink scheduling based on call admission control , IEEE International Conference on ICT Convergence (ICTC), 2012, pp. 548 - 552.

- [91] H. Lebreit and S. Boyd, Antenna array pattern synthesis via convex optimization , *IEEE transactions on signal processing*, vol. 45, no. 3, pp. 526 532, 1997.
- [92] S. Sadr, A. Anpalagan, and K. Raahemifar, Radio resource allocation algorithms for the downlink of multiuser ofdm communication systems , *IEEE Communications Surveys & Tutorials*, vol. 11, no. 3, 2009.
- [93] T. Jiang, L. Song, and Y. Zhang, *Orthogonal Frequency Division Multiple Access Fundamentals and Applications*. CRC Press, 2010.
- [94] Z. Cao and E. W. Zegura, Utility max-min: An application-oriented bandwidth allocation scheme , IEEE INFOCOM '99. Conference on Computer Communications. Proceedings. Eighteenth Annual Joint Conference of the IEEE Computer and Communications Societies. The Future is Now (Cat. No.99CH36320), vol. 2, 1999, pp. 793 801.